Chapter – 3

RESULTS AND DISCUSSION

3. RESULTS AND DISCUSSION

The work carried out towards achieving the proposed plan has been discussed under the following four main headings.

3.1. Syntheses

3.2. Hydrolyses kinetics

3.3. Biological evaluation

3.4. Biodistribution and Gamma imaging studies

3.1. SYNTHESES

The work carried out under this head has been discussed under the following subheadings:

3.1.1. Aminoalcohol ester derivatives of 4-biphenylacetic acid

3.1.2. Aminoalcohol ester derivatives of flurbiprofen

3.1.3. Attempted synthesis of the aminoalcohol ester derivatives of diclofenac

3.1.4. Aminoalcohol ester derivatives of diclofenac

3.1.5. Attempted synthesis of the aminoalcohol ester derivatives of indomethacin

3.1.6. Aminoalcohol ester derivatives of indomethacin

3.1.7. Aminoalcohol ester derivatives of aspirin

3.1.8. Aminoalcohol ester derivatives of ketorolac

3.1.1. AMINOALCOHOL ESTER DERIVATIVES OF 4-BIPHENYLACETIC ACID

4-Biphenylacetic acid (45)

Fenbufen (**44**) is a potent anti-inflammatory agent that is metabolized into 4-hydroxy-4-biphenylbutanoic acid and 4-biphenylacetic acid (**45**). 4-Biphenylacetic acid (**45**) is an active metabolite of fenbufen (**44**) with three times more activity than the parent drug but is also considerably more ulcerogenic than fenbufen (**44**) or its other metabolites[101, 102].

considering its higher level of gastrotoxicity it was thought of decreasing the gastrotoxicity of 4-biphenylacetic acid (**45**) using the approach as described in earlier chapter.

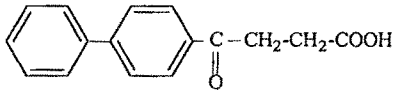

(44)

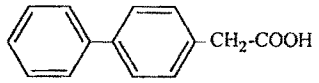

(45)

The intermediate 4-biphenylacetic acid (**45**) required for the synthesis of the final compounds (**45a-f**) was synthesized[103] starting from biphenyl (**46**). Biphenyl (**46**) was reacted with acetic anhydride in the presence of anhydrous aluminium trichloride to yield 4-phenylacetophenone (**47**). The compound (**47**) showed an intense peak at 1680 cm^{-1} for the carbonyl (C=O) stretching in the IR spectrum. The ketone (**47**) was converted to 4-biphenylacetic acid (**45**) by the modified Willgerodt reaction which was carried out in two steps. The first step involved the conversion of ketone (**47**) to thiomorpholide (**48**) by

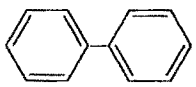

(46)

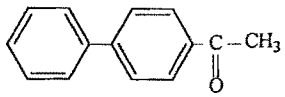

(47)

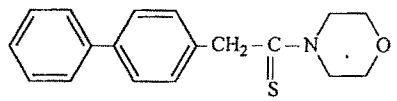

(48)

reacting the ketone (**46**) with sulfur in presence of morpholine. In the second step, the thiomorpholide (**48**) was hydrolysed under basic condition to obtain the required acid (**45**).

Compound (**45**) showed the carbonyl stretching band at 1690 cm^{-1} and a broad peak for hydroxyl stretching at 3400 cm^{-1}. The PMR spectrum showed a sharp singlet for the methylene protons (ArCH_2-) at δ 3.70 and signal for the aromatic protons appeared as a multiplet at δ 7.25-7.66.

The targeted aminoalcohol ester derivatives (**45a-f**) of 4-biphenylacetic acid (**45**) have been synthesized as outlined in Scheme-I

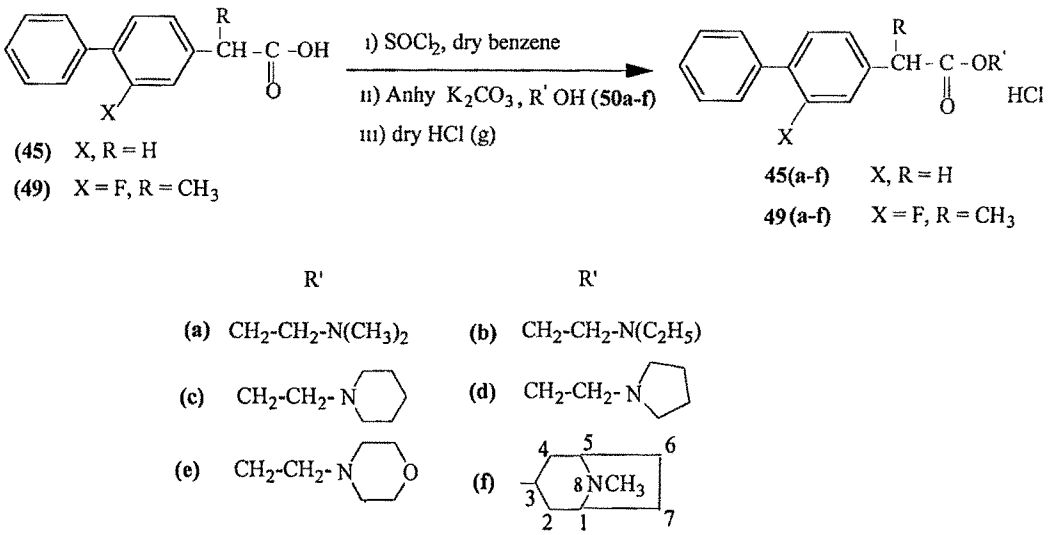

SCHEME –I

2-Dimethylaminoethyl 4-biphenylacetate hydrochloride (45a)

4-Biphenylacetic acid (**45**) on treatment with thionyl chloride in dry benzene gave the acid chloride which was reacted with excess of 2-dimethylaminoethanol (**50a**) under basic conditions i.e in the presence of anhydrous potassium carbonate in dry alcohol-free

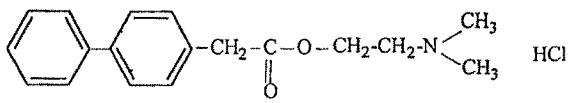

(45a)

chloroform. During the processing of the reaction mixture, excess of the aminoalcohol (**50a**) was removed by successive washings with cold water to get an oily material, which was converted into the corresponding hydrolchloride salt (**45a**) and crystallized from acetone-isopropyl ether. The compound (**45a**) showed the characteristic ester carbonyl (C=O) stretching at 1743 cm^{-1} in the IR spectrum. The PMR spectrum showed a sharp singlet at δ 2.75 for the six protons of [-N(CH_3)$_2$], a triplet for the two protons of (-CH_2N-) was observed at δ 3.33, a sharp singlet at δ 3.79 for the (Ar-CH_2) protons and the signal for the deshielded protons (-O-CH_2-) appeared as a multiplet at δ 4.56-4 61.

Multiplet for the nine aromatic protons appeared at δ 7.33-7.63 and a broad singlet at δ 12.75 was observed for the proton of (.N*H*Cl).

2-Diethylaminoethyl 4-biphenylacetate hydrochloride (45b)

The synthesis and work up of the reaction between the acid (**45**) and 2-diethylaminoethanol (**50b**) was carried out in same fashion as described for the compound (**45a**) to yield compound (**45b**). The ester carbonyl (C=O) stretching was obs-

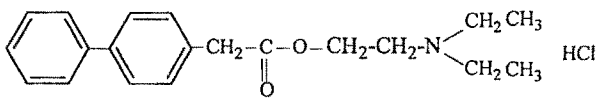

(45b)

erved at 1749 cm^{-1} in the IR spectrum. Its PMR spectrum showed a triplet at δ 1.30 for the six protons [–N(CH_2CH_3)$_2$] and a quartet at δ 3.02 for four protons [-N(CH_2CH_3)$_2$]. Signals for (-CH_2-CH_2-N-) protons appeared as a triplet at δ 3.26 and the deshielded protons (-O-CH_2-) gave a multiplet at δ 4.60-4.65. The Ar-CH_2 protons appeared as a sharp singlet at δ 3.75 and the multiplet for the nine aromatic protons appeared at δ 7.27-7.59.

1-[2-(1-Piperidino)]ethyl 4-biphenylacetate hydrochloride (45c)

The compouind (**45c**) was obtained by reacting 4-biphenylacetic acid (**45**) with 2-piperidinoethanol (**50c**) as described above. The IR spectrum of compound (**45c**) showed

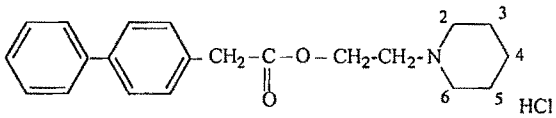

(45c)

the characteristic ester carbonyl (C=O) stretching at 1743 cm^{-1}. In the PMR spectrum a multiplet was observed at δ 1.25-1.77 for six protons of the three methylene groups of the piperidine ring system (3-CH_2, 4-CH_2, 5-CH_2). Three triplets were observed at δ 2.45, 3.19 and 3.38 for the three methylene group protons (2-CH_2, 6-CH_2, -CH_2N-)

directly bonded to the nitrogen atom. A multiplet at δ 4.63-4.66 was observed for the (-O-C*H*$_2$-) protons. A sharp singlet at δ 3.74 appeared for the (Ar-C*H*$_2$) protons and a multiplet for the aromatic protons appeared at δ 7.27-7.57 with a broad signal corresponding to (N.*H*Cl) at δ 12.25, which was exchangeable in deuterium exchange PMR spectrum.

1-[2-(1-Pyrrolidino)]ethyl 4-biphenylacetate hydrochloride (45d)

Using Scheme-I, 4-biphenylacetic acid (**45**) and 2-pyrrolidinoethanol (**50d**) were reacted as described above to obtain the desired compound as hydrochloride salt (**45d**). The ester carbonyl stretching appeared as an intense sharp peak at 1743 cm^{-1} in its IR spectrum.

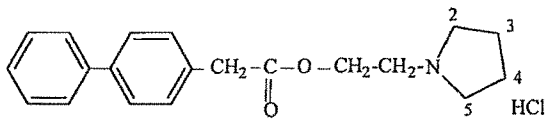

(45d)

Triplet for the four protons of the two (-CH$_2$-) groups of the pyrrolidine system not directly bonded to nitrogen (3-C*H*$_2$, 4-C*H*$_2$) appeared at δ 2.02 in the PMR spectrum. A multiplet for six protons was observed for (2-C*H*$_2$, 5-C*H*$_2$, -C*H*$_2$N) between δ 2.25-2.60 with a sharp singlet at 3.78 for (Ar-C*H*$_2$-) protons. The characteristic signal for (-O-C*H*$_2$) two protons appeared at δ 4.58-4.63. The multiplet for the aromatic protons appeared between δ 7.27-7.58 with a broad signal at δ 12.50 for the proton attached to nitrogen (N.*H*Cl).

1-[2-(4-Morpholino)]ethyl 4-biphenylacetate hydrochloride (45e)

The compound (**45e**) was prepared as described for (**45a**) by reacting 4-biphenylacetic acid (**45**) and 4-(hydroxyethyl)morpholine (**50e**). It showed characteristic ester (C=O) stretching at 1743 cm^{-1} in the IR spectrum (Figure 3.1). A multiplet at δ 2.60-2.67 for the (C*H*$_2$-N) protons and a multiplet at δ 3.25-3.29 for the four protons of two (-CH$_2$-) group directly bonded to nitrogen (3-C*H*$_2$, 5-C*H*$_2$) were observed in the PMR spectrum A

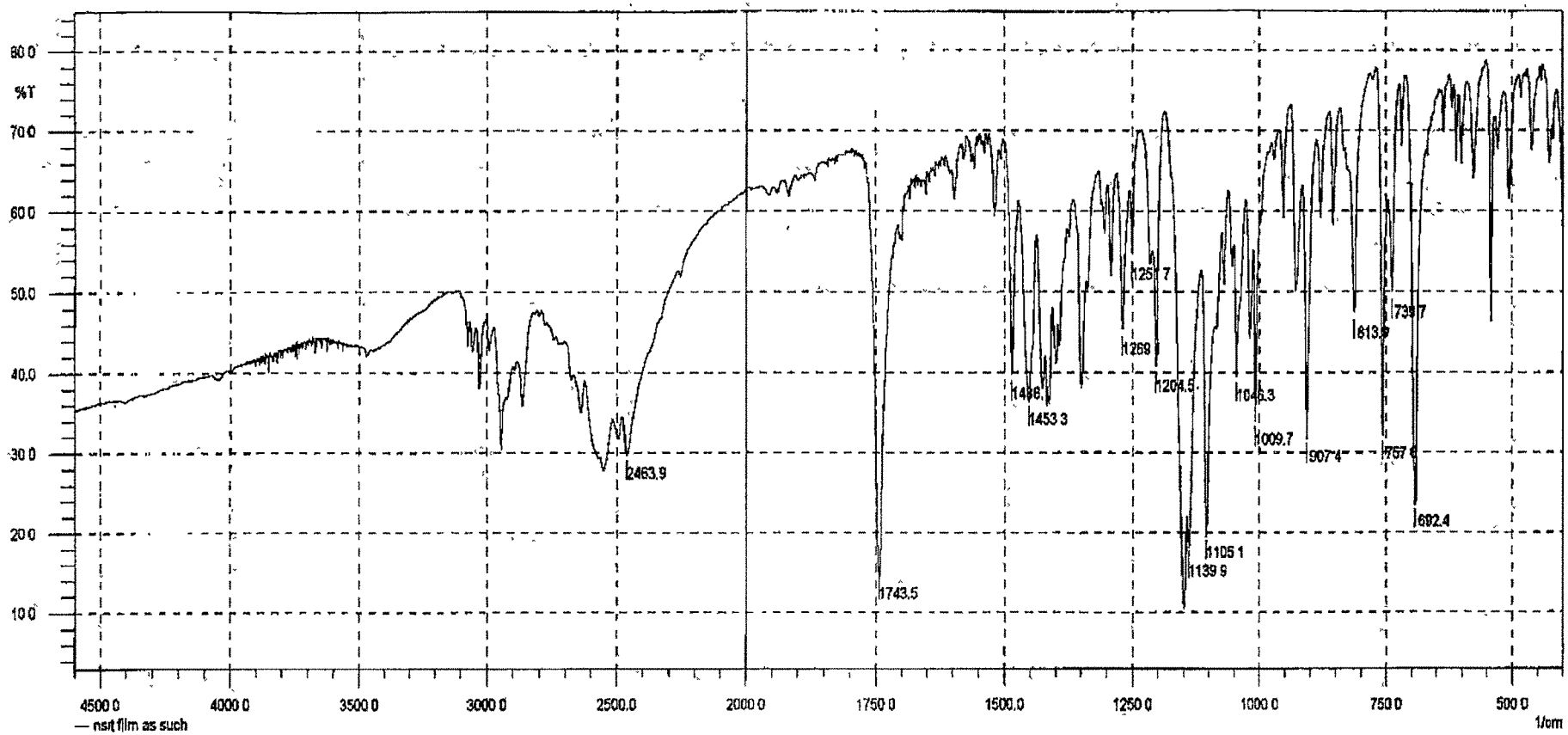

Figure 3.1 IR spectrum of compound (45e)

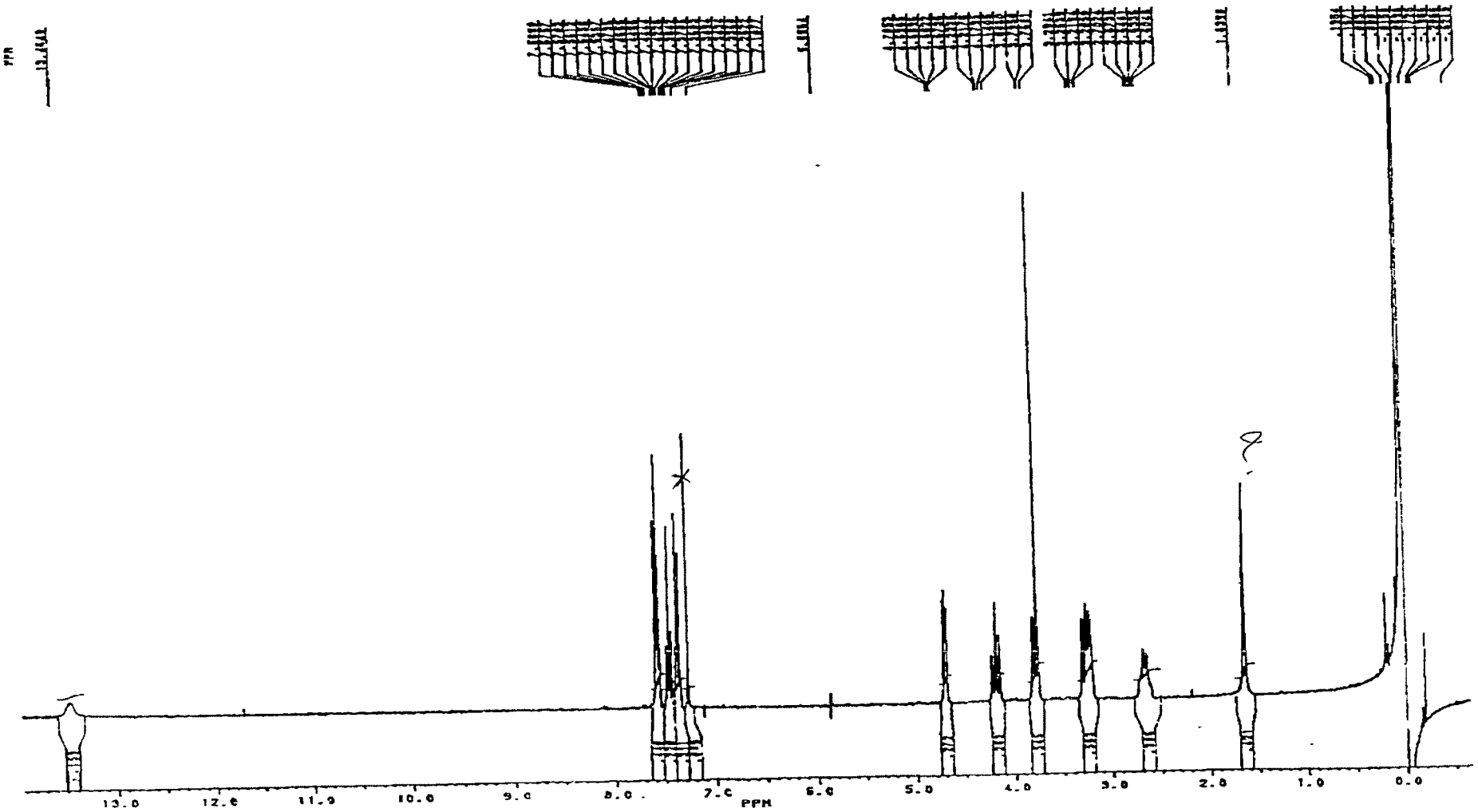

Figure 3.2 PMR spectrum of compound (45e)

sharp singlet appeared at δ 3.76 for the (Ar-C*H*$_2$) protons. Signals at δ 3 80-4 22 for the methylene protons (2-C*H*$_2$, 6-C*H*$_2$-) of the morpholine system, a multiplet at δ 4.67-4.70

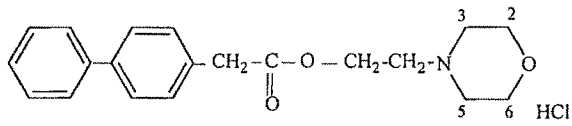

(45e)

for the protons of (-CO-O-C*H*$_2$-) group, a multiplet at δ 7.33-7.58 for the aromatic protons and a broad signal at δ 13.50 for (N *H*Cl) protons were also observed (Figure 3.2).

8-Methyl-8-azabicyclo[3,2,1]octan-3-yl 4-biphenylacetate (45f)

Tropinol (**50f**) was obtained by alkaline hydrolysis of atropine sulphate. The compound (**45f**) was prepared by reaction of 4-biphenylacetic acid (**45**) and tropinol (**50f**) adopting Scheme-I as described for the compound (**45a**) It gave a sharp intense band at 1727 cm^{-1}

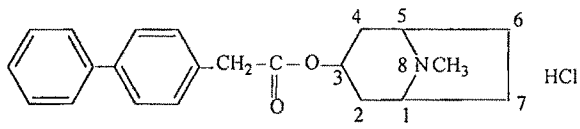

(45f)

for the ester carbonyl stretching in the IR spectrum. The compound (**45f**) showed signals at δ 1.62-1.65 (m, 2H, 2-C*H* and 4-C*H*), 1.86-1.94(m, 4H) for (6-C*H*$_2$ and 7-C*H*$_2$), 2.65(s, 3H, NC*H*$_3$), δ 2.75-3.00 (m, 2H) for (1-C*H* and 5-C*H*), 3.49-3.61 (m, 2H, 2-C*H* and 4-C*H*), 3.68 (s, 2H, Ar-C*H*$_2$), 5.13-5.17 (m, 1H, 3-O-C*H*) and 7.31-7.60(m, 9H, Ar-*H*) in the PMR spectrum.

3.1.2. AMINOALCOHOL ESTER DERIVATIVES OF FLURBIPROFEN

Flurbiprofen (**49**) is a potent, clinically used[104] NSAID belonging to the arylpropionic acid class. The ester derivatives (**49a-f**) were synthesized as depicted in Scheme-I.

2-Dimethylaminoethyl 2-(2-fluoro-4-biphenyl)propionate hydrochloride (49a)

The compound (**49a**) was prepared by reacting flurbiprofen (**49**) and 2-dimethylamino-ethanol (**50a**) as described for the derivatives (**45a-f**) in the above paragraphs as per the Scheme-I. The compound (**49a**) showed characteristic band at 1743 cm^{-1} for the ester (C=O) in the IR spectrum (Figure 3.3). A doublet at δ 1.55 for the three protons of [Ar-CH(CH_3)] group and a singlet at δ 2.72 for the six protons of [N(CH_3)$_2$] group were observed in its PMR spectrum. A triplet for (-CH_2-N-) protons at δ 3.27, a quartet for

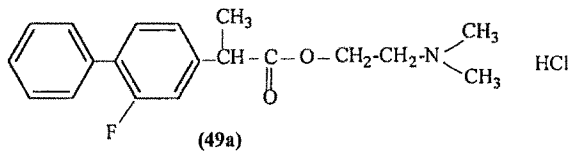

(**49a**)

(ArC*H*-) at δ 3.88, a multiplet at δ 4.49-4.66 for the (-O-CH_2-) protons and a multiplet at δ 7.09-7.53 for the aromatic protons were also observed in the PMR spectrum (Figure 3.4).

2-Diethylaminoethyl 2-(2-fluoro-4-biphenyl)propionate hydrochloride (49b)

The compound (**49b**) was prepared by reaction of flurbiprofen (**49**) and 2-diethylamino-ethanol (**50b**) as described above. It showed absorption band at 1732 cm^{-1} ester carbonyl stretching in its IR spectrum. The PMR spectrum of **49b** showed signals at δ 1.28 (t, 6H,

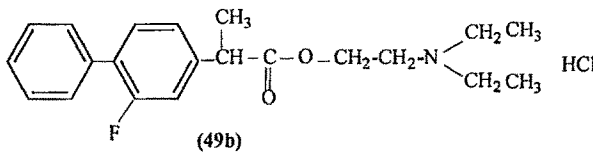

(**49b**)

N(CH_2CH_3)$_2$), 1.55 (d, 3H, Ar-CH(CH_3)), 2.94-3.04 [m, 4H, N(CH_2CH_3)$_2$], 3.26 (t, 2H, CH_2-N), 3.82 (q, 1H, ArC*H*-), 4.58-4.62 (m, 2H, OCH_2-) and at 7.08-7.53 (m, 8H, ArH).

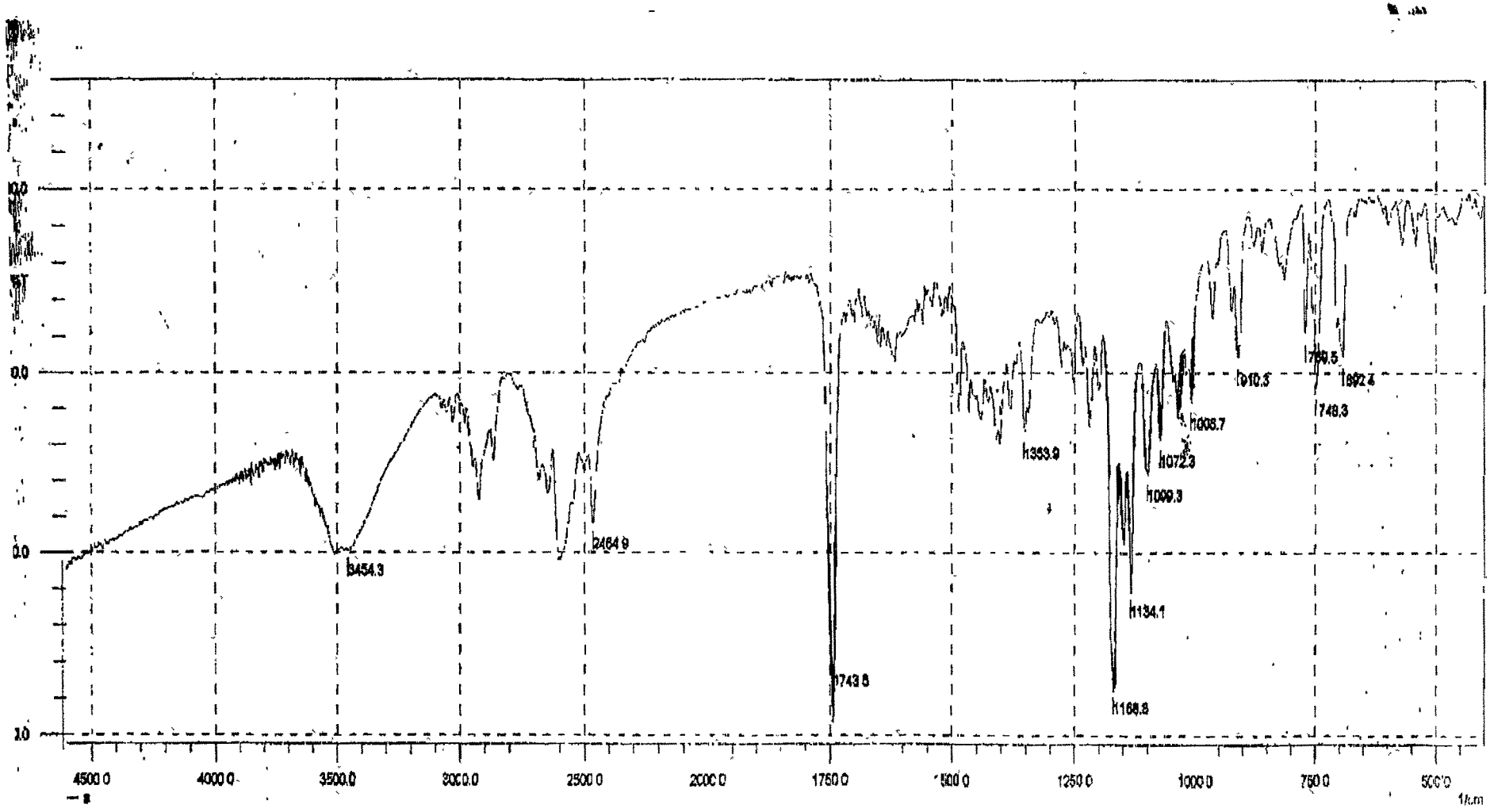

Figure 3.3 IR spectrum of compound (49a)

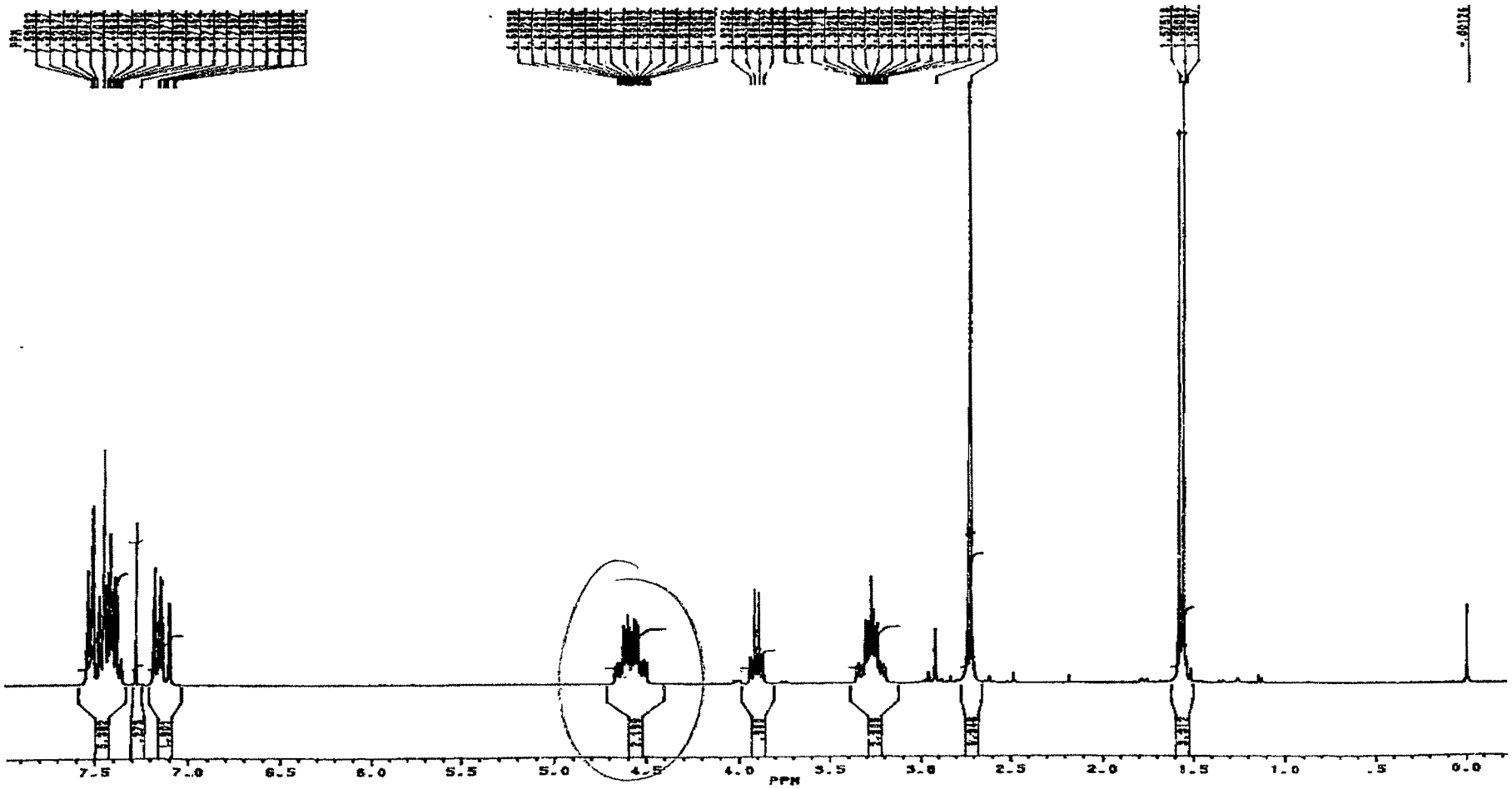

Figure 3.4 PMR spectrum of compound (49a)

1-[2-(1-Piperidino)]ethyl 2-(2-fluoro-4-biphenyl)propionate hydrochloride (49c)

Flurbiprofen (**49**) was reacted with 1-piperidinoethanol (**50c**) as described above to afford compound (**49c**). The IR spectrum of compound (**49c**) showed the ester carbonyl stretching as a sharp intense band at 1736 cm^{-1}. The PMR spectrum showed signals at δ 1.54 (d, 3H, ArCH-C*H*$_3$), 1.69-2.21 (m, 6H, 3-C*H*$_2$, 4-C*H*$_2$ and 5-C*H*$_2$), 2.35-3.40 (m, 6H

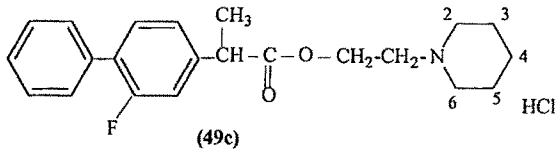

(49c)

C*H*$_2$-N, 2-C*H*$_2$ and 6-C*H*$_2$), 3.83 (q, 1H,Ar-C*H*-CH$_3$), 4.59-4.64 (m, 2H, OC*H*$_2$), 7.08-7.53 (m, 8H, Ar-*H*) and 12.25 (b, 1H, N.*H*Cl disappeared on deuterium exchange)

1-[2-(1-Pyrrolidino)]ethyl 2-(2-fluoro-4-biphenyl)propionate hydrochloride (49d)

On reacting flurbiprofen (**49**) with 2-(1-pyrrolidino)ethanol (**50d**) by the above described procedure compound (**49d**) was obtained as hydrochloride salt. The characteristic carbonyl stretching vibrations gave an intense peak at 1733 cm^{-1} in the IR spectrum. A doublet at δ 1.54 for [Ar-CH(C*H*$_3$)-] protons, multiplet at δ 2.02-2.16 for the two methylene protons of the pyrrolidine ring system not bonded to nitrogen (3-C*H*$_2$ and 4-C*H*$_2$) and multiplet at δ 2.63-3.70 for the three methylene protons bonded to the nitrogen

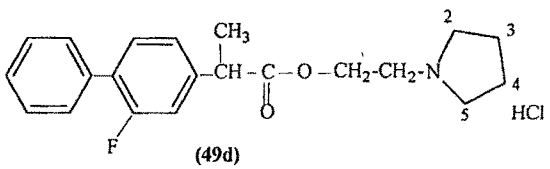

(49d)

atom (2-C*H*$_2$, 5-C*H*$_2$ and C*H*$_2$N) were observed in its PMR spectrum. The multiplet for the (O-C*H*$_2$) proton at δ 4.53-4.64, quartet for (ArC*H*-) at δ 3.86, multiplets at δ 7.09-7.53 for the aromatic protons and a broad signal at δ 12.45 for the (.N*H*Cl) proton also appeared in the PMR spectrum.

1-[2-(4-Morpholino)]ethyl 2-(2-fluoro-4-biphenyl)propionate hydrochloride (49e)

On reacting flurbiprofen (**49**) with 2-(4-morpholino)ethanol (**50e**) by the above described procedure compound (**49e**) was obtained as hydrochloride salt. The characteristic carbonyl stretching vibration gave an intense peak at 1740 cm^{-1} in the IR spectrum. A doublet at δ 1.54 for [Ar-CH(C*H*$_3$)-] protons, multiplet at δ 2.58- 3.29 for the six protons of three methylene groups bonded to nitrogen (3-C*H*$_2$, 5-C*H*$_2$ and C*H*$_2$N), a signal at 3.75-4.20 for five protons [(Ar-C*H*), 2-C*H*$_2$, 6-C*H*$_2$] and broad signal for the protons of

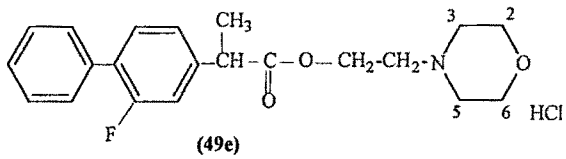

(49e)

(O-C*H*$_2$-) at δ 4.66 were observed in the PMR spectrum. Multiplet at δ 7.09-7.53 for the aromatic protons and a broad signal at δ 13.30 for (.N*H*Cl) were also observed.

8-Methyl-8-azabicyclo[3,2,1]octan-3-yl 2-(2-fluoro-4-biphenyl)propionate hydrochloride (49f)

Compound (**49f**) was obtained by reacting flurbiprofen (**49**) and tropinol (**50f**) as described for compound (**45f**). Characteristic peak at 1727 cm^{-1} was observed in the IR spectrum of **49f** for the ester carbonyl stretching. In the PMR spectrum signals appeared

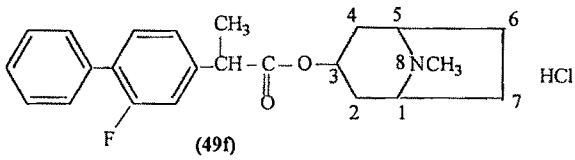

(49f)

at δ 1.53 [d, 3H, Ar-CH(C*H*$_3$)-], 1.85-1.96 (m, 4H) for (6-C*H*$_2$ and 7-C*H*$_2$), 2.04-2.09 (m, 2H, 2-C*H* and 4-C*H*), 2.64 (s, 3H, NC*H*$_3$), δ 2.99-3.13 (m, 2H) for (1-C*H* and 5-C*H*), 3.55-3.65 (m, 2H, 2-C*H* and 4-C*H*), 3.69-3.76 (m, 1H, Ar-C*H*), 5.13-5.16 (m, 1H, O-C*H*), 7.07-7.53 (m, 9H, Ar-*H*) and 12.51 (b, 1H, .N*H*Cl).

3.1.3. ATTEMPTED SYNTHESIS OF AMINOALCOHOL ESTER DERIVATIVES OF DICLOFENAC

Diclofenac (**51**), a heteroaryl acetic acid derivative has been used worldwide since its introduction in Japan[105] in 1974. The incidence of gastrointestinal side effects may approach 30-40%[106] in the diclofenac (**51**) treated patients and hence diclofenac (**51**) was one of the NSAIDs chosen for the present work.

In our attempt to synthesize the ester derivatives of diclofenac (**51**), the general method of converting carboxylic acid into ester via the acid chloride method was tried. A solution of diclofenac (**51**) in dry, alcohol-free dichloromethane was treated with thionyl chloride at room temperature with further stirring for 2 hours followed by treatment with 2-dimethylaminoethanol (**50a**) at room temperature. Work up of the reaction mixture yielded a dark red coloured product. By reacting different aminoalcohols (**50 a-d**) in this fashion with diclofenac (Scheme-II, Method-A) dark colored reaction mixtures were obtained every time. On further purification using repeated crystallization, lactam (**52**)

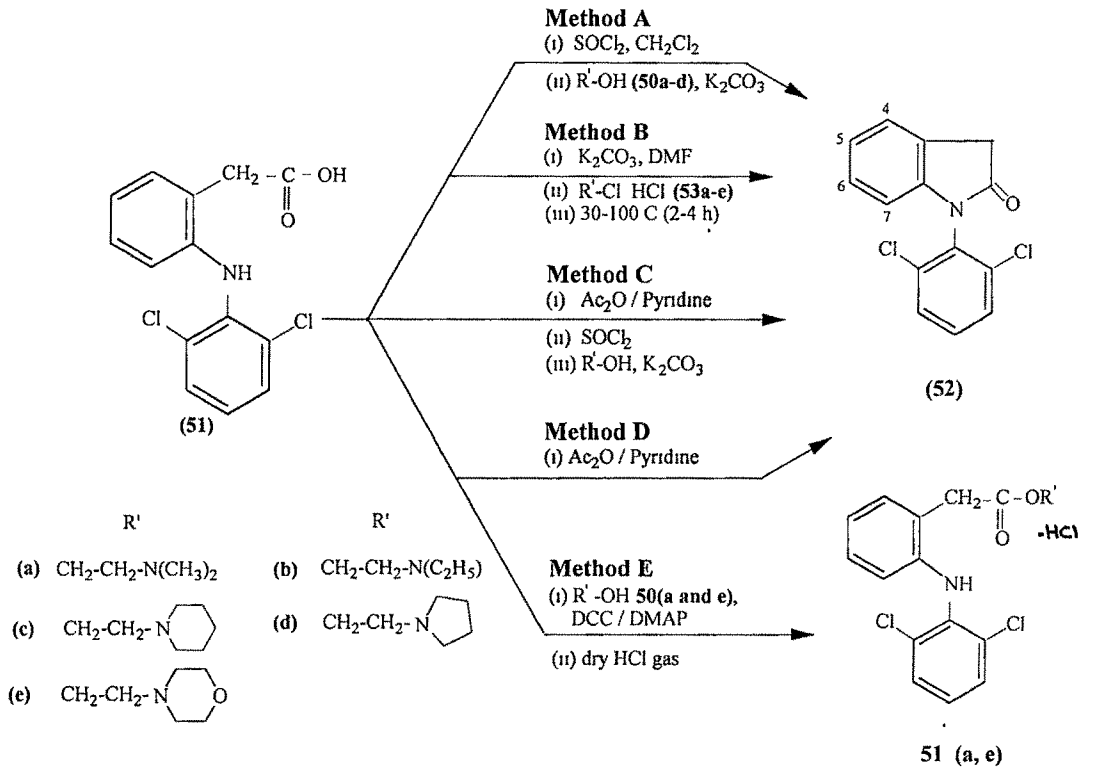

SCHEME-II

was isolated in all the cases in the above described reaction mixtures. The compond (**52**) showed an intense peak at 1732 cm^{-1} for the γ-lactam (C=O) in the IR spectrum (Figure 3.5). PMR spectrum gave signals at δ 3.78 (s, 2H) for (Ar-C*H*$_2$) protons and at δ 6.39-6.41(d, 1H, Ar-7-C*H*), 7.07-7.12 (m, 1H, Ar-5-C*H*), 7.18-7.23 (m, 1H, Ar-4'-C*H*), 7.33-7.37 (m, 1H, Ar-6-C*H*), 7.38-7.40 (d, 1H, Ar-4-C*H*) and 7.49-7.52 (d, 2H, Ar-3'-C*H*, Ar-5'-C*H*) (Figure 3.6). Formation of the lactam (**52**) can be explained through internal nucleophilic attack by the amino 'N', which can easily take place, on the carbonyl of the acid chloride due to the entropy advantage (Scheme-III). To prevent the formation of lactam (**52**) it was thought of converting the aminoalcohol component into an electrophile by converting it into the chloro derivative and making carboxylic group to a carboxylate nucleophile, and performing the reaction in a polar aprotic solvent like DMF (Method B). In this method, 2-dimethylaminoethanol (**50a**) was reacted with thio-

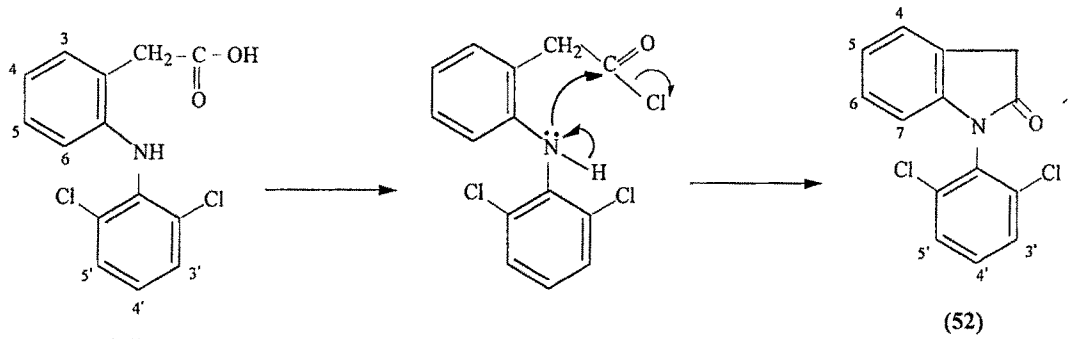

(51) (52)

SCHEME-III

nyl chloride to obtain hydrochloride salt of the chloro-derivative (**53a**). This chloro-derivative (**53a**) was reacted with diclofenac (**51**) in presence of anhydrous potassium carbonate and anhydrous DMF with heating on a water bath over different time intervals. But, the same product (**49**) was obtained here again in all the cases.

To prevent the formation of lactam (**52**) it was thought of blocking the amino group of diclofenac (**51**) by acetylating it, and then to synthesize the esters adopting Method-A (Scheme-I) via the acid chloride route. With this aim in mind diclofenac (**51**) was treated with acetic anhydride in dry pyridine and left overnight at room temperature. The excess of the solvent and acetic anhydride were removed under vacuum, the residue obtained

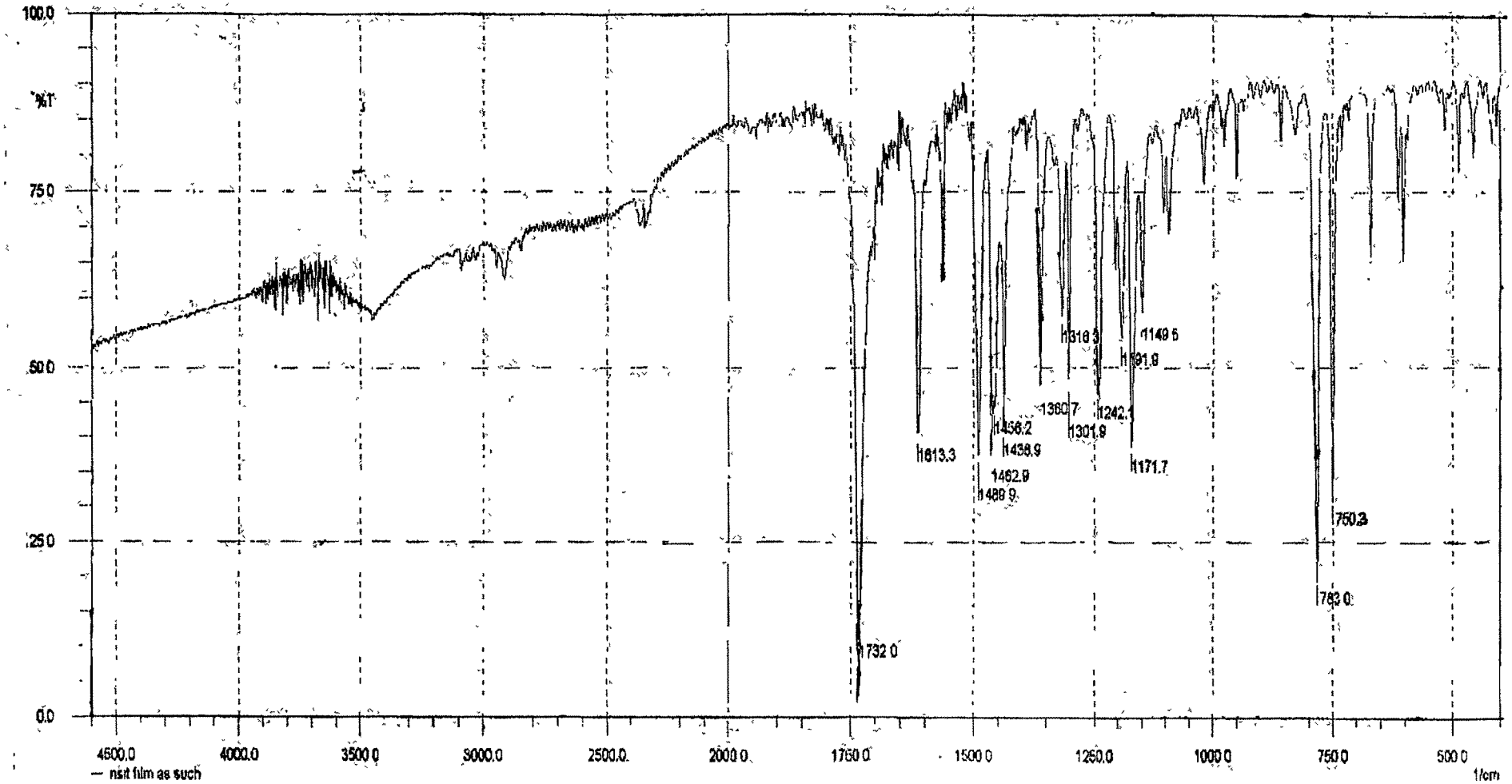

Figure 3.5 IR spectrum of compound (52)

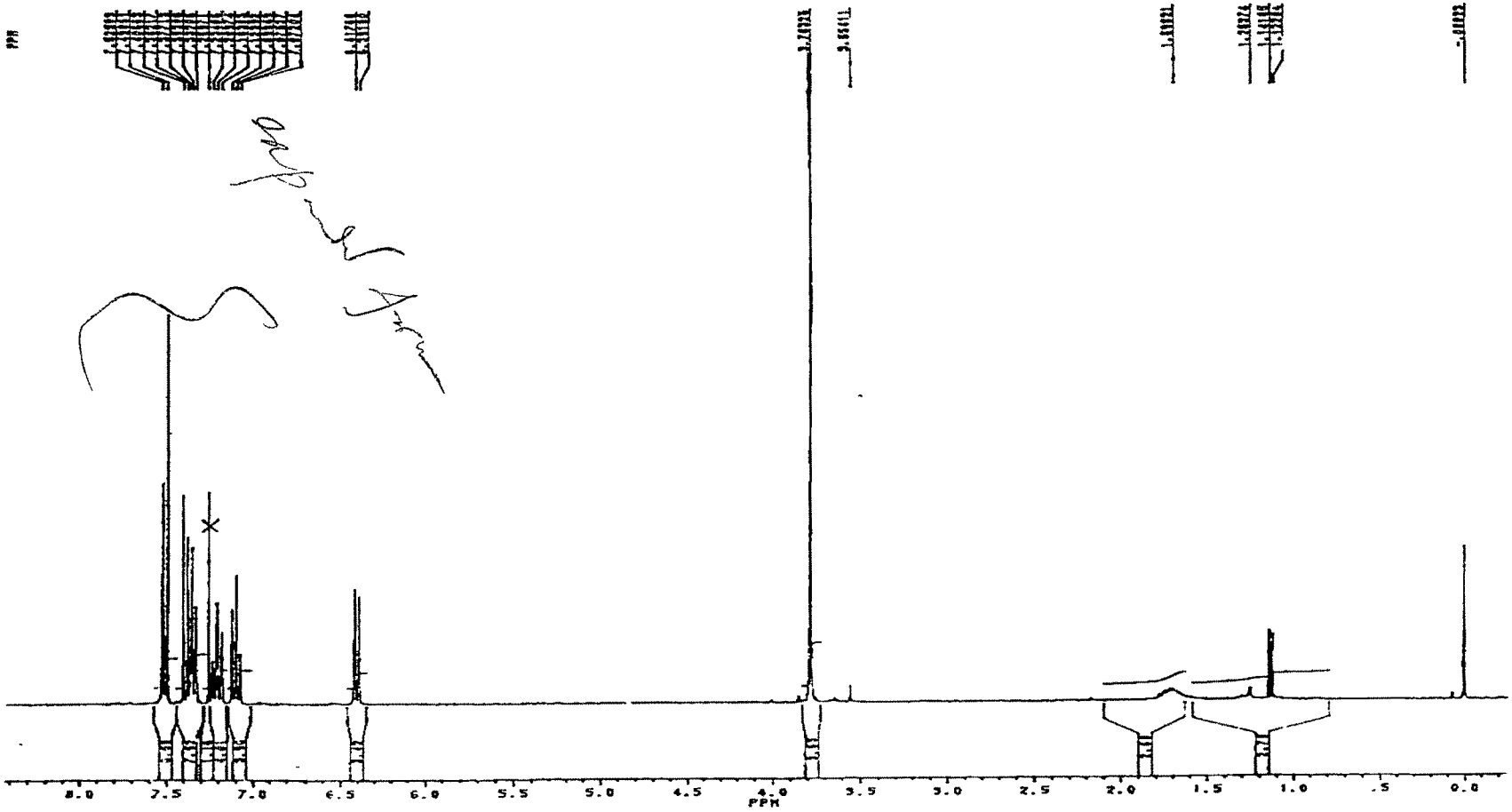

Figure 3.6 PMR spectrum of compound (52)

was dissolved in dry, alcohol-free chloroform and treated dropwise with thionyl chloride at room temperature (Method-C). Further procedure was similar as described in method A. Surprisingly here too the same lactam product (**52**) got isolated.

In the above discussed methods (Method-A, B and C) the lactam (**52**) was the only product isolated from the reaction mixtures. To confirm the formation of this lactam (**52**) upon treatment of diclofenac (**51**) with acetic anhydride in basic medium, the drug diclofenac (**51**) was treated with acetic anhydride in dry pyridine at room temperature The reaction mixture was left overnight and poured into ice-cold water, acidified with concentrated hydrochloric acid and extracted into chloroform, dried and complete removal of the solvent gave a semisolid which upon crystallization was identified to be lactam (**52**) by taking the mixed melting point, co-TLC and co-IR with the product isolated in the above discussed methods (Methods A, B, C, and D).

3.1.4. AMINOALCOHOL ESTER DERIVATIVES OF DICLOFENAC

After failing to obtain the desired aminoesters of diclofenac (**51**) by the above described methods (Methods A, B, C and D) it was thought of adopting a reported[99] method (Method E). Diclofenac (**51**) was added to a stirred solution of 2-(4-morpholino)ethanol (**50e**), 4-dimethylaminopyridine and dicyclohexylcarbodiimide (DCC) in dry dichloromethane followed by the work up and purification through column (Silica gel G) to give a yellow oily residue, which was converted to the hydrochloride salt (**51e**).

In the reported method[99] compound (**51e**) was said to be obtained in 42% yield but, in our attempt following the same procedure the desired compound (**51e**), was obtained in a very poor yield (5% only). The method (Method E), was also tried for 2-dimethylamino-ethanol (**50a**) but again, here too, the compound (**51a**) was obtained in a very low yield (7%). Theoretically, there is a high probability of formation of lactam (**52**) here too, and that could be the reason for obtaining low yields of esters (**51a, e**). It was not tried to isolate compound (**52**), as that was not our aim.

In brief, different synthetic routes (Method A, B, C, D and E) were tried for the synthesis of esters of diclofenac as discussed above but, most of them failed to give the desired product or if at all succeeded (Method E), the yield was very poor. So, an alternative

method was tried for the synthesis of the esters of diclofenac (**51**) involving the reaction of diclofenac (**51**) with chloro derivatives (**53a-e**) of aminoalcohols (**50a-e**) (Scheme-IV) in a biphasic medium using a phase transfer catalyst. The reaction was carried out using a phase transfer catalyst (tetraethylammonium bromide), diclofenac (**51**) (nucleophile) as a salt and the chloro-derivatives (**53a-e**) (electrophile) of the various amino alcohols Here, the carboxylate anion of diclofenac, which as such is a poor nucleophile in itself, would be carried by the PTC into the organic phase where it would attack the electron deficient carbon of the chloro-derivative (electrophile, substrate) leading to the formation of the ester product. The ester so formed would remain in the organic phase and the PTC molecule will return back to the aqueous phase and would carry a new carboxylate ion

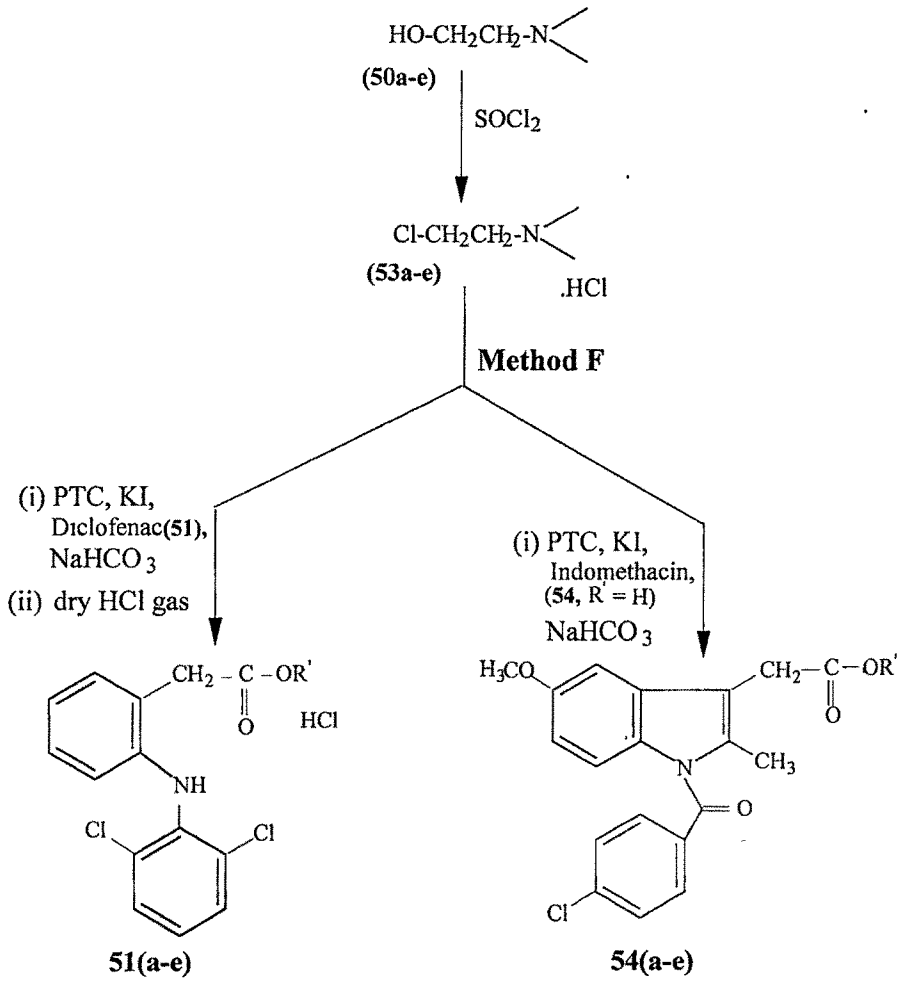

SCHEME-IV

into the organic phase till the completion of the reaction. The synthetic plan is outlined in Scheme-IV.

Finally, the esters (**51a-e**) were synthesized by the route as given in Scheme-IV (Method F) This method (Method F) involved the reaction of the aminoalcohols (**50a-e**) with thionyl chloride to yield the chloro-derivative (electrophile, substrate), which remained as the hydrochloride salt in the solvent, the excess of the thionyl chloride was destroyed by adding water. This solution was vigorously stirred with the PTC, potassium- iodide, diclofenac (**51**) and sodium bicarbonate. Presence of excess of sodium bicarbonate not only neutralized the amine salt into free amine but also converted free carboxylic acid into carboxylate anion. Potassium iodide was added for the purpose of halogen exchange. The reaction got completed over a period of 12-18 hours for various aminoalcohols (**50a-e**) as indicated by TLC monitoring. The work up involving the washing of the organic phase with ice-cold water, drying and solvent removal yielded the oily esters which were converted to the hydrochloride salts. Recrystallization of the products yielded the crystalline compounds (**51a-e**) with a yield in the range of 47 to 56%. This method (Method F) involving two steps reaction followed by a simple work up offered a synthetic route, which provided the desired compounds (**51a-e**) in a much better yield than the reported method[99]. However unfortunately, even this method (Method F) did not yield the desired ester when the reaction was carried out with diclofenac (**51**) and tropinol (**50f**). The reaction conditions were varied in various attempts to synthesize the tropinol ester of diclofenac (**51**), like replacing the solvent chloroform with benzene/toluene, using other PTCs, and increasing the temperature of the reaction mixture. But, the desired ester could not be prepared.

2-Dimethylaminoethly 2-(2,6-dichlorophenylaminophenyl)acetate hydrochloride (51a)

2-Dimethylaminoethanol (**50a**) was treated with thionyl chloride in dry, alcohol-free chloroform to yield the chloro derivative as the hydrochloride salt. Excess of the thionyl chloride was destroyed by adding water slowly to the reaction mixture. Tetraethyl ammonium bromide (PTC), potassium iodide and diclofenac (**51**) were added to the above reaction mixture with vigorous stirring and the reaction mixture was made alkaline with addition of sodium bicarbonate. The reaction was monitored by TLC. Simple work up involving the washing of the organic phase with ice-cold water, drying and complete recovery of the organic solvent yielded the oily esters. The oil so obtained was converted to hydrochloride salt by passing dry hydrogen chloride gas through the solution of the oil

in dry *iso*propyl ether followed by filtration of the precipitated solid and recrystalization to yield the crystalline compound (**51a**). IR spectrum of compound (**51a**) showed a sharp band at 3283 cm^{-1} for the NH stretching with the characteristic intense peak at 1734 cm^{-1} for the ester carbonyl stretching (Figure 3.7). PMR spectrum showed a singlet at δ 2 75 for ($N(CH_3)_2$) protons with a triplet at δ 3.32 for ($-CH_2N$) protons and a singlet at 3.93

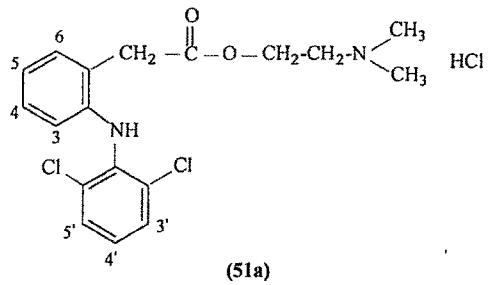

(51a)

for ($ArCH_2$). The desheilded ($O-CH_2$) protons appeared at δ 4.61-4.64 as a multiplet. Aromatic protons appeared at δ 6.48-6.51(d, 1H, Ar-3-C*H*), 6.90-6.95 (m, 1H, Ar-5-C*H*), 6.99-7.04 (m, 1H, Ar-4'-C*H*), 7.09-7.14 (m, 1H, Ar-4-C*H*), 7.22-7.25 (d, 1H, Ar-6-C*H*) and 7.34-7.36 (d, 2H, Ar-3'-C*H* and Ar-5'-C*H*). A broad signal at δ 12.74 was observed for (N.*H*Cl) and the proton of secondary amine (ArN*H*) appeared at δ 6.62 (Figure 3.8).

2-Diethylaminoethly 2-(2,6-dichlorophenylamino)phenylacetate hydrochloride (51b)

Reacting 2-diethylaminoethanol (**50b**) and diclofenac (**51**) by the procedure as described above for compound (**51a**) yielded the desired compound (**51b**). It showed characteristic bands at 3315 and 1730 cm^{-1} for the (N-H) and ester carbonyl stretching respectively in

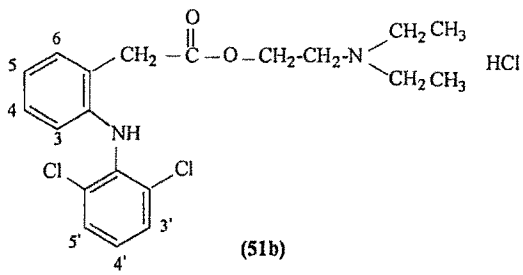

(51b)

the IR spectrum. The PMR spectrum showed a triplet at δ 1.31 for the six protons of ($-N(CH_2CH_3)_2$) with a quartet at 3.06 for the four protons of ($-N(CH_2CH_3)_2$) group. A tri-

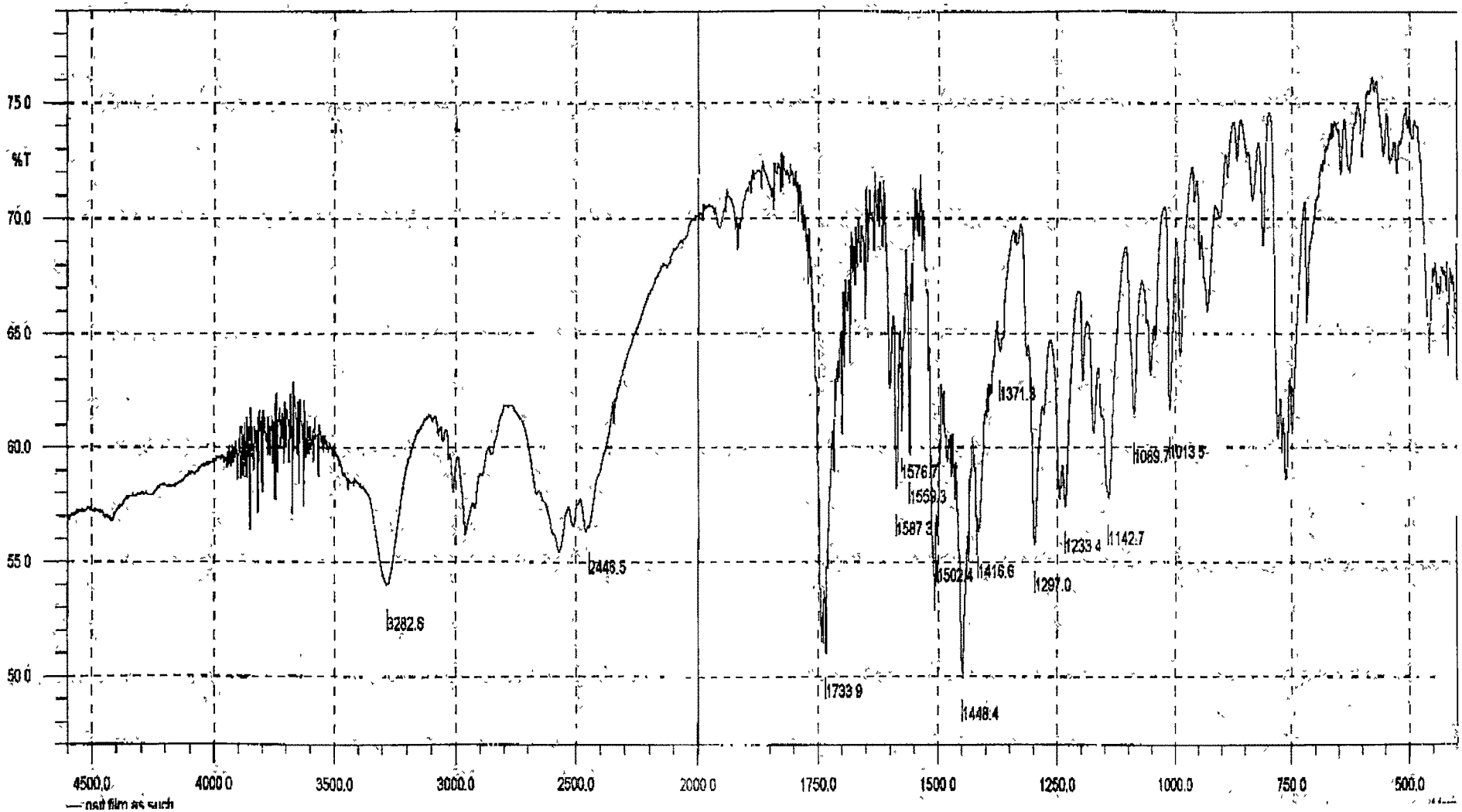

Figure 3.7 IR spectrum of compound (51a)

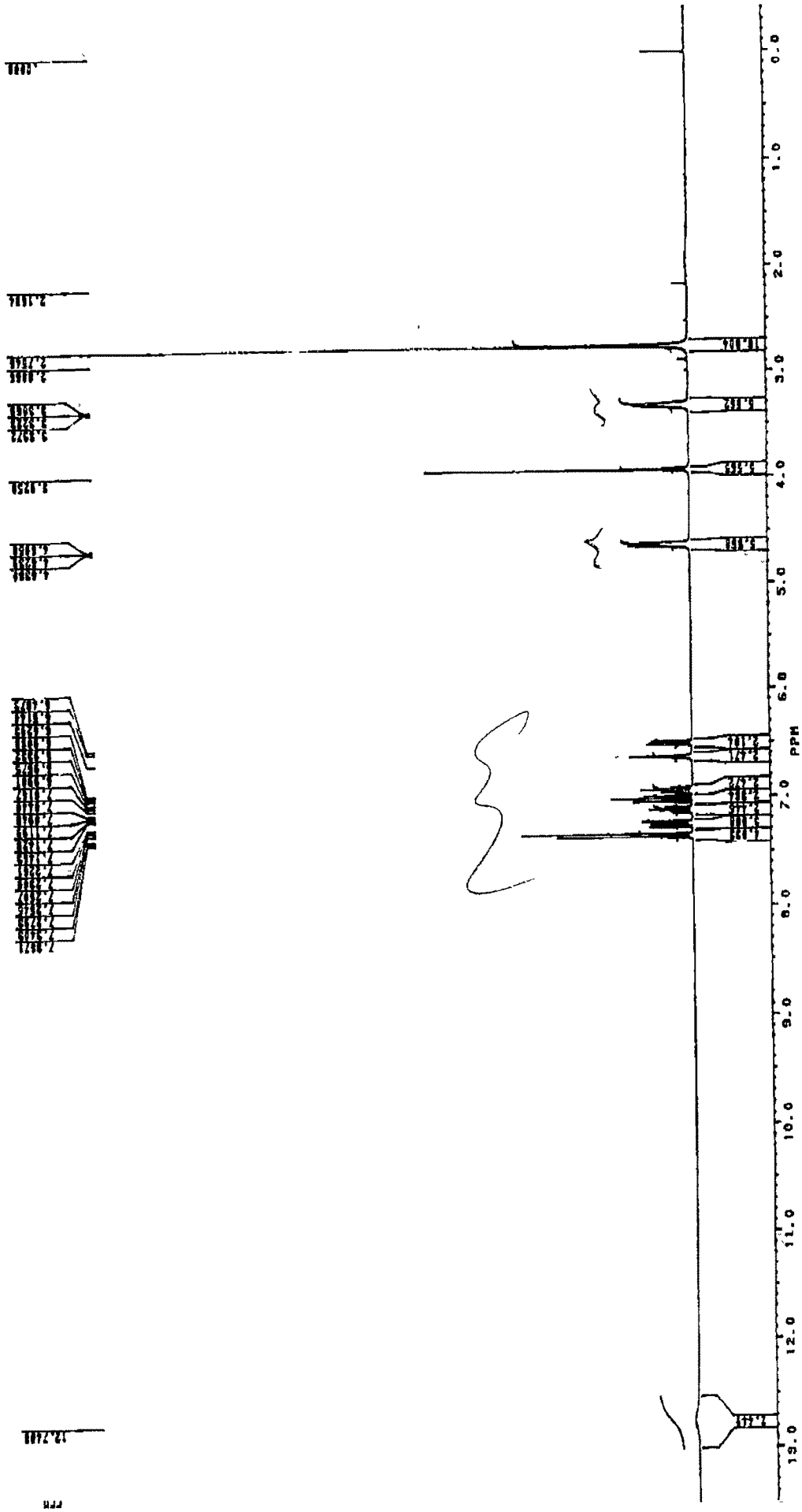

Figure 3.8 PMR spectrum of compound (51a)

plet for two protons (CH_2N-) at δ 3.28 and a singlet at δ 3.86 for ($ArCH_2$) group protons were observed. The characteristic multiplet for two protons of (-OCH_2) appeared at δ 4.66-4.69. The signals at δ 6.50-7.37 can be explained as follows: δ 6 50-6.53 (d, 1H, Ar-3-C*H*), 6.59 (b, 1H, ArN*H*), 6.92-6.97 (m, 1H, Ar-5-C*H*), 6.99-7.04 (m, 1H, Ar-4'-C*H*), 7.10-7.16 (m,1H, Ar-4-C*H*), 7.20-7.23 (d, 1H, Ar-6-C*H*) and 7.34-7.37 (d, 2H, Ar-3'-C*H*, Ar-5'-C*H*). Broad signal at δ 12.5 was also observed for the (N.*H*Cl).

1-[2-(1-Piperidino)]ethyl 2-(2,6-dichlorophenylaminophenyl)acetate hydrochloride (51c)

The compound (**50c**) was prepared by reacting 2-piperidinoethanol with diclofenac (**51**) as described above. The characteristic sharp bands appeared at 3271 and 1735 cm^{-1} for the NH and ester carbonyl stretching respectively, in its IR spectrum. The PMR spectrum showed a multiplet at δ 1.21-1.79 for six protons of three methylene groups of piperidine ring (3-CH_2, 4-CH_2 and 5-CH_2), a multiplet at δ 2.17-3.44 for the six protons of the three

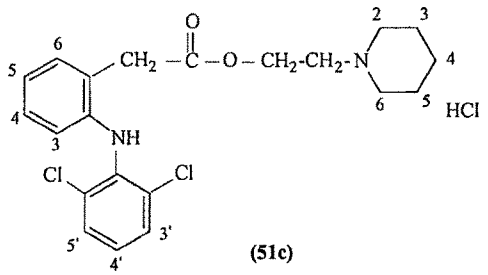

(51c)

methylene groups directly bonded to nitrogen (2-CH_2, 6-CH_2 and –CH_2N), a singlet at δ 3.87 for ($ArCH_2$) protons, and a multiplet for two protons of (OCH_2) at δ 4.70-4.73. The signals at δ 6.50-7.37 have been assigned to the various protons as follows: δ 6.50-6.52 (m, 1H, Ar-3-C*H*), 6.53 (b, 1H, ArN*H*), 6.92-6.97 (t, 1H, Ar-4-C*H*), 7.00-7.06 (t, 1H, Ar-4'-C*H*), 7.10-7.16 (m, 1H, Ar-4-C*H*), 7.21-7.23 (d, 1H, Ar-6-C*H*) and 7.36-7.38 (d, 2H, Ar-3'-C*H*, Ar-5'-C*H*) and a broad signal at δ 12.80 for (N.*H*Cl).

1-[2-(1-Pyrrolidino)]ethyl 2-(2,6-dichlorophenylaminophenyl)acetate hydrochloride (51d)

Diclofenac (**51**) was reacted with 2-pyrrolidinoethanol (**50d**) as described above to yield

the desired compound (**51d**). Intense sharp bands at 3351, 1741 cm^{-1} appeared in the IR spectrum of compound (**50d**) for the NH and ester carbonyl stretching. The PMR spectrum showed multiplets at δ 1.91-2.17 for the four protons (3-CH_2 and 4-CH_2) of the pyrolidine ring and at δ 2.56-3.73 for the six protons of the three methylene groups covalently bonded to nitrogen (2-CH_2, 5-CH_2 and CH_2N). Signals at δ 3.90 (s, 2H, ArCH_2), 4.66-4.69 (m, 2H, -OCH_2), 6.49-6.51 (d, 1H, Ar-3-C*H*), 6.58 (b, 1H, ArN*H*),

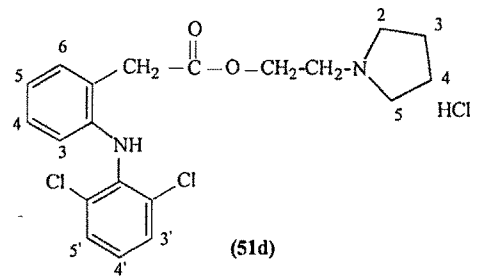

(51d)

6.91-6.96 (m, 1H, Ar-5-C*H*), 7.00-7.05 (m, 1H, Ar-4'-C*H*), 7.09-7.15 (m, 1H, Ar-4-C*H*), 7.22-7.25 (d, 1H, Ar-6-C*H*), 7.35-7 37 (d, 2H, Ar-3'-C*H* and Ar-5'-C*H*) and at δ 12.60 (b, 1*H*, .N*H*Cl) were also observed.

1-[2-(4-Morpholino)]ethyl 2-(2,6-dichlorophenylamino)phenylacetate hydrochloride (51e)

The compound (**51e**) was prepared by reaction of diclofenac (**51**) and 2-(4-morpholino)ethanol (**50e**) as described above for compound (**51a**). Its IR spectrum show-

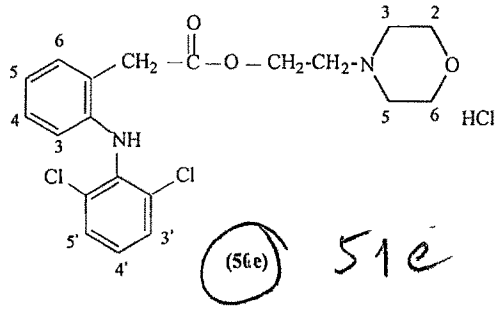

(51e) 51e

ed intense sharp bands at 3348 and 1738 cm^{-1} for the NH and ester carbonyl stretching respectively. The PMR spectrum showed signals at δ 2.65 (t, 2H, -CH_2N), 3.23-3 41(m, 4H, N(CH_2)$_2$), 3.77-4.21 (m, 4H ,CH_2-O-CH_2), 4.67 (s, 2H, ArCH_2) and 4.72-4.75 (m,

2H, O-CH_2). The signals at δ 6.48-6.49 (d, 1H, Ar-3-C*H*), 6.58 (b, 1H, ArN*H*), 6 92-6.97 (m, 1H, Ar-5-C*H*), 7.01-7.07 (m, 1H, Ar-4'-C*H*), 7.10-7.16 (m, 1H, Ar-4-C*H*), 7.22-7.25 (d, 1H, Ar-6-*H*), 7.36-7.37 (d, 2H, Ar-3'-C*H* and Ar-5'-C*H*) and 13.30 (b, 1H, .N*H*Cl) were also observed in its PMR spectrum.

3.1.5 ATTEMPTED SYNTHESIS OF AMINOALCOHOL ESTER DERIVATIVES OF INDOMETHACIN

Indomethacin (**54**), an indole acetic acid derivative[107] was introduced in the year 1963, for the treatment of rheumatoid arthritis and related disorders. Although indomethacin is used widely, its gastrointestinal toxicity often limits its use.

In order to make its aminoalcohol esters indomethacin (**54**) was reacted with thionyl chloride followed by its reaction with 2-dimethylaminoethanol (**50a**) as described in Method-A for diclofenac, to obtain an oily residue on processing. The oily residue on conversion to hydrochloride salt offered compound (**55a**), as an unusual product. It showed an intense peak at 1731 cm^{-1} in the IR spectrum for the ester (C=O) group (Figure 3.9). PMR spectrum gave signals at δ 2.94 (s, 6H, N (CH_3)$_2$), 3.47-3.50 (m, 2H, NCH_2), 4.82-4.85 (m, 2H, OCH_2), 7.43-7.46 (d, 2H, Ar-3-C*H* and Ar-5-C*H*-) and 8.02-

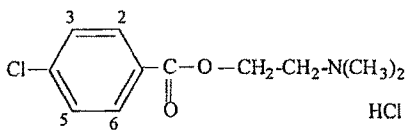

(55a)

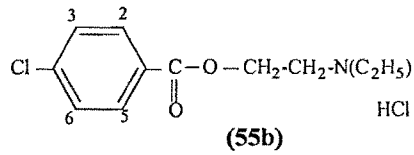

(55b)

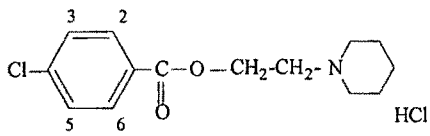

(55c)

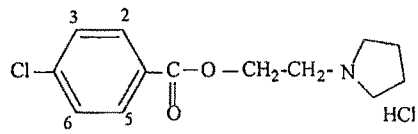

(55d)

8.05 (d, 2H, Ar-2-C*H* and Ar-6-C*H*) (Figure 3.10). Similarly, when 2-diethylamino-ethanol (**50b**) was reacted as above, compound (**55b**) was obtained. The compound (**55b**) showed band at 1727 cm^{-1} in its IR spectrum. Signals appeared at δ 1.44 (t, 6H, N(CH_2CH_3)$_2$), 3.19-3.24 (q, 4H, N(CH_2CH_3)$_2$, 3.41-3.45 (m, 2H, -CH_2N), 4.83-4.85 (m, 2H, -OCH_2), 7.43-7.46(d, 2H, Ar-3-C*H* and Ar-5-C*H*-) and 7.97-8.04 (d, 2H, Ar-2-C*H* and Ar-6-C*H*) in its PMR spectrum. In order to confirm the formation of 4-chlorobenzo-

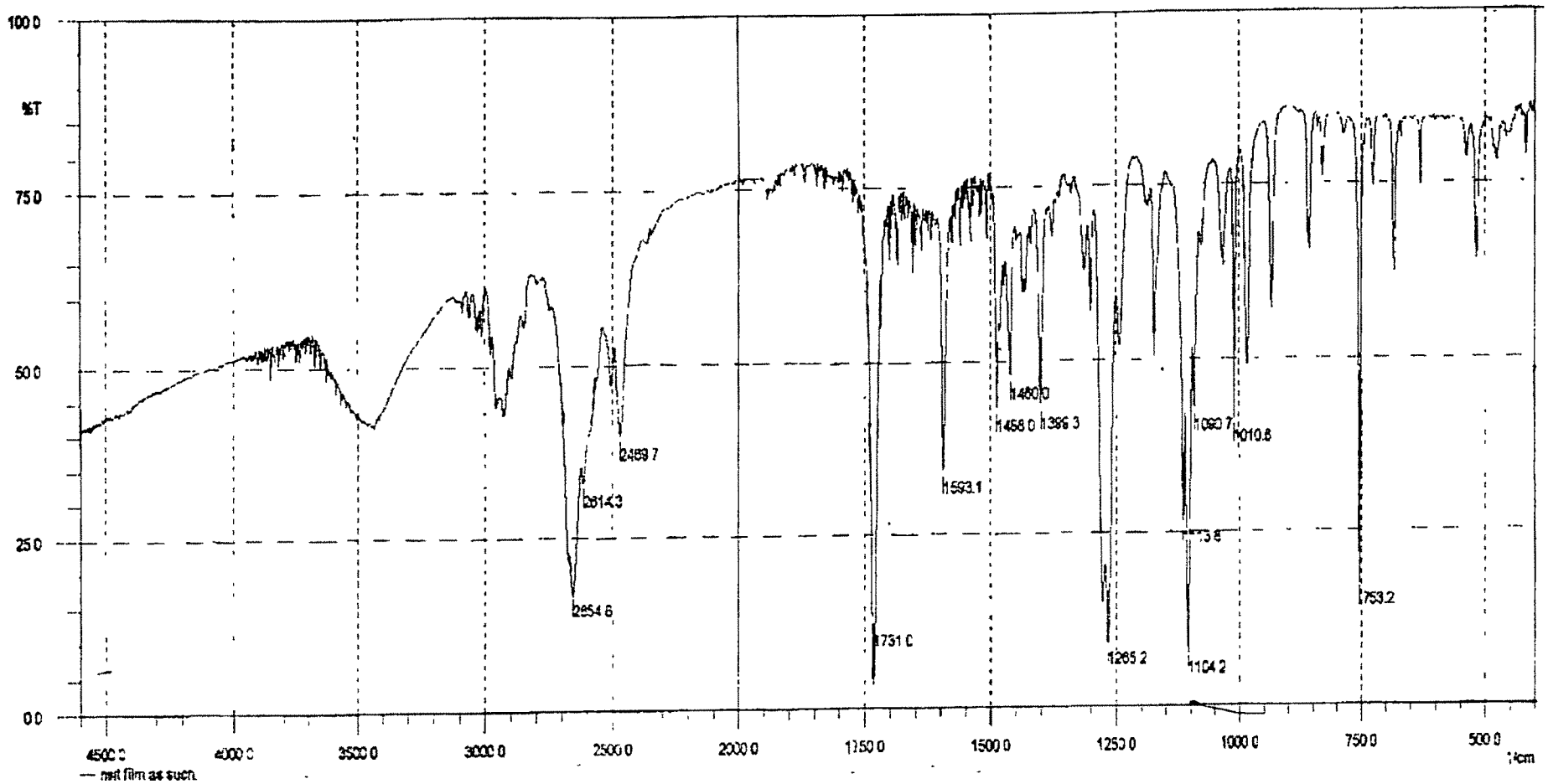

Figure 3.9 IR spectrum of compound (55a)

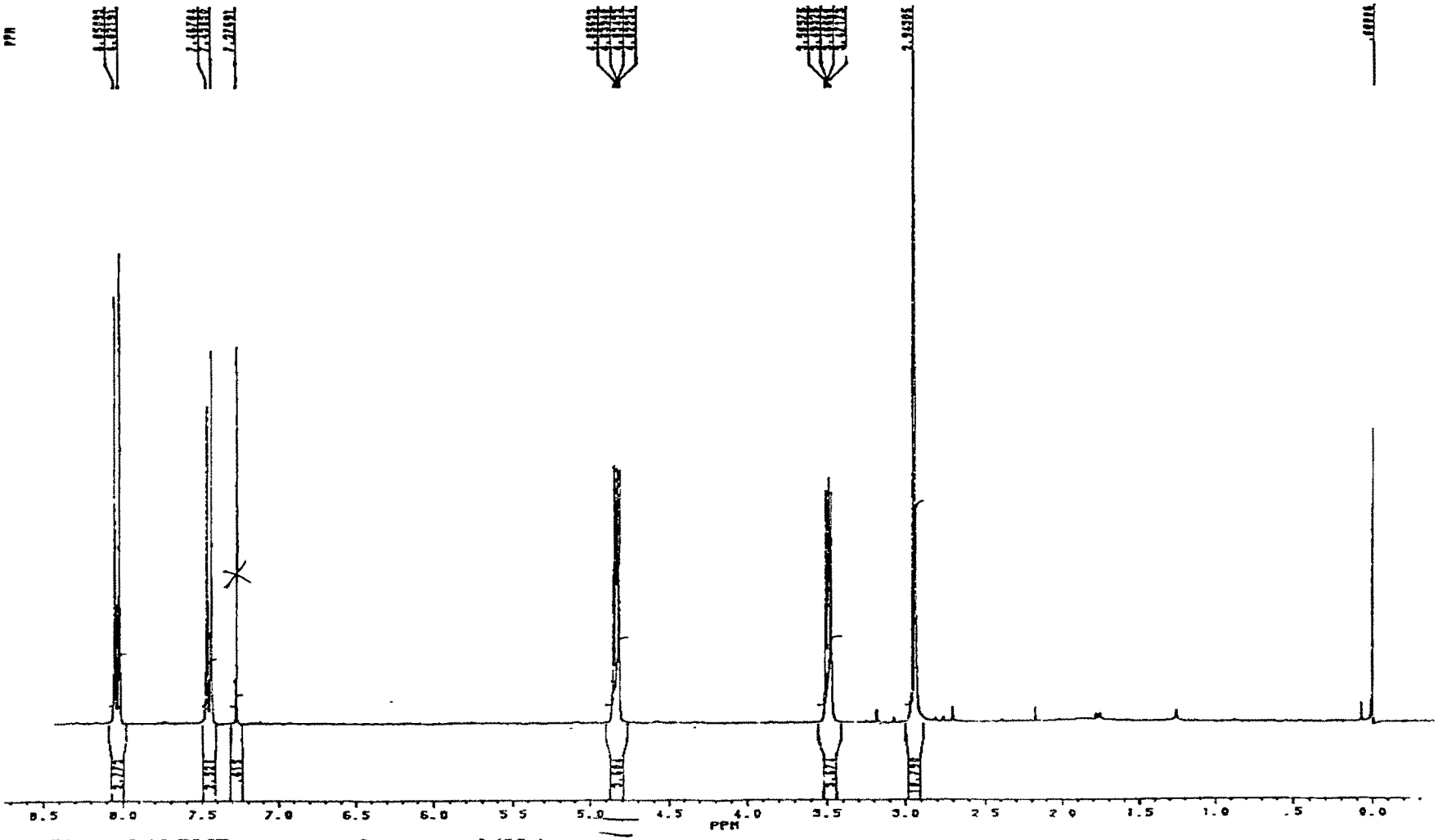

Figure 3.10 PMR spectrum of compound (55a)

ate esters, 1-hydroxyethylpiperidine (**50c**) and 1-hydroxyethylpyrrolidine (**50d**) were also reacted with indomethacin (**54**) in a similar fashion to afford the two esters (**55c and 55d**). The esters (**55c and 55d**) showed the characteristic absorption bands at 1727 and 1739 cm^{-1}, respectively, in their IR spectra. Formation of these products (**55a-d**) could be explained as shown in Scheme-V:

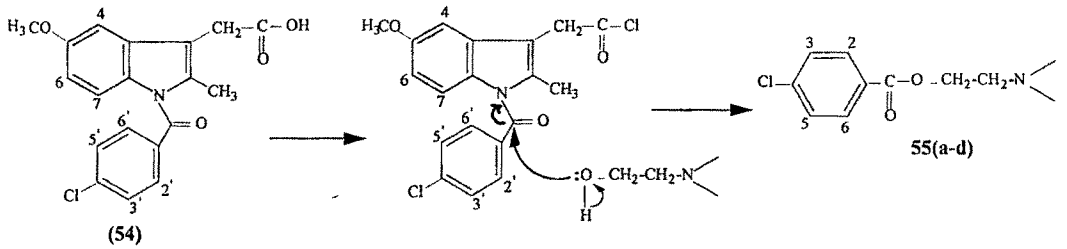

Scheme-V

After failing to acquire the desired aminoesters of indomethacin (**54**) by the Method-A, Method-B as described for diclofenac (**51**) was also tried. Unfortunately, here again same unusual products (**55a-d**) were obtained on reaction with different amino alcohols. After this unsuccessful endeavor of obtaining the desired aminoesters, DCC method (Method-E) as described for diclofenac (**51**) was adopted for indomethacin (**54**) also. The reaction mixture on processing offered a dark colored residue showing a number of spots in TLC. The mixture could not be salvaged by any means.

3.1.6. SYNTHESIS OF AMINOESTER DERIVATIVES OF INDOMETHACIN

Ultimately, Method-F as described for diclofenac (**51**) was followed for the synthesis of derivatives of indomethacin (**54**). The derivatives (**54a-e**) were found to be unstable in the form of hydrochloride salts as gauged by development of dark color of the products, and absence of ester (C=O) bands in their IR spectra. Hence, the derivatives (**54a-e**) were characterized and preserved as oils for further studies. Scheme-IV was followed for the synthesis of these derivatives (**54a-e**).

2-Dimethylaminoethyl 1-(4-chlorobenzoyl)-5-methoxy-2-methyl-1*H*-indole-3-acetate (54a)

Reacting 2-dimethylaminoethanol (**50a**) and indomethacin (**54**) as per the Scheme-IV yielded the compound (**54a**). IR spectrum of **54a** showed a charcteristic peak for the

ester carbonyl stretching at 1733 cm^{-1}. The PMR spectrum showed signals at δ 2 31 (s, 6H, $N(CH_3)_2$), 2.40 (s, 3H, Ar-CH_3), 2.63-2.69 (m, 2H, CH_2N), 3.65 (s,2H, Ar-CH_2), 3.80

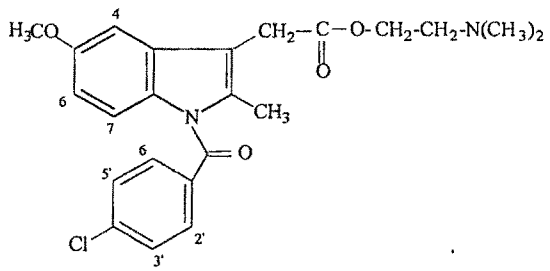

(54a)

(s, 3H, Ar-OCH_3), 4.24-4.26 (m, 2H, -OCH_2), 6.64-6.68 (m, 1H, Ar-6-C*H*), 6.81-6.87 (d, 1H, Ar-7-C*H*), 6.94-6.95 (d, 1H, Ar-4-C*H*), 7.47-7.48 (d, 2H, Ar-3'-C*H* and Ar-5'-C*H*) and 7.63-7.67(d, 2H, Ar-2'-C*H* and Ar-6'-C*H*).

2-Diethylaminoethyl 1-(4-chlorobenzoyl)-5-methoxy-2-methyl-1*H*-indole-3-acetate (54b)

The compound (**54b**) was prepared by reacting indomethacin (**54**) and 2-diethylaminoethanol (**50b**) as described for the compound (**54a**). Its IR spectrum showed

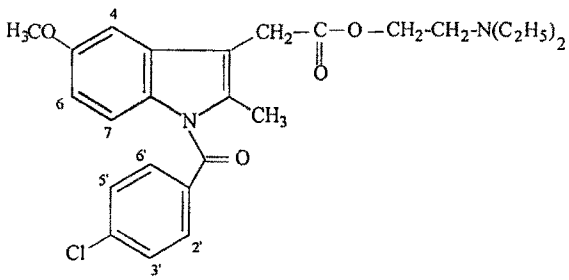

(54b)

the ester carbonyl stretching peak at 1733 cm^{-1}. In the PMR spectrum signals were observed at δ 1.11(t, 6H, $N(CH_2CH_3)_2$), 2.35 (s, 3H, Ar-C*H*3), 2.73-2.85(q, 4H, $N(CH_2CH_3)_2$), 2.98 (t, 2H,-CH_2N), 3.64 (s, 2H, Ar-CH_2), 3.78 (s, 3H, Ar-OCH_3), 4.21-4.26 (m, 2H, OCH_2), 6.60-6.65 (m, 1H, Ar-6-C*H*), 6.84-6.88 (d, 1H, Ar-7-C*H*), 6.93-6.95(d, 1H, Ar-4-C*H*), 7.43-7.48(d, 2H, Ar-3'-C*H*, Ar-5'-C*H*) and 7.60-7.66(d, 2H, Ar-2'-C*H*, Ar-6'-C*H*).

1-[2-(1-Piperidino)]ethyl 1-(4-chlorobenzoyl)-5-methoxy-2-methyl-1*H*-indole-3-acetate (54c)

Indomethacin (**54**) and 2-piperidinoethanol (**50c**) were reacted as described above to yield compound (**54c**). The IR spectrum showed the characteristic ester carbonyl peak at 1733 cm^{-1}. The PMR spectrum of the compound (**54c**) showed signals for the protons of the three methylene groups of the piperidine ring at δ 1.25-1.68 (m, 6H, b-C*H*$_2$, c-C*H*$_2$, d-C*H*$_2$), 2.34 (s, 3H, Ar-C*H*$_3$), 2.55-2.77 for the four protons of the methylene group of the piperidine ring bonded to nitrogen (m, 4H, a-C*H*$_2$, e-C*H*$_2$), 2.93 (t, 2H, -C*H*$_2$N), 3 60 (s, 2H, Ar-C*H*$_2$), 3.79 (s, 3H, Ar-OC*H*$_3$) and the characteristic multiplet for (OC*H*$_2$) appeared at 4.29-4.55 (m, 2H). The aromatic protons gave signals at 6.65-6.74 (m, 1H,

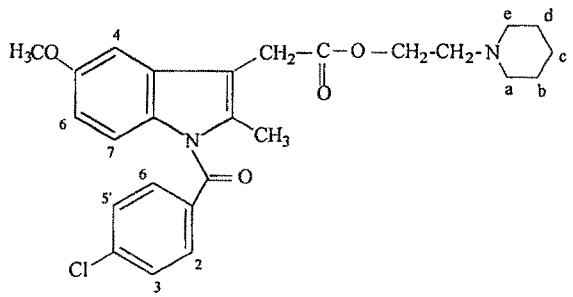

(54c)

Ar -6-C*H*), 6.85-6.93 (d, 1H, Ar-7-C*H*), 7.01-7.02 (d, 1H, Ar-4-C*H*), 7.36-7.45 (d, 2H, Ar-3'-C*H*, Ar-5'-C*H*) and 7.92-7.97 (d, 2H, Ar-2'-C*H*, Ar-6'-C*H*).

1-[2-(1-Pyrrolidino)]ethyl 1-(4-chlorobenzoyl)-5-methoxy-2-methyl-1*H*-indole-3-acetate (54d)

Compound (**54d**) was prepared by reacting indomethacin (**54**) with 2-pyrrolidinoethanol as described for the above compound (**54c**). The characteristic peak for the ester carbonyl stretching appeared at 1733 cm^{-1} in the IR spectrum. The PMR spectrum of the compound (**54d**) showed a signal at δ 1.90-1.95 for the two methylene protons of the pyrrolidine ring (m, 4H, b-C*H*$_2$, c-C*H*$_2$), 2.33 (s, 3H, Ar-C*H*$_3$), and the signal for the protons of the methylene group of pyrrolidine ring attached to the nitrogen appeared at 2.71-2.99 (m, 4H, a-C*H*$_2$, d-C*H*$_2$), 3.16 (t, 2H, C*H*$_2$N), 3.60 (s, 2H, Ar-C*H*$_2$), 3.81(s, 3H,

Ar-OC*H*$_3$) and 4.52-4.58 (t,2H, OC*H*$_2$). The aromatic protons gave signals at δ 6.68-6.69

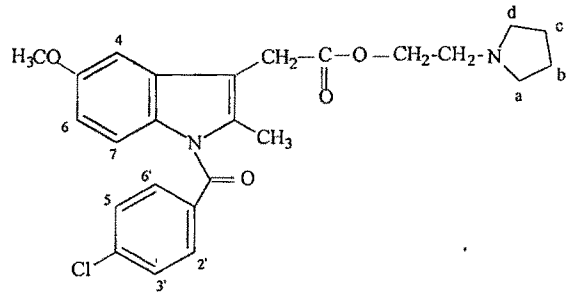

(54d)

(m, 1H, Ar-6-C*H*), 6.72-6.86 (d, 1H, Ar-7-C*H*), 6.90-7.02 (d, 1H, Ar-4-C*H*), 7.28-7.37 (d, 2H, Ar-3'-C*H*, Ar-5'-C*H*) and 7.92-7.97 (d, 2H, Ar-2'-C*H*, Ar-6'-C*H*).

1-[2-(4-Morpholino)]ethyl 1-(4-chlorobenzoyl)-5-methoxy-2-methyl-1*H*-indole-3-acetate (54e)

The compound (**54e**) was obtained by reacting indomethacin (**54**) and 2-(4-morpholino)ethanol as per the Scheme-IV. The compound (**54e**) showed an ester carbon-

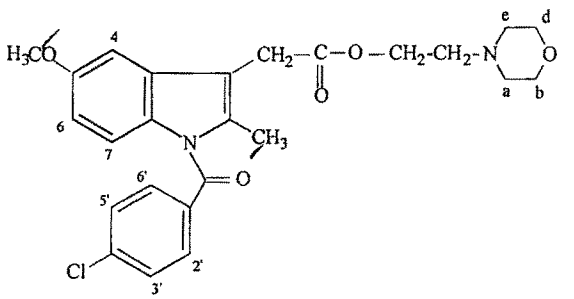

(54e)

yl stretching at 1733 cm^{-1} in the IR spectrum (Figure 3.11). The PMR spectrum showed singlet at δ 2.40 (s, 3H, Ar-CH$_3$). Protons for the three methylene groups appeared as multiplet at δ 2.43-2.75 (m, 6H, a-C*H*2, e-CH$_2$ and C*H*$_2$N). Signals also appeared at δ 3.57-3.77 (m, 4H, b-C*H*$_2$, d-C*H*$_2$), 3.68 (s, 2H, Ar-C*H*$_2$), 3.83 (s, 3H, Ar-OC*H*$_3$) and 4.24-4.27 (m, 2H, O-C*H*$_2$). The aromatic protons gave signals at 6.64-6.68 (m, 1H, Ar-6-C*H*), 6.83-6.86 (d, 1H, Ar-7-C*H*), 6.95-6.96 (d, 1H, Ar-4-C*H*), 7.46-7.49 (d, 2H, Ar-3'-C*H*, Ar-5'-C*H*) and 7.65-7.67 (d, 2H, Ar-2'-C*H*, Ar-6'-C*H*) (Figure 3.12).

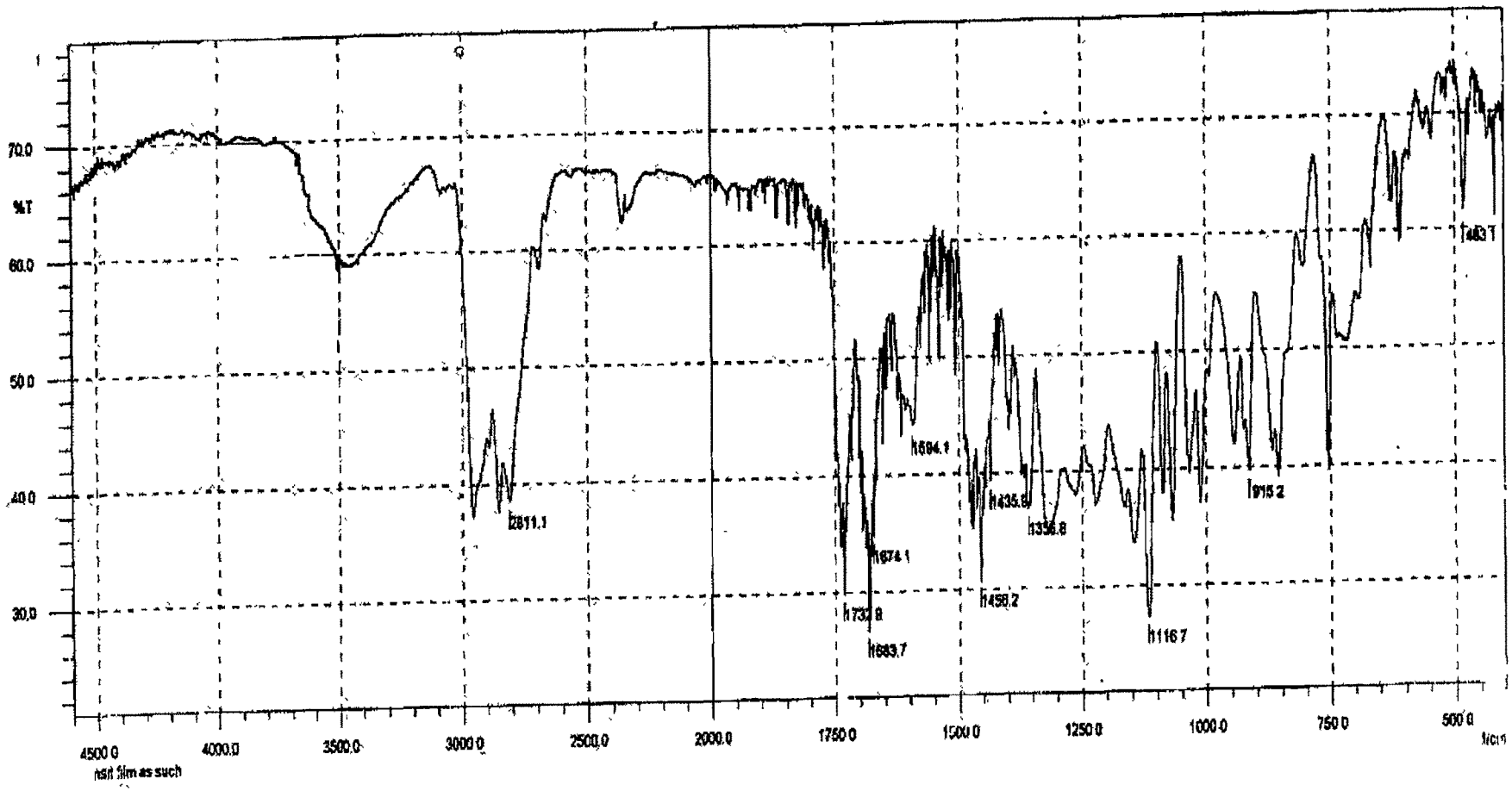

Figure 3.11 IR spectrum of compound (54e)

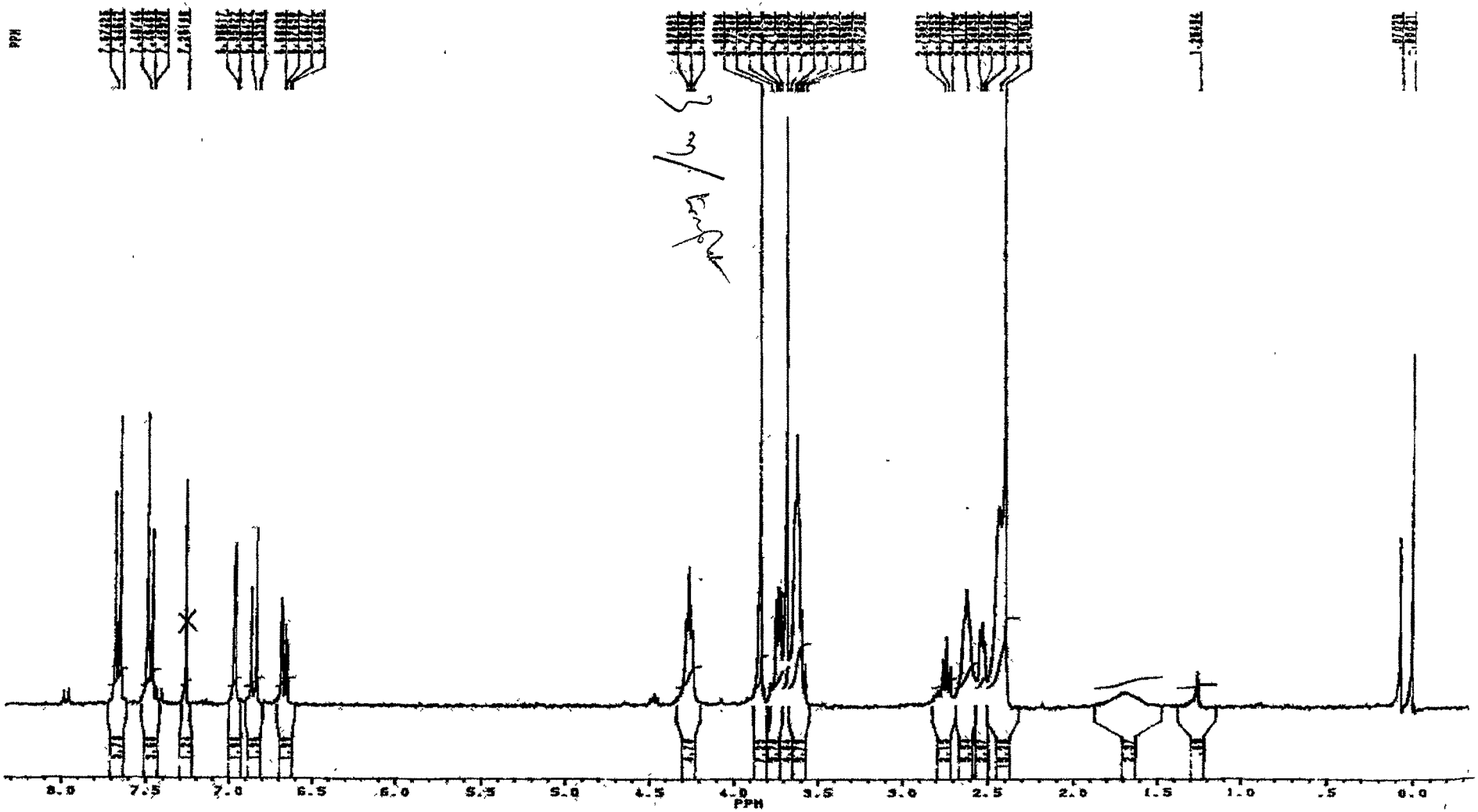

Figure 3.12 PMR spectrum of compound (54e)

3.1.7. AMINOALCOHOL ESTER DERIVATIVES OF ASPIRIN

Despite the introduction of many new drugs, aspirin (**56**) is still the most widely prescribed analgesic, antipyretic and anti-inflammatory agent[108]. It is being used as a standard for comparison and evaluation of other NSAIDs but, it too suffers from the gastrointestinal side effects. So, it was one of the drugs chosen for the present work.

2-Dimethylaminoethyl 2-acetoxybenzoate hydrochloride (56a)

Aspirin (**56**) on treatment with thionyl chloride in dry benzene yielded the acid chloride, which was reacted with excess of 2-dimethylaminoethanol (**50a**) under basic conditions i.e. in presence of anhydrous potassium carbonate in dry chloroform. During the work up of the reaction mixture excess of the amino alcohol (**50a**) was removed by successive washings with cold water to yield an oily residue, which was converted to the hydrochlo-

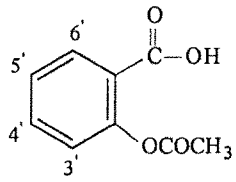

(56)

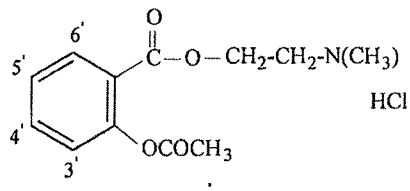

(56a)

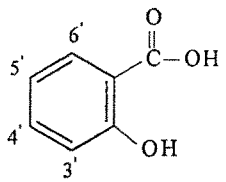

(57)

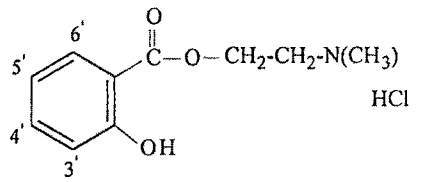

(57a)

ride salt by passing dry hydrogen chloride gas through the solution of the oil in dry isopropyl ether. Unfortunately, the product got deacetylated during the course of reaction/processing as it was identified to be **57a** on the basis of spectral evidences. IR spectrum of the product showed an intense peak at 1678 cm^{-1} which corresponded for the (Ar-C=O) stretching (Figure 3.13). Its PMR spectrum showed a singlet at δ 2.97 for ($N(CH_3)_2$), a triplet at δ 3.58 for ($-CH_2N$) and a triplet at δ 4.88 for (OCH_2) protons. Multiplet for the four aromatic protons appeared at δ 6.87-7.89. A sharp singlet at δ 10.40 was observed for the (-OH) proton and a broad singlet at δ 12.81 for (.NHCl) also appeared in the PMR spectrum (Figure 3.14). The compound (**57a**) showed λ_{max} at 306

nm in its UV spectrum, which corresponded with the UV spectrum of salicylic acid (**57**) The product (**57a**) was acetylated finally with acetic anhydride in presence of sulphuric acid and then converted to hydrochloride salt (**56a**) by passing hydrogen chloride gas into the base (Scheme-VI). The compound (**56a**) showed a UV maximum at 279 nm and

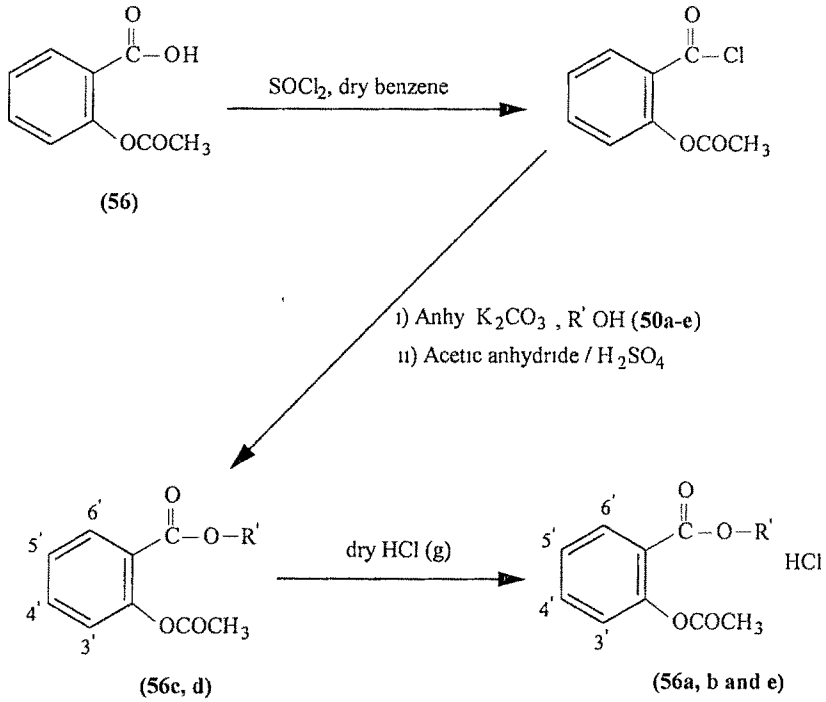

Scheme-VI

the IR spectrum showed two characteristic intense peaks at 1763 for (-O-COC*H*$_3$) and 1736 cm^{-1} for (Ar-COO-) (Figure 3.15). Its PMR spectrum showed signals at δ 2.35 (s, 3H, OCOC*H*$_3$), 2.60 (s, 6H, N (C*H*$_3$)$_2$), 3.48 (t, 2H, C*H*$_2$N), 4.75 (t, 2H, OC*H*$_2$) and the aromatic protons appeared at δ 7.08-7.15 (d, 1H, Ar-3'-C*H*), 7.29- 7.38 (m, 1H, Ar-5'-C*H*), 7.55-7.65 (m, 1H, Ar-4'-C*H*), 8.02-8.08 (d, 1H, Ar-6'-C*H*) and 12.60 (b, 1H, .N*H*Cl) (Figure 3.16).

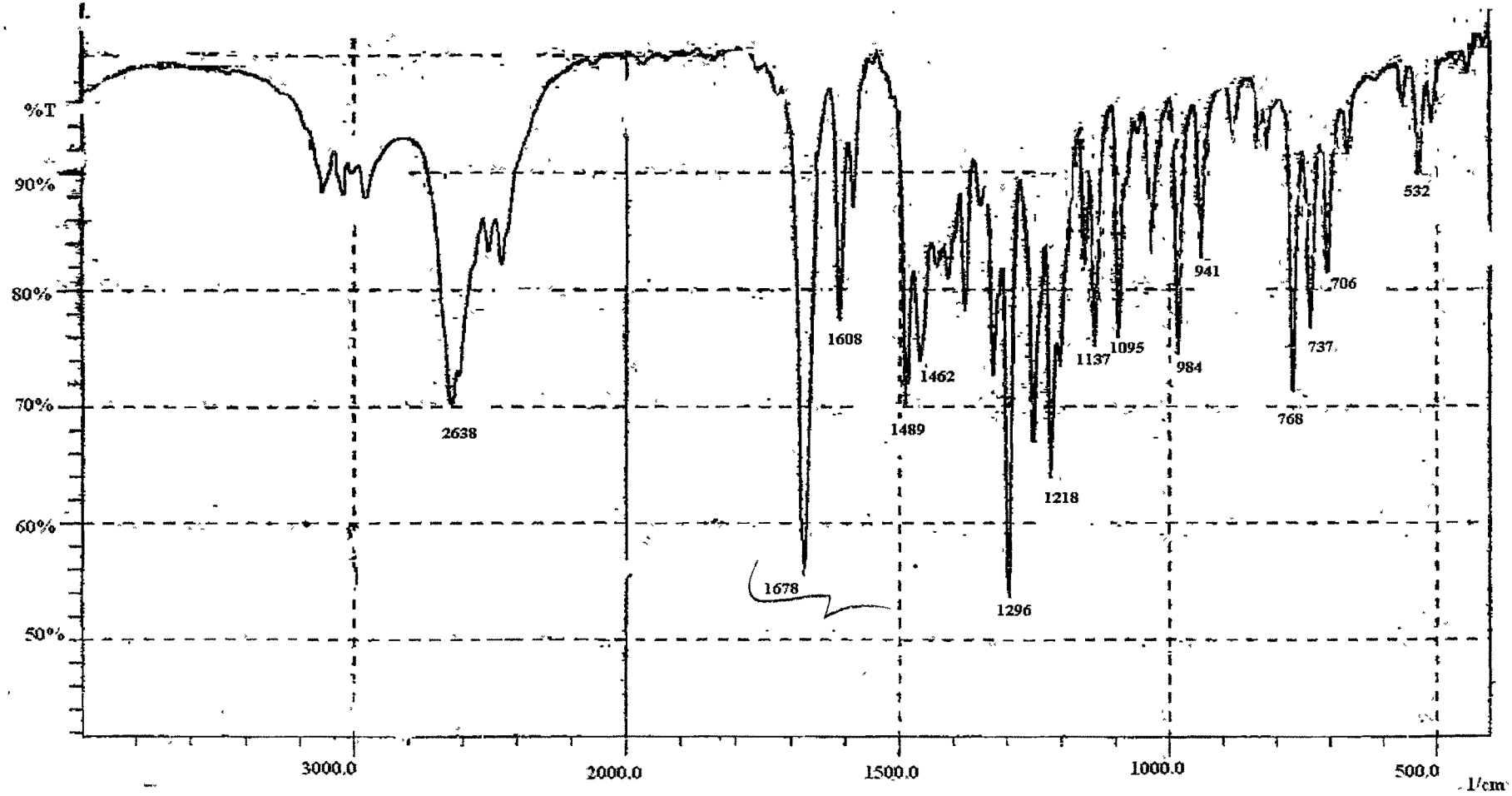

Figure 3.13 IR spectrum of compound (57a)

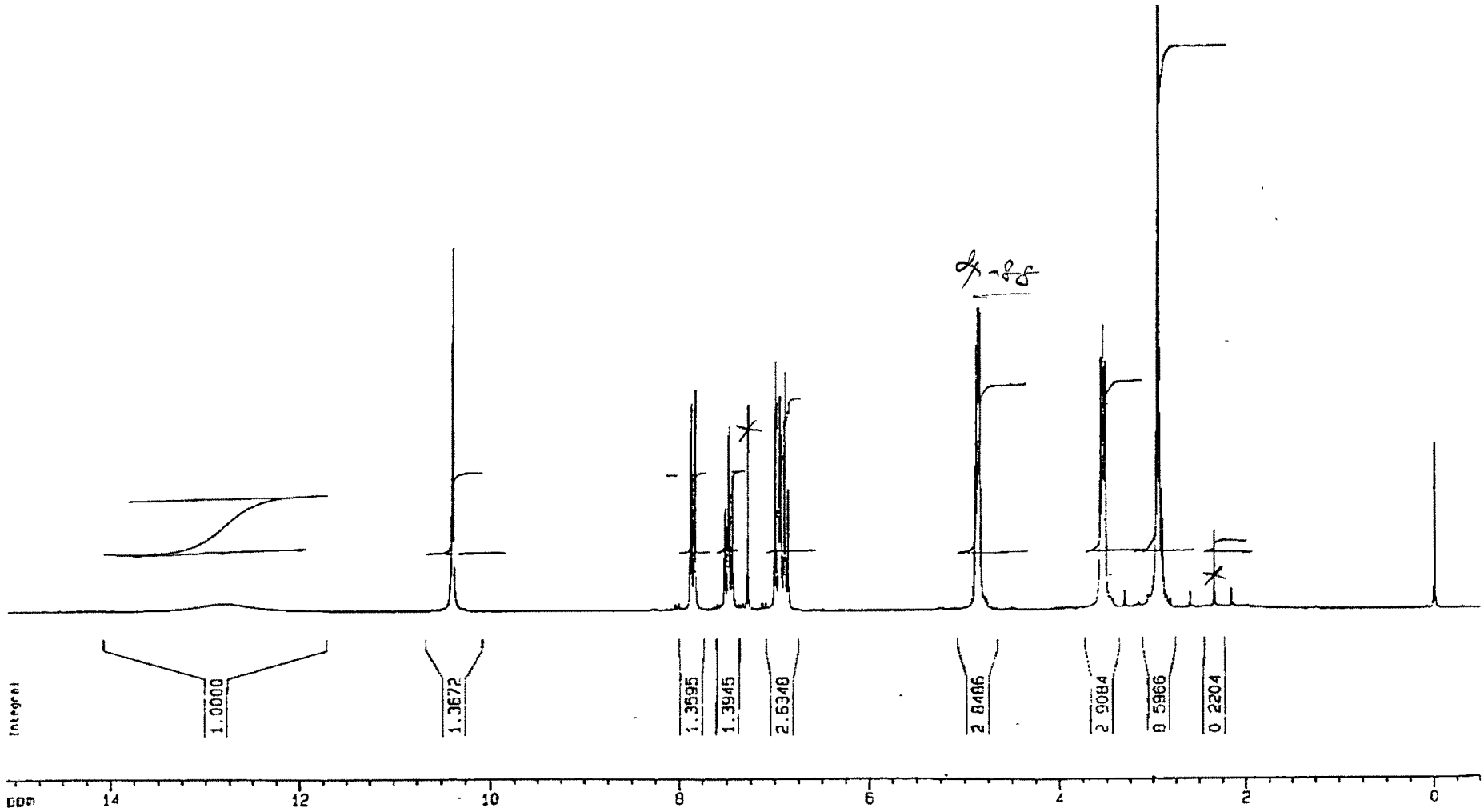

Figure 3.14 PMR spectrum of compound (57a)

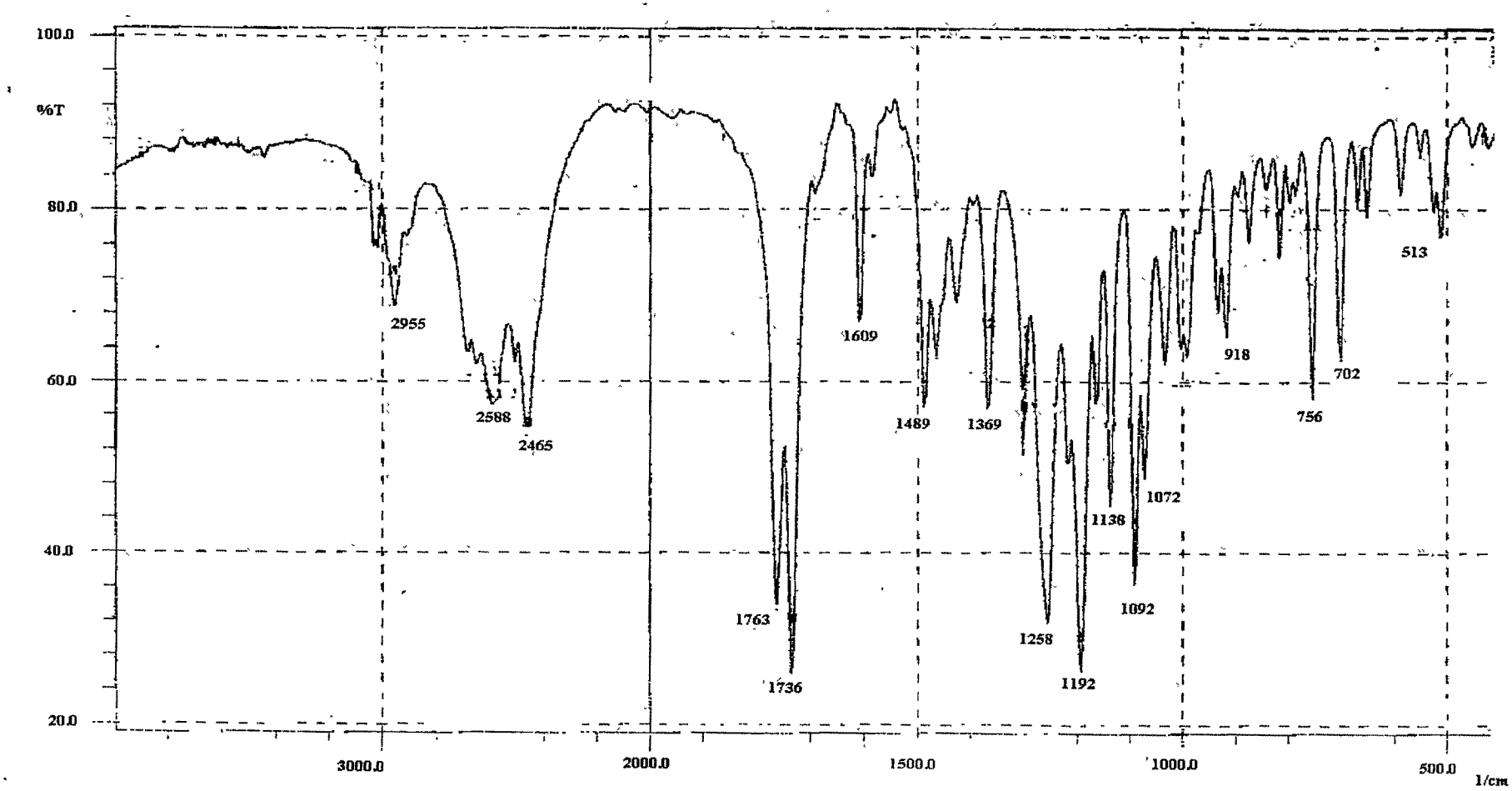

Figure 3.15 IR spectrum of compound (56a)

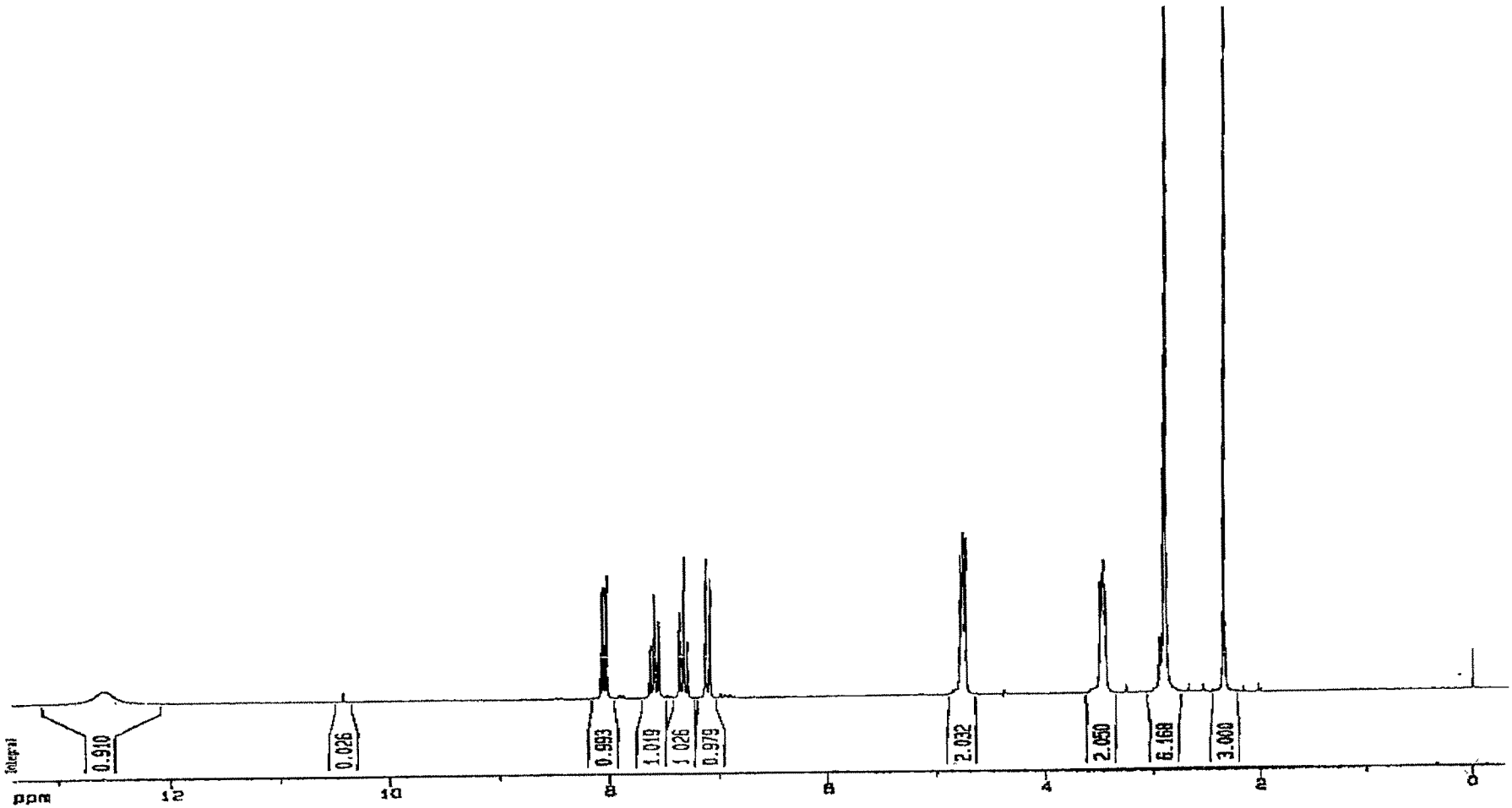

Figure 3.16 PMR spectrum of compound (56a)

2-Diethylaminoethyl 2-acetoxybenzoate hydrochloride (56b)

The synthesis and work up of the reaction between aspirin (**56**) and 2-diethylamino-ethanol (**50b**) was carried out in the same fashion as described for the compound (**56a**) to yield compound (**56b**). The characteristic ester carbonyl stretchings appeared at 1765 and

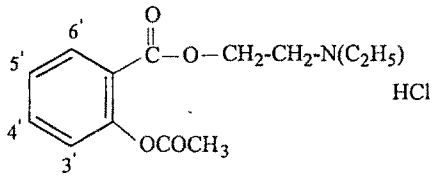

(56b)

1724 cm^{-1} in its IR spectrum. The PMR spectrum gave signals at δ 1.43 (t, 6H, $N(CH_2CH_3)_2$), 2.36 (s, 3H, $COCH_3$), 3.15-3.29 (m, 4H, $N(CH_2CH_3)_2$) and 3.38 (t, 2H, CH_2N). A characteristic triplet appeared at δ 4.85 for the (OCH_2) protons and the signals for the aromatic protons appeared at 7.11-7.15 (d, 1H, Ar-3'-C*H*), 7.30- 7.38 (m, 1H, Ar-5'-C*H*), 7.57-7.66 (m, 1H, Ar-4'-C*H*), 8.00-8.01 (d, 1H, Ar-6'-C*H*).

1-[2-(1-Piperidino)]ethyl 2-acetoxybenzoate hydrochloride (56c)

The compound (**56c**) was prepared by reacting aspirin (**56**) with 2-piperidinoethanol (**50c**) as described in Scheme-VI. The compound (**56c**) showed the characteristic sharp

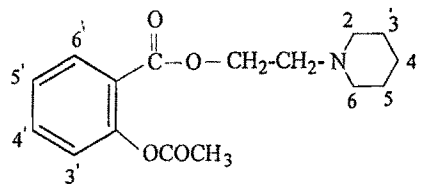

(56c)

intense peaks at 1769 and 1725 cm^{-1} in its IR spectrum. The PMR spectrum for the compound (**56c**) showed a multiplet at δ 1.72-1.76 for the methylene protons (3-CH_2, 4-CH_2 and 5-CH_2) of the piperidine ring, a singlet at 2.35 for ($COCH_3$) protons, a multiplet at 2.98-3.04 for the methylene protons (2-CH_2 and 6-CH_2), a triplet at 3.07 for (-CH_2N-) a characteristic triplet for (OCH_2) protons at 4.60. The aromatic protons appeared at

7.14-7.19 (d, 1H, Ar-3'-C*H*), 7.28-7.33 (m, 1H, Ar-5'-C*H*), 7.55-7.59 (m, 1H, Ar-4'-C*H*) and 7.98-8.00 (d,1H, Ar-6'-C*H*).

1-[2-(1-Pyrrolidino)]ethyl 2-acetoxybenzoate hydrochloride (56d)

Aspirin (**56**) was treated with 2-pyrrolidinoethanol (**50d**) as described above for compound (**56c**) to afford the desired compound (**56d**). Intense sharp bands were observed at 1769 and 1725 cm^{-1} in the IR spectrum of the compound (**56d**). The PMR spectrum

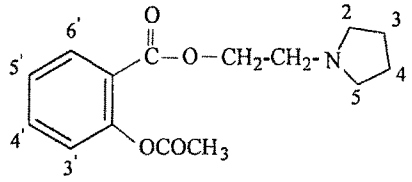

(56d)

showed a multiplet at δ 1.93-1.96 for the methylene protons (3-CH_2 and 4-CH_2) of the pyrrolidine ring system, at 2.35 (s, 3H, COCH_3), 3.04-3.07 (m, 4H, 2-CH_2, 5-CH_2), 3.21-3.27 (t, 2H, CH_2N) and 4.61 (t, 2H, OCH_2). The aromatic protons appeared at 7.09-7.11 (d, 1H, Ar-3'-C*H*), 7.28- 7.33 (m, 1H, Ar-5'-C*H*), 7.55-7.59 (m, 1H, Ar-4'-C*H*), and 8.00-8.02 (d, 1H, Ar-6'-C*H*).

1-[2-(4-Morpholino)]ethyl 2-acetoxybenzoate hydrochloride (56e)

The compound (**56e**) was synthesized by reacting aspirin (**56**) and 2-(4-morpholino) ethanol (**50e**) as described for compound (**56a**). Work up of the reaction mixture yielded

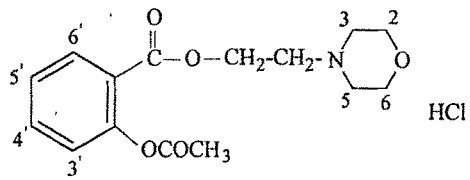

(56e)

the hydrochloride salt (**56e**). The IR spectrum of the compound (**56e**) showed intense bands at 1769 and 1722 cm^{-1}. The PMR spectrum of **56e** showed signals at 2 36 (s, 3H, COCH_3), 3.51 (t, 2H, CH_2N), 3.95-4.02 for the methylene protons of the morpholine ring

(m, 4H, 3-CH_2 and 5-CH_2), 4.29(t, 4H, 2-CH_2, 6-CH_2), 4.90 (t, 2H, OCH_2), 7.12-7.14 (d, 1H, Ar-3'-C*H*), 7.33-7.36 (m, 1H, Ar-5'-C*H*), 7.49-7.53 (m, 1H, Ar-4'-C*H*) and 7.94-7 96 (d, 1H, Ar-6'-C*H*). A broad signal appeared at δ 13.74 for the proton (.N*H*Cl).

3.1.8. AMINOALCOHOL ESTER DERIVATIVES OF KETOROLAC

2-Dimethylaminoethyl 5-benzoyl-2,3-dihydro-1*H*-pyrrolizine-1-carboxylate (58a)

Ketorolac (**58**), structurally related to heteroarylacetic acid derivatives with some desirable pharmacological features[109], also exhibits gastrointestinal side effects. Hence, it was chosen as one of the drugs for the proposed work.

Synthesis of the aminoalcohol esters of ketorolac (**58**) was tried as per the Scheme-I described for the compounds (**45a-f**). But, it was observed that upon treatment of ketorolac (**58**) with thionyl chloride in dry benzene, the solution turned dark brown within a few minutes and further addition of 2-dimethylaminoethanol (**50a**) to it and work up of the reaction mixture yielded a black sticky residue. Although IR spectrum of the reaction mixture showed peak for ester carbonyl but TLC showed many spots indicating the presence of degraded products. So, it was decided to synthesize the esters of ketorolac (**58**) through Method F (Scheme-IV) using PTC (Tetraethylammonium bromide). The aminoalcohol (**50a**) was treated with thionyl chloride to yield the choloro derivative (**53a**), which was reacted with ketorolac (**58**) using the catalyst in a biphasic alkaline medium. Work up of the reaction mixture yielded a yellow colored oil (**58a**).

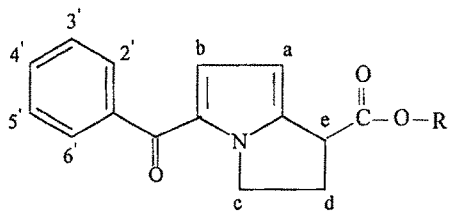

(58) R = H

(58a) R = CH_2-CH_2-N(CH_3)$_2$

When dry hydrogen chloride gas was passed through this solution of the oil in dry isopropyl ether a white-salt precipitated out which dissolved in no time and the solution turned black. Complete removal of the solvent under vacuum yielded a black sticky residue which, did not show any peak for the ester carbonyl stretching in the IR spectrum. Keeping this observation in mind the ester derivatives (**58a-e**) were

synthesized and preserved as oils without conversion to the hydrochloride salt. The compound (**58a**) showed the characteristic ester carbonyl stretching at 1733 cm^{-1} in the IR spectrum. The PMR spectrum showed signals at δ 1.2-1.3 (m, 2H, d-CH_2), 2.30-2.34 (s, 6H, N (CH_3)$_2$), 2.62-2.67 (t, 2H, CH_2N) and 2.75-2.95 (m, 3H, c-CH_2, e-C*H*). The characteristic multiplet for (-OCH_2) appeared at δ 4.42-4.62 and the signals for the aromatic protons were seen at δ 6.10-6.12 (d, 1H, Ar-a-C*H*), 6.79-6.81 (d, 1H, Ar-b-C*H*), 7.41-7.56 (m, 3H, Ar-3'-C*H*, Ar-4'-C*H*, Ar-5'-C*H*) and 7.79-7.81 (d, 2H, Ar-2'-C*H*, Ar-6'-C*H*).

2-Diethylaminoethyl 5-benzoyl-2,3-dihydro-1*H*-pyrrolizine-1-carboxylate (58b)

The compound (**58b**) was synthesized by the procedure as described above for compound (**58a**) by reacting ketorolac (**58**) with 2-diethylaminoethanol (**50b**). The IR spectrum of the compound (**58b**) showed the characteristic peak at 1733 cm^{-1}. The PMR

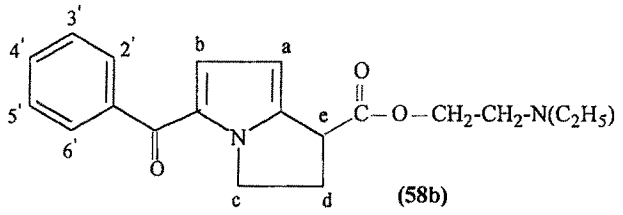

(58b)

spectrum of (**58b**) showed signals at δ 1.02-1.06 (t, 6H, N(CH$_2$CH_3)$_2$), 1.22-1.26 (m, 2H, d-CH$_2$), 2.58-2.63 (m, 4H, N(CH_2CH$_3$)$_2$), 2.76 (t, 2H, CH_2N), 2.92-2.94 (m, 2H, c-CH$_2$), 3.00-3.02 (m, 1H, e-C*H*), 4 35-4.62 (m, 2H, OCH_2), 6.10-6.12 (d, 1H, Ar-a-C*H*), 6.81-6.82 (d, 1H, Ar-b-C*H*), 7.42-7.47 (m, 3H, Ar-3'-C*H*, Ar-4'-C*H*, Ar-5'-C*H*) and 7.77-7.82 (d, 2H, Ar-2'-C*H*, Ar-6'-C*H*).

1-[2-(1-Piperidino)]ethyl 5-benzoyl-2,3-dihydro-1*H*-pyrrolizine-1-carboxylate (58c)

Ketorolac (**58**) was reacted with 2-piperidinoethanol (**50c**) as described in Scheme-IV to yield to compound (**58c**) as a yellow oil. Intense sharp band at 1733 cm^{-1} was observed in the IR spectrum. The PMR spectrum showed multiplet at δ 1.25-1.30 for (2H, d-CH_2), a triplet at 1.58-1.81 (2H, 4-CH_2) and a multiplet at 1.83-1.89 (4H, 3-CH_2, 5-CH_2). Signals at δ 2.75-2.93 (m, 3H) and 2.97-3.06 (m, 6H) were observed for (e-C*H*, *c*-CH_2,

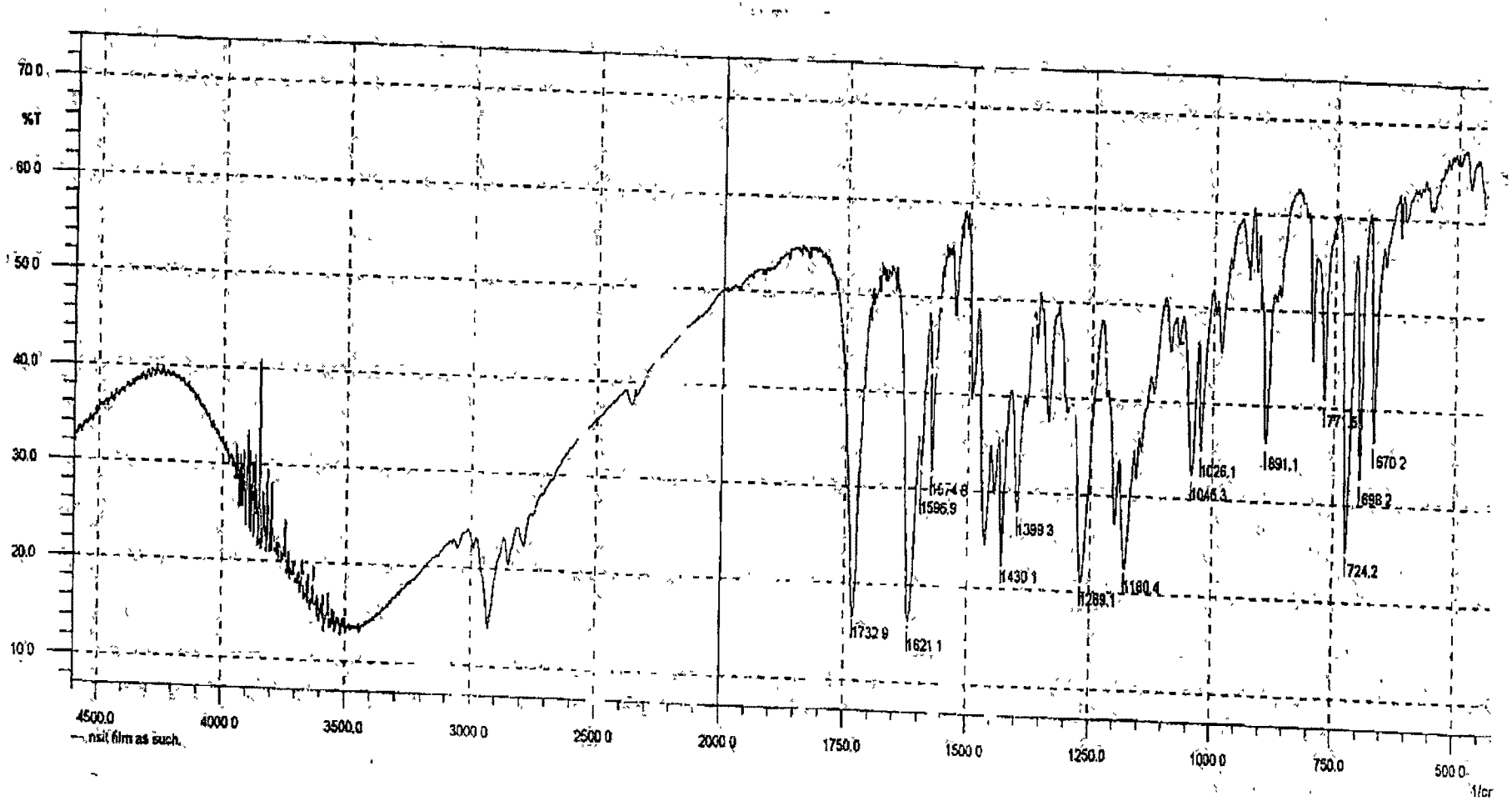

Figure 3.17 IR spectrum of compound (58b)

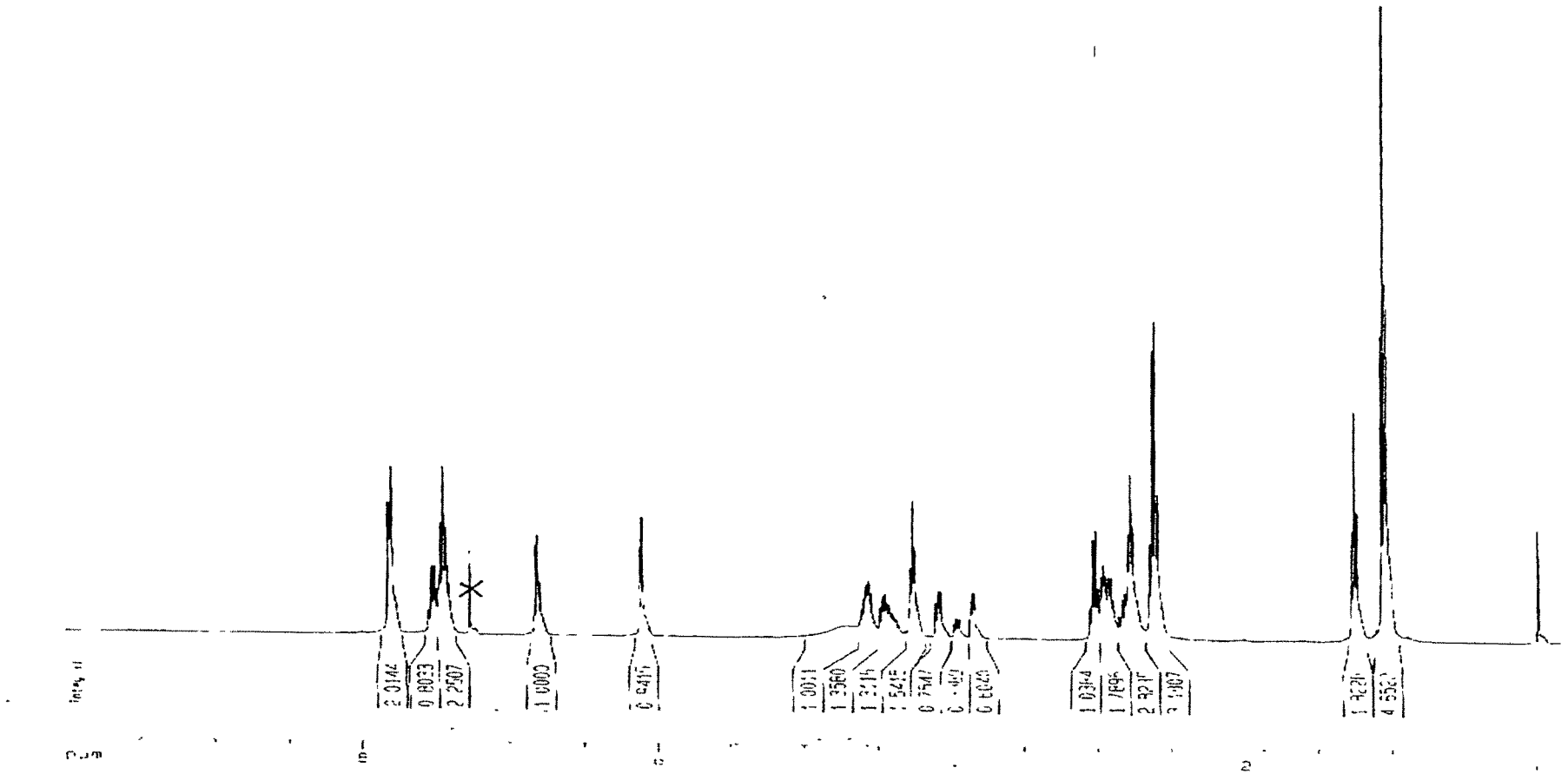

Figure 3.18 PMR spectrum of compound (58b)

CH_2N, 6-CH_2 and 2-CH_2). The multiplet for (OCH_2) appeared at δ 4.3-4.5 and signals for

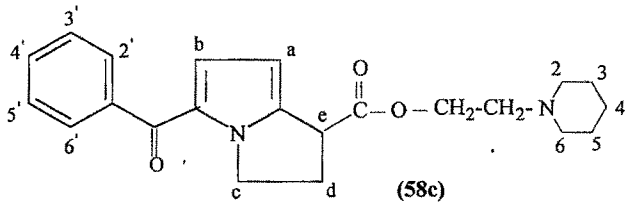

aromatic protons appeared at 6.10-6.12 (d, 1H, Ar-a-C*H*), 6.79-6.81 (d, 1H, Ar-b-C*H*), 7.38-7.51 (m, 3H, Ar-3'-C*H*, Ar-4'-C*H*, Ar-5'-C*H*) and 7.77-7.81 (d, 2H, Ar-2'-C*H*, Ar-6'-C*H*).

1-[2-(1-Pyrrolidino)]ethyl 5-benzoyl-2,3-dihydro-1*H*-pyrrolizine-1-carboxylate (58d)

The reaction of ketorolac (**58**) with 2-pyrrolidinoethanol (**50d**) as described for the compound (**58a**) yielded the desired compound (**58d**) as a yellow oil. IR spectrum of the compound (**58d**) showed the characteristic band at 1739 cm^{-1} for the ester carbonyl stretching vibrations. In the PMR spectrum of **58d** signals were observed at δ 1.2-1.3 (m,

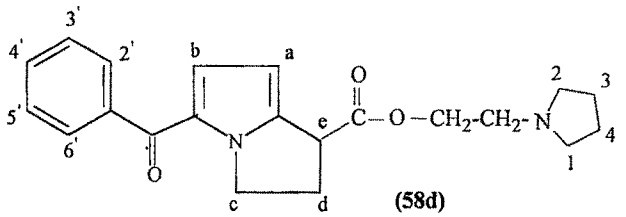

2H, d-CH_2)), 1.80-1.84 (t, 2H, 4-CH_2), 1.99-2.03 (t, 2H, 3-CH_2), 2.65-2.90 (m, 6H, CH_2N, 2-CH_2, 5-CH_2), 3.08-3.12 (m, 3H, c-CH_2, e-C*H*), 4.32-4.59 (m, 2H, OCH_2), 6.10-6.11 (d, 1H, Ar-a-C*H*), 6.79-6.81 (d, 1H, Ar-b-C*H*), 7.40-7.52 (m, 3H, Ar-3'-C*H*, Ar-4'-C*H*, Ar-5'-C*H*) and 7.78-7.81 (d, 2H, Ar-2'-C*H*, Ar-6'-C*H*).

1-[2-(4-Morpholino)]ethyl 5-benzoyl-2,3-dihydro-1*H*-pyrrolizine-1-carboxylate (58e)

Compound (**58e**) was synthesized by reacting ketorolac (**58**) and 2-(4-morpholino)ethanol (**50e**) as described for compound (**58a**). Work up of the reaction mixture afforded the

desired compound as a yellow oil, the IR spectrum of which showed intense band at 1739 cm^{-1}. The PMR spectrum of the compound (**58e**), showed signals at δ 1.25 (m, 2H, d-C*H*$_2$), 2.62-2.66 (m, 6H, C*H*$_2$N, 3-C*H*$_2$, 5-C*H*$_2$), 2 80-2.91 (m, 3H, c-C*H*$_2$, e-C*H*), 3.68-

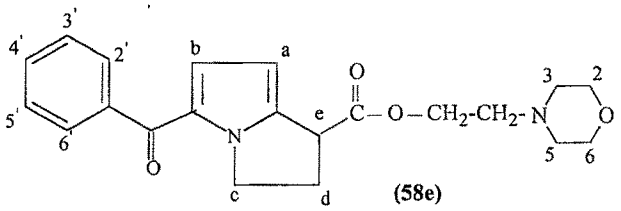

(58e)

3.80 (m, 4H, 2-C*H*$_2$, 5-C*H*$_2$), 4.50-4.57 (m, 2*H*, OC*H*$_2$), and the signals for the aromatic protons were observed at 6.10-6.12 (d, 1H, Ar-a-C*H*), 6.80-6.82 (d, 1H, Ar- b-C*H*), 7.44-7.49 (m, 3H, Ar-3'-C*H*, Ar-4'-C*H*, Ar-5'-C*H*) and 7.77-7.81 (d, 2H, Ar-2'-C*H*, Ar-6'-C*H*).

3.2. HYDROLYSES STUDIES

It was proposed that the aminoalcohol ester derivatives synthesized for the present work, would remain in the protonated form (amine salts) in the acidic pH of stomach which would prevent the absorption of these ionized compounds into the mucosal cells and thereby prevent/minimize the local irritation (due to the absence of free acidic carboxyl group). Further, the protonated derivatives were expected to revert back into the unionized form in the alkaline pH of the intestine where they were expected to be absorbed intact due to their lipophilic character. For such an event to happen, the drug derivatives must remain stable throughout the span they stay in GIT, prior to their absorption. To check this hypothesis, all the synthesized ester derivatives were evaluated *in vitro* for their stability at 37±1°C in buffers (pH 2.0 and 7.4) which simulated the pH existing in the stomach and intestine. After absorption into the system, the aminoalcohol esters should cleave enzymatically/non-enzymatically, to release the parent NSAIDs for eliciting the normal pharmacological activity. Hence, the *in vitro* hydrolyses studies were performed in pooled human serum (80%) at 37±1°C for all the synthesized derivatives.

The hydrolyses studies performed are discussed under the following headings:

3.2.1. Hydrolyses studies of derivatives of 4-biphenylacetic acid (45a-f)

3.2.2. Hydrolyses studies of derivatives of flurbiprofen (49a-f)

3.2.3. Hydrolyses studies of derivatives of diclofenac (51a-e)

3.2.4. Hydrolyses studies of derivatives of indomethacin (54a-e)

3.2.5. Hydrolyses studies of derivatives of aspirin (56a-e)

3.2.6. Hydrolyses studies of derivatives of ketorolac (58a-e)

3.2.1. HYDROLYSES STUDIES OF DERIVATIVES OF 4-BIPHENYLACETIC ACID (45a-f)

3.2.1.1 Hydrolyses studies in buffers

Exploiting the physicochemical properties of tertiary alkylamines and carboxylic acids, analytical procedures were developed for the quantitative estimation of free NSAIDs in presence of their aminoalcohol ester derivatives using UV spectrophotometry as an analytical tool. NSAIDs possessing free carboxylic group (pKa ~ 4) are freely soluble in

basic aqueous media as salts while the free acids are soluble in organic solvents in acidic media. Reverse is the case with aminoalcohol esters of these NSAIDs. They are soluble in organic solvents in the basic media while as hydrochloride salts (in acidic media) they are freely soluble in the aqueous medium. Since the hydrochloride salts of amines have approximately same pKa (i.e. 4) as the free carboxylic acid compounds, both of these compounds could fully be partitioned in a medium with a pH decreased by two units (i.e. pH 2.0) from their pKa values, into organic and aqueous phases. That is, at this pH (2.0) carboxylic acid compounds would remain soluble exclusively in organic phase while, the aminoalcohol esters would be exclusively present in aqueous medium.

Since both, the free NSAIDs and the aminoalcohol esters, have same chromophoric systems, partitioning of both of them in separate phases is an essential requirement to estimate either of them by UV spectrophotometry. Keeping the above points in mind, it was first established that no partitioning takes place for aminoalcohol ester derivatives at this pH (2.0) in the organic phase i.e. the NSAIDs derivatives at this pH are not extractable in organic solvents like n-hexane, chloroform or isopropyl ether while, the NSAIDs are fully extractable in organic solvents. It was also established that the parent drugs (NSAIDs) could be completely extracted by sodium hydroxide solution (0.1 N) from the organic solvents without any significant extraction of aminoalcohol ester derivatives of these parent drugs into the aqueous phase.

Keeping the above described philosophy and observations in mind, estimations of various parent drugs (**45, 49, 51, 54, 56, 57** and **58**) were carried out as and when they got liberated after hydrolysis from the aminoalcohol ester derivatives (**45a-f, 49a-f, 51a-e, 54a-e, 56a-e, and 58a-e**) during the hydrolyses studies.

Preliminary investigations indicated a very high partitioning of 4-biphenylacetic acid (**45**) in chloroform at pH 2.0 and high aqueous solubility in alkaline medium (0.1 N sodium hydroxide solution). Calibration curve was prepared for 4-biphenylacetic acid (**45**) by dissolving it in alkaline solutions and then partitioning in chloroform in acidic medium (pH 2.0), further extraction into sodium hydroxide solution (0.1 N) and taking the absorbance at its UV maximum (253 nm). Traces of chloroform from the aqueous solutions were removed by heating the aqueous solutions so that there is no interference of chloroform at this wavelength. This sequence of events, i.e. partitioning, heating etc.

in the preparation of calibration curve of 4-biphenylacetic acid (**45**) was essential since the same sequence has been followed in its estimation in the two buffer solutions (pH 2.0 and pH 7.4). Three sets of readings were taken for the preparation of the calibration curve. Two closest sets (Table 3.2.1.1) were retained for regression analysis. It was observed that Beer-Lambert law was followed in the range of 2-16 ug/ml. Regression analysis of the data within this range offered Equation-1. Graphical representation of the data for the regressed values, which prove the linearity of data, is given in Figure-3.2.1.1.

Table 3.2.1.1 Data for preparation of calibration curve for estimating 4-Biphenyl - acetic acid (45) in buffers

Sr. No	Concentration ug/ml	Absorbance		Regressed values
		A	B	C
1	2.0	0.125	0.123	0.107
2	4.0	0.228	0.220	0.229
3	6.0	0.345	0.343	0.353
4	8.0	0.472	0.462	0.475
5	10.0	0.621	0.613	0.598
6	12.0	0.703	0.689	0.721
7	14.0	0.834	0.829	0.844
8	16.0	0.996	0.985	0.966

$A = 0.0614*C - 0.0155$ Equation-1

$r = 0.9993$, $s = 0.0182$

[A = absorbance, C = concentration (ug/ml)]

Figure 3.2.1.1 Calibration plot for estimating 4-biphenylacetic acid (45) in buffers

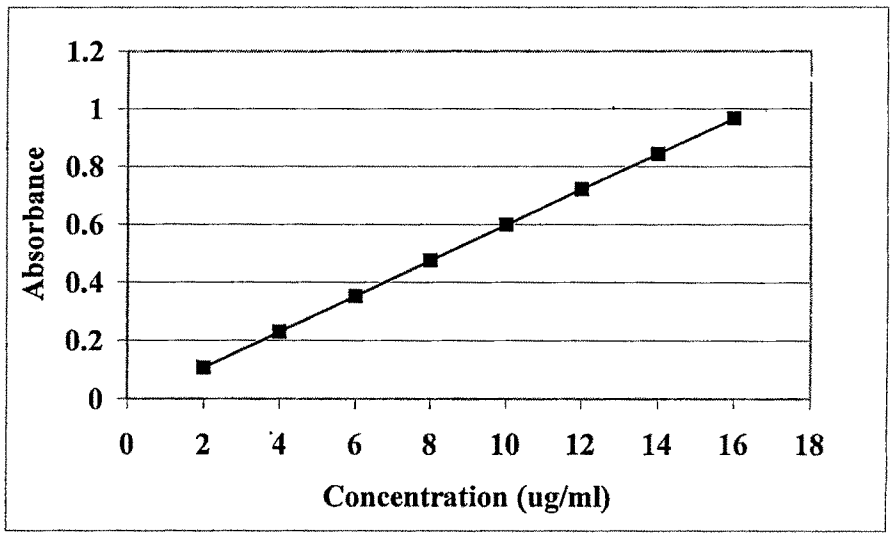

The UV spectrophotometric method developed for estimating the amount of biphenylacetic acid (**45**) released from the chemical hydrolysis of the derivative was based on the principle described above. Aliquots (1.0 ml) withdrawn at different time intervals from the test solution kept at 37±1°C at pH 2.0 and 7.4 were acidified with buffer solution (pH 2.0) so that the parent drug (**45**) released from the hydrolysis of the derivatives (**45a-f**) would be in the non-ionic (lipophilic) form and the ester derivative (**45a-f**) would be in the ionic-form (since the 'N' would be protonated). Extraction of this acidified aliquot (pH ~ 2.0) with chloroform would result in the extraction of the parent drug and the protonated intact derivative (**45a**) would be retained in the aqueous phase. The chloroform layer was again extracted with sodium hydroxide solution (0.1 N) where the parent drug (**45**) would be extracted into the aqueous phase and remained as the sodium salt. To prevent the error in measurement of the absorbance due to the interference of traces of chloroform, the aqueous extract was heated on a waterbath to remove the traces of chloroform and the absorbance measured at 253 nm against a blank sodium hydroxide solution. The concentration of the parent drug was calculated using the Equation-1 for each set of the absorbance (values in parentheses indicate the dilutions done before measuring the absorbance) at pH 2.0 and 7.4 (Table 3.2.1.2). The rate constants for hydrolysis of the derivatives were determined by the linear regression of the logarithm of residual drug derivative (**45a**) concentration versus time plots as shown in Table 3.2.1.3 for one set of readings (Sample-A).

Table 3.2.1.2 The absorbance readings of (45) for the studies of (45a) in buffers

Time	pH 2.0	Sample A pH 7.4	Sample B pH 7.4	Sample C pH 7.4
(h)	Absorbance			
0.0	0.092	0.125	0.126	0.169
0.5	0.096	0.625	0.820	0.717
1.0	0.081	0.294 (1:3)	0.376 (1:4)	0.315 (1:4)
2.0	0.118	0.633 (1:3)	0.465 (1:4)	0 436 (1·4)
4.0	0.088	0.642 (1:4)	0.606 (1:4)	0.542 (1:4)
6.0	0.137	0.778 (1:4)	0.691 (1:5)	0.704 (1:5)
8.0	0.077	0.967 (1:4)	0.778 (1:5)	0.793 (1:5)

No change in absorbance was observed for the study of compound (**45a**) in buffer (pH 2.0) so average concentration obtained (1.61 ug/ml) from these observations was taken as the concentration of the parent drug (**45**) for the '0' hour readings in the calculations for the studies carried at pH 7.4 for (**45a**). Table 3.2.1.3 describes the set of data required for calculation of rate constant of hydrolysis for Sample A readings of the derivative (**45a**) in buffer pH 7.4.

The concentrations of parent drug (**45**) for the absorbance readings of Sample A of **45a** were calculated using Equation-1. These concentration values were further converted to the corresponding quantity (x, ug/ml) of the derivative (**45a**). The actual concentration of the intact derivative (**45a**) (y, ug/ml) in the stock solution at zero hour was calculated from the average reading [1.61 ug/ml of (**45**) in buffer pH 2.0] to give a value of 975.7 ug/ml (y). Considering that the hydrolysis of the aminoalcohol ester derivatives followed psuedo-first order kinetics, calculations were done for finding the rate constant (k) for Sample A readings.

Table 3.2.1.3 Data presentation for Set A (45a) for calculation of rate constant k

Time (h)	Absorb-ance	Conc. of (45) (ug/ml)	x (ug/ml)	(y-x) (ug/ml)	(y-x) (mol/litre)	Log(y-x)	Calculated Log(y-x)
0	0.125	1.61	0	975.7	$3.051*10^{-3}$	-2.516	-2.521
0.5	0.625	10.43	13.29	962.41	$3.007*10^{-3}$	-2.522	-2.524
1	0.294 (1:3)	20.16	27.96	947.74	$2.963*10^{-3}$	-2.528	-2.528
2	0.633 (1:3)	42.25	61.24	914.46	$2.859*10^{-3}$	-2.548	-2.534
4	0.642 (1:4)	53.54	78.26	897.44	$2.806*10^{-3}$	-2.552	-2.548
6	0.778 (1:4)	64.62	94.94	880.76	$2.754*10^{-3}$	-2.560	-2.561
8	0.967 (1:4)	80.01	118.14	857.56	$2.681*10^{-3}$	-2.572	-2.575

x = concentration of the derivative (**45a**) at various time intervals which got hydrolysed

y = initial concentration of the derivative (**45a**) at 0 hour, i.e. 975.7 ug/ml

y-x = concentration of the derivative (**45a**) left intact in the solution at various time intervals.

Equation-2 was obtained by regressing time vs. log(y-x).

$$\log(y-x) = 0.0067*t - 2.521 \qquad \text{Equation-2}$$

The values for log (y-x) were calculated substituting these values of m (0.0067) and c (-2.521) in the linear equation (Equation-2) so obtained. The calculated values of log (y-x) obtained are shown in Table 3.2.1.3 for sample A and the line demonstrating the pseudo-first order kinetics has been shown graphically in Figure 3.2.1.2. for all the three samples A, B and C.

Comparing the above obtained linear equation with the general equation for the psuedofirst order kinetics, $\log (Z_0 - Z) = -k*t/2.303 + \log Z_0$ (Z_0 is initial concentration of a substance, Z is the constant fraction degrading from it in time interval 't', k is the rate constant and t is time), we get the rate constant k (for Sample A) = m*2.303 = 0.01536.

Similarly, the data for sample B and sample C of (**45a**) were treated to give the rate constants k (Sample B, k = 0.0144, and Sample C, k = 0.0152). Finally the average rate

constant (k) was found and half-life was calculated using equation $t_{1/2}$ = 0.693/k. The half life for derivative (**45a**) has been tabulated in Table 3.2.1.13.

The same procedure as described above was followed for rest of the derivatives (45b-f) and the data presentations have been shown in tables (from Table 3.2.1.4 to 3.2.1.12 and figures (from Figures 3.2.1.3 to 3.2.1.12).

Figure 3.2.1.2 Graphical presentation for calculated log(y-x) values vs time for samples A, B and C of 45a

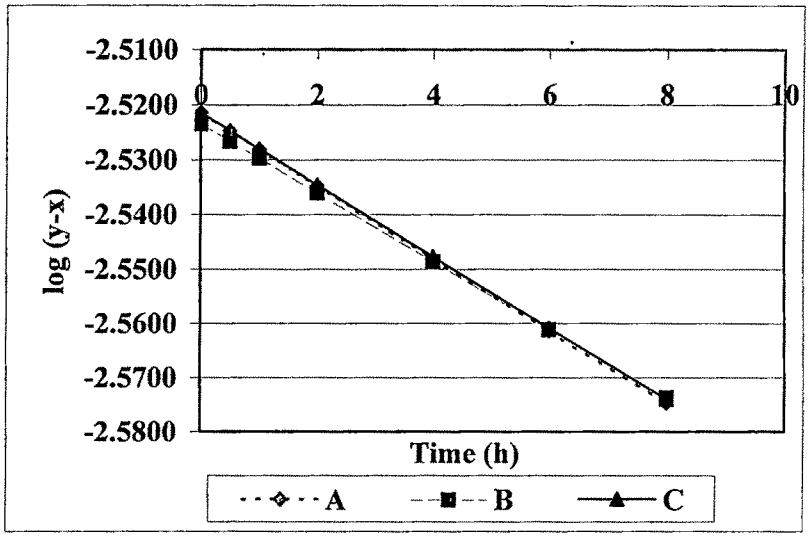

Table 3.2.1.4 The absorbance readings of (45) for the studies of (45b) in buffers

Time	pH 2.0	Sample A pH 7.4	Sample B pH 7.4	Sample C pH 7.4
(h)	Absorbance			
0.0	0.074	0.198	0.105	0.163
0.5	0.081	0.46	0.477	0.457
1.0	0.087	0.707	0.939	0.683
2.0	0.100	0.328 (1:3)	0.401 (1:3)	0.254 (1:3)
4.0	0.096	0.559 (1:3)	0.558 (1:3)	0.469 (1:3)
6.0	0.089	0.778 (1:3)	0.683 (1:3)	0.653 (1:3)
8.0	0.084	0.960 (1:3)	0.584 (1:4)	0.892 (1.3)

Table 3.2.1.5 Data presentation for set A (45b) for calculation of the rate constant k

Time (h)	Absorb-ance	Conc. of (45) (ug/ml)	x (ug/ml)	(y-x) (ug/ml)	(y-x) (mol/litre)	Log(y-x)	Calculated Log(y-x)
0	0.198	1.67	0	972.7	$2.796*10^{-3}$	-2.553	-2.555
0.5	0.460	7.74	9.96	962.74	$2.768*10^{-3}$	-2.558	-2.558
1	0.707	11.77	16.55	956.15	$2.749*10^{-3}$	-2.561	-2.561
2	0.328 (1:3)	22.38	33.94	938.76	$2.699*10^{-3}$	-2.569	-2.567
4	0.559 (1:3)	37.43	58.61	914.09	$2.628*10^{-3}$	-2.580	-2.579
6	0.778 (1:3)	51.69	81.99	890.71	$2.561*10^{-3}$	-2.592	-2.591
8	0.960 (1:3)	63.55	101.42	871.28	$2.505*10^{-3}$	-2.601	-2.603

Figure 3.2.1.3 Graphical presentation for calculated log(y-x) values vs time for the samples A, B and C of 45b

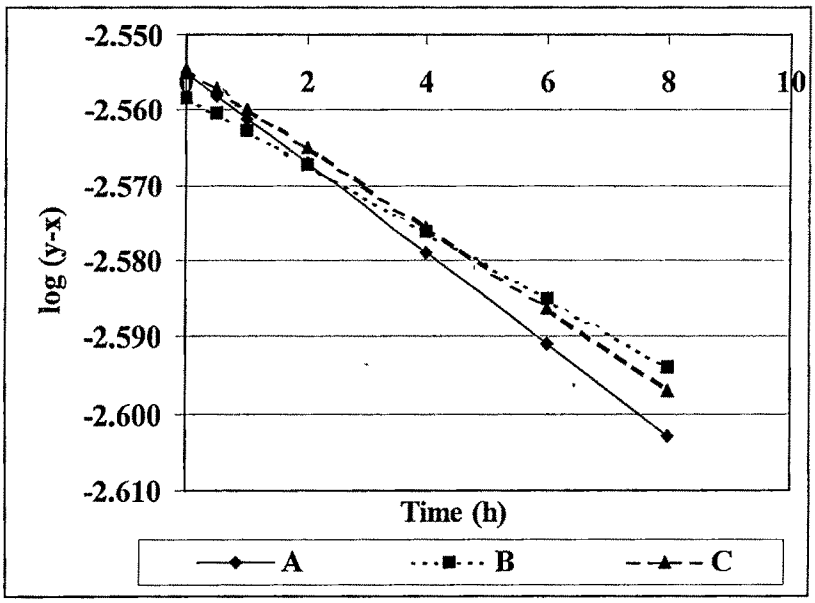

Table 3.2.1.6 The absorbance readings of (45) for the studies of (45c) in buffers

Time	pH 2.0	Sample A pH 7.4	Sample B pH 7.4
(h)	Absorbance		
0.0	0.104	0.094	0.083
0.5	0.104	0.376	0.457
1.0	0.068	0.689	0.714
2.0	0.043	0.269 (1:5)	0.288 (1:5)
4.0	0.081	0.293 (1:5)	0.313 (1:5)
6.0	0.083	0.439 (1:5)	0.442 (1:5)
8.0	0.076	0.476 (1:5)	0 465 (1:5)

Table 3.2.1.7 Data presentation for set A (45c) for calculation of the rate constant k

Time (h)	Absorb-ance	Conc. of (45) (ug/ml)	x (ug/ml)	(y-x) (ug/ml)	(y-x) (mol/litre)	Log(y-x)	Calculated Log(y-x)
0	0.094	1.55	0	973.7	$2.706*10^{-3}$	-2.568	-2.571
0.5	0.376	6.38	8.18	965.52	$2.683*10^{-3}$	-2.571	-2.574
1	0.689	11.47	16.83	956.87	$2.659*10^{-3}$	-2.575	-2.576
2	0.269 (1:5)	27.80	44.51	929.19	$2.582*10^{-3}$	-2 588	-2.581
4	0.293 (1:5)	30.15	48.49	925.21	$2.571*10^{-3}$	-2.590	-2 590
6	0.439 (1:5)	44.41	72.68	901.02	$2.504*10^{-3}$	-2.601	-2.599
8	0.476 (1:5)	48.03	78.81	894.89	$2.487*10^{-3}$	-2.604	-2.608

Figure 3.2.1.4 Graphical presentation for calculated log(y-x) values vs time for samples A and B of (45c)

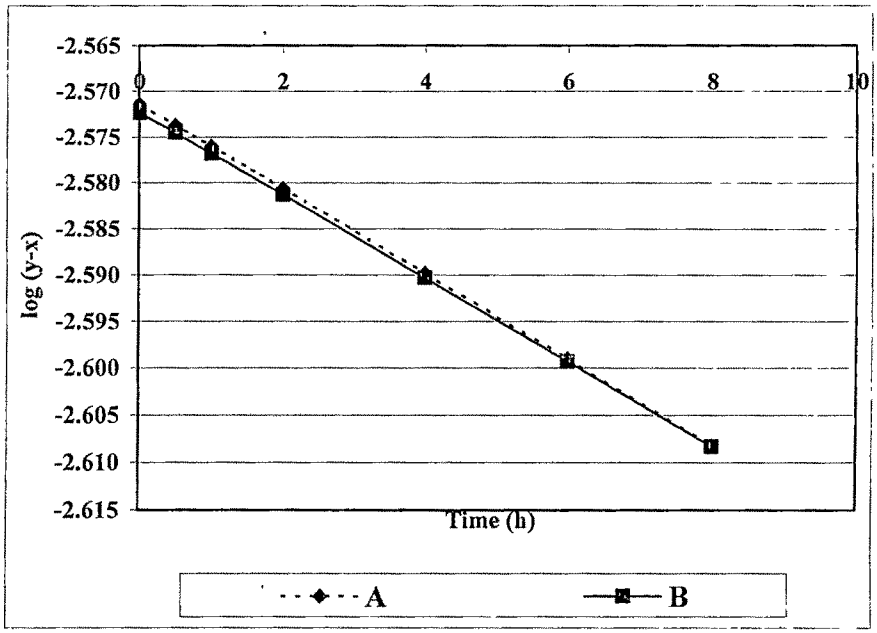

Table 3.2.1.8 The absorbance readings of (45) for the studies of (45d) in buffers

Time	pH 2.0	Sample A pH 7.4	Sample B pH 7.4
(h)	Absorbance		
0.0	0.225	0.157	0.130
0.5	0.163	0.384	0.505
1.0	0.125	0.716	0.699
2 0	0 184	0.263 (1:3)	0.246 (1:3)
4.0	0.172	0.428 (1:3)	0.504 (1.3)
6.0	0.162	0.635 (1:3)	0.615 (1:3)
8.0	0.151	0.733 (1:3)	0.744 (1:3)

Table 3.2.1.9 Data presentation for set A (45d) for calculation of the rate constant k

Time (h)	Absorb-ance	Conc. of (45) (ug/ml)	x (ug/ml)	(y-x) (ug/ml)	(y-x) (mol/litre)	Log(y-x)	Calculated Log(y-x)
0	0.157	3.00	0	951.11	$2.750*10^{-3}$	-2.561	-2.562
0.5	0.384	6.51	5.71	945.40	$2.734*10^{-3}$	-2.563	-2.564
1	0.716	11.91	14.52	936.59	$2.708*10^{-3}$	-2.567	-2.567
2	0.263 (1:3)	18.14	24.68	926.43	$2.679*10^{-3}$	-2.572	-2.571
4	0.428 (1:3)	28.89	42.19	908.92	$2.628*10^{-3}$	-2.580	-2.580
6	0.635 (1:3)	42.38	64.17	886.94	$2.565*10^{-3}$	-2.591	-2.589
8	0.733 (1:3)	48.76	74.57	876.54	$2.535*10^{-3}$	-2.596	-2.598

Figure 3.2.1.5 Graphical presentation for calculated log(y-x) values vs time for the samples A and B of (45d)

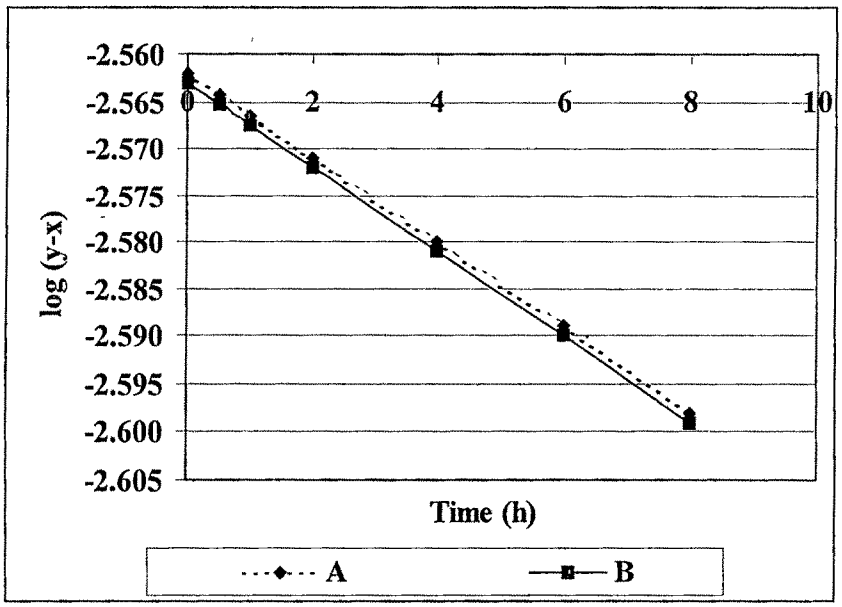

Table 3.2.1.10 The absorbance readings of (45) for the studies of (45e) in buffers

Time	pH 2.0	Sample A pH 7.4	Sample B pH 7.4	Sample C pH 7.4
(h)	Absorbance			
0.0	0.219	0.254	0.198	0.200
0.5	0.362	0.306	0.411	0.364
1.0	0.333	0.435	0.490	0.489
2.0	0.265	0.621	0.607	0.658
4.0	0.263	0.867	0.847	0.762
6.0	0.272	0.404 (1:2)	0.414 (1:2)	0.356 (1.2)
8.0	0.322	0.513 (1:2)	0.493 (1:2)	0.458 (1:2)

Table 3.2.1.11 Data presentation for set A of (45e) for calculation of rate constant k

Time (h)	Absorb-ance	Conc. of (45) (ug/ml)	x (ug/ml)	(y-x) (ug/ml)	(y-x) (mol/litre)	Log(y-x)	Calculated Log(y-x)
0	0.254	4.99	0	914.9	2.528	-2.597	-2.597
0.5	0.306	5.24	0.42	914.48	2.527	-2.597	-2.598
1	0.435	7.34	4.00	910.90	2.517	-2.599	-2.599
2	0.621	10.37	9.17	905.73	2.503	-2.602	-2.601
4	0.867	14.37	16.00	898.90	2.484	-2.605	-2.606
6	0.404(1:2)	20.50	26.44	888.46	2.455	-2.610	-2.610
8	0.513(1:2)	25.82	35.52	879.38	2.430	-2.614	-2.615

Figure 3.2.1.6 Graphical presentation for calculated log(y-x) values vs time for samples A and B of (45e)

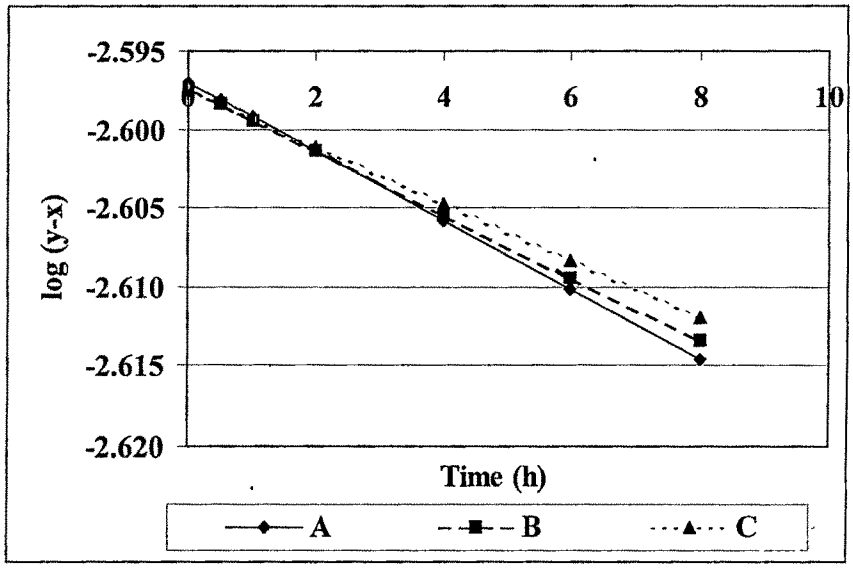

Table 3.2.1.12 The absorbance readings of (45) for the studies of (45f) in buffers

Time	pH 2.0	Sample A pH 7.4	Sample B pH 7.4	Sample C pH 7.4
(h)	Absorbance			
0.0	0.068	0.044	0.040	0.093
0.5	0.073	0.066	0.047	0.136
1.0	0.065	0.066	0.070	0.093
2.0	0.062	0.043	0.085	0 044
4.0	0.065	0.042	0.131	0.052
6.0	0.058	0.058	0.108	0.049
8.0	0.063	0.045	0.106	0.105

Table 3.2.1.13 Chemical Hydrolyses of Derivatives (45a-f)

Compound	t ½ (h) pH7.4 Buffer
45a	46
45b	52
45c	68
45d	66
45e	143

The studies in buffer (pH 2.0) indicated that all of the drug derivatives (**45a-f**) showed no observable hydrolysis till 8 hours. Table 3.2.1.13 shows the half-lives calculated for these derivatives (**49a-e**). The half-lives range vary from 46-143 hours. It was interesting to note that no hydrolysis was observed for **45f** even in buffer (pH 7.4) till 8 hours. The long half-lives of the derivatives (**45a-f**) assure that these derivatives would be absorbed intact from the GIT and would successfully prevent the local GI irritation caused by the parent drug (**45**).

3.2.1.2 Hydrolyses studies in human serum (80%)

For the estimation of 4-biphenylacetic acid (**45**) released during enzymatic hydrolysis during the kinetic studies of the derivatives (**45a-f**), it was planned to adopt the same method as described for the hydrolyses studies of the derivatives (**45a-f**) in both the buffer solutions (pH 2.0 and 7.4). But the usage of chloroform as an organic phase for partitioning posed serious problem of emulsification. In the current study, to stop the enzymatic (hydrolysis) reaction by the esterases present in the serum, trichloroacetic acid was used for inactivating (precipitating) the proteins. Presence of these denatured proteins in the solutions gave stable emulsions with chloroform. Due to the formation of emulsions with chloroform, it was substituted with isopropyl ether as the partitioning solvent. The choice of selection of partitioning organic solvent fell on isopropyl ether due to the following reasons:

- Chloroform formed an emulsion with the precipitated serum proteins which was difficult to separate while isopropyl ether was observed to form no such emulsion, separating clearly as the upper layer with the precipitated proteins settling down in the lower aqueous layer.

- A solvent, with good solubility for the parent drug but at the same time with no affinity for the protonated derivative in the acidic pH was needed and isopropyl ether satisfied these requirements.
- Besides these, during the synthesis of the derivatives (**45a-f**), these compounds were precipitated as hydrochloride salts from isopropyl ether. This confirmed that the protonated derivatives would not be soluble in isopropyl ether.

Calibration curve for 4-biphenylacetic acid (**45**) was prepared essentially based on the same principle as described for the buffer solutions (pH 2.0 and 7.4) with a difference of change of partitioning solvent from chloroform to isopropyl ether. Solutions of 4-biphenylacetic acid (**45**) with varying concentrations were prepared in sodium hydroxide solution (0.1 N) and the same sequence of extraction and reextraction was carried out as described above before taking the absorbance readings on the UV spectrophotometer Beer-Lambert law was followed in the range of 1-14 ug/ml. Two closest observations were regressed to give Equation-3 and the regressed values are also given in Table 3.2.14 and represented by graph in Figure 3.2.1.7.

Table 3.2.1.14 Calibration curve data for estimating 4-biphenylacetic acid (45) in pooled human serum (80%)

Sr. No	Concentration ug/ml	Absorbance		Regressed values
		A	B	C
1	1.0	0.106	0.107	0.108
2	2.0	0.227	0.229	0.193
3	4.0	0.381	0.353	0.363
4	6.0	0.551	0.475	0.532
5	8.0	0.719	0.598	0.702
6	10.0	0.862	0.721	0.871
7	12.0	1.032	0.844	1.041
8	14.0	1.226	1.218	1.210

$A = 0.0848*C - 0.0235$ Equation-3

$r = 0.999$, $s = 0.0203$

[A = absorbance, C = concentration (ug/ml)]

Figure 3.2.1.7 Calibration plot for estimating 4-biphenylacetic acid (45) in pooled human serum (80%)

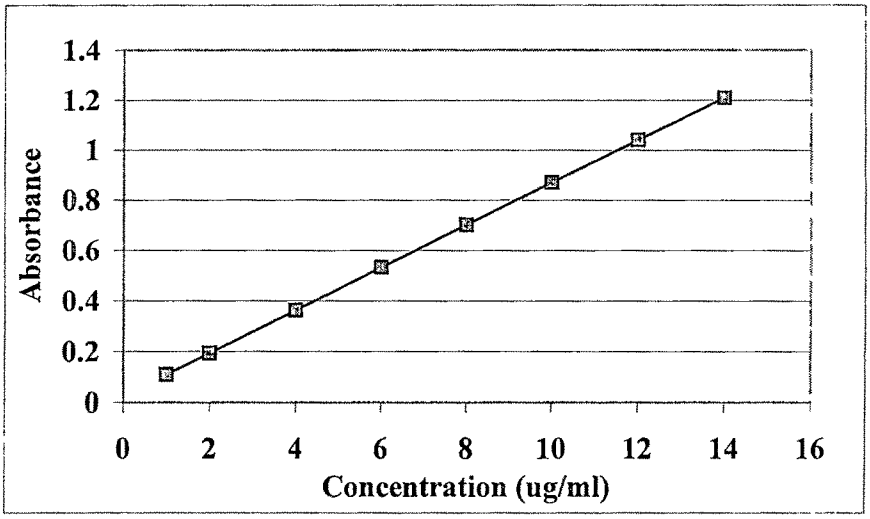

Hydrolyses studies of the derivatives (**45a-f**) were carried out in pooled human serum (80%). The stock solution of (**45a**) (1 mg/ml) in human serum (80%) was maintained at 37±1°C. Aliquots (0.5 ml) were treated with trichloroacetic acid (TCA) (1.0 ml, 10%) to arrest further (chemical and enzymatic) hydrolysis by deactivating the serum proteins (enzymes) as well as bringing the pH to acidic side. The acidified solution was extracted into isopropyl ether. The organic extract was further extracted with sodium hydroxide solution (0 1 N), heated on a water bath and the absorbance measured at 253 nm. Concentration of the parent drug was calculated using the Equation-3. Samples were analysed in duplicate for all the derivatives (**45a-f**) as shown in Tables 3.2.1.15 and 3.2.1.16.

Taking initial concentration (y, 975.7 ug/ml) of the drug derivatives (**45a-f**) from the data of hydrolyses studies in acidic pH 2.0 buffer solution equivalent concentration of the parent drug (**45**) was calculated in each case. Taking this to be 100%, the release of the parent drug (**45**) from various drug derivatives (**45a-f**) at different time intervals was calculated as shown in Table 3.2.1.17.

Table 3.2.1.15 The absorbance data for the studies of (45a-c) in human serum (80%)

Time (min)	45a (Sample A and B) Absorbance		45b (Sample A and B) Absorbance		45c (Sample A and B) Absorbance	
	A	B	A	B	A	B
15	0.220 (1:3)	0.245 (1:4)	0.546	0.588	0.289	0.285
30	0.388 (1:3)	0.362 (1:4)	0.863	0.822	0.378	0 362
60	0.607 (1:3)	0.505 (1:4)	0.174 (1:5)	0.191 (1:5)	0.511	0.733
120	0.850 (1:5)	0.793 (1:5)	0.312 (1:5)	0.421 (1:5)	0.824 (1:1)	0.862 (1:1)

Table 3.2.1.16 The absorbance data for the studies of (45d-f) in human serum (80%)

Time (min)	45d (Sample) Absorbance		45e (Sample) Absorbance		45f (Sample) Absorbance	
	A	B	A	B	A	B
15	0.561	0.628	0.269	0.295	0.044	0.091
30	0.769	0.875	0.381	0.445	0 052	0.053
60	0.287 (1:3)	0.471 (1:3)	0.413 (1:1)	0.527 (1:1)	0.058	0 065
120	0.479 (1:3)	0.509 (1:3)	0.503 (1:1)	0.593 (1:1)	0.021	0.072

Table 3.2.1.17 Enzymatic hydrolyses of derivatives (45a-f)

Compound	% Release of parent NSAID 45) (80% human serum)		
	½ h	1 h	2h
45a	27.3	40.5	81.4
45b	11.4	15.8	43.4
45c	4.0	11.7	31.6
45d	10.7	11.7	23 2
45e	3.3	11.9	15.6
45f	0.0	0.0	0.0

The results of Table 3.2.1.17 lead us to conclude that all the derivatives (**45a-e**) of 4-biphenylacetic acid (**45**) except for compound (**45f**) would be cleaved by the action of

esterases following absorbtion into systemic circulation from GIT, to liberate the parent drug (**45**).

3.2.2 HYDROLYSES STUDIES OF DERIVATIVES OF FLURBIPROFEN (49a-f)

3.2.2.1 Hydrolyses studies in buffers

The basic principle involved in the UV spectrophotometric method for estimating flurbiprofen (**49**) released in the hydrolyses studies of (**49a-f**), is same as discussed in 3.2.1.1 for estimating 4-biphenylacetic acid (**45**). For preparing the calibration curve for estimating flurbiprofen (**49**), it was dissolved in sodium hydroxide solution (0.1 N) and partitioned into n-hexane in acidic medium, dried (to remove traces of aqueous solution) and the absorbance measured at the UV maximum (237 nm) of **49**. n-Hexane was chosen for extraction as it was observed to have good solubility for flurbiprofen (**49**) with no partitioning for the intact derivatives in acidic medium (pH ~ 2), and above all it would not interfere in the absorbance measurement at 237 nm due to its low UV cut off (below 190 nm). Three determinations were made and regressed to give Equation-4. The Beer-Lambert law was obeyed in the concentration range of 2-20 ug/ml. The absorbance data for preparing the calibration curve with the graphical presentation has been shown in Table-3.2.2.1 and Figure 3.2.2.1, respectively.

Table 3.2.2.1 Calibration curve data for estimating flurbiprofen (49) in buffers and pooled human serum (80%)

Sr. No	Concentration ug/ml	Absorbance			Regressed values
		A	B	C	D
1	2.0	0.082	0.103	0.113	0.135
2	4.0	0.196	0.217	0.218	0.214
3	6.0	0.284	0.332	0.339	0.314
4	8.0	0.392	0.440	0.418	0.414
5	10.0	0.521	0.552	0.556	0.514
6	12.0	0.648	0.653	0.620	0.614
7	14.0	0.704	0.748	0.801	0.714
8	16.0	0.796	0.823	0.818	0.814
9	18.0	0.870	0.932	0.886	0.915
10	20.0	0.978	1.032	0.989	1.015

$A = 0.0501*C + 0.0134$ Equation-4

$r = 0.997$, $s = 0.024$

[A = absorbance, C = concentration (ug/ml)]

Figure 3.2.2.1 Calibration plot for estimating flurbiprofen (49) in buffers and pooled 80% human serum

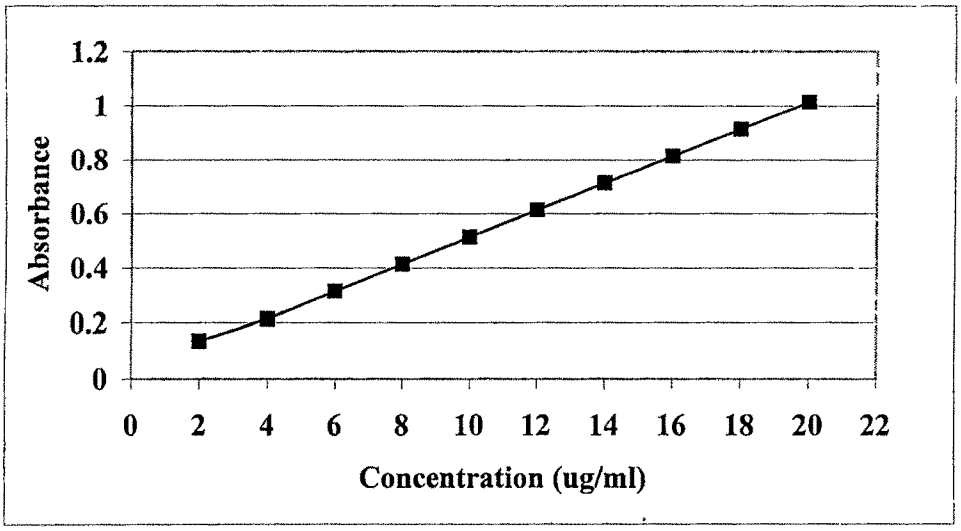

Table 3.2.2.3 Data presentation for set A (49a) for calculation of the rate constant k

Time (h)	Absorb-ance	Conc. of (49) (ug/ml)	x (ug/ml)	(y-x) (ug/ml)	(y-x) (mol/litre)	Log(y-x)	Calculated Log(y-x)
0	0.153	2.84	0	959.1	$2.726*10^{-3}$	-2.564	-2.565
0.5	0.329	6.30	4.98	954.12	$2.712*10^{-3}$	-2.567	-2.566
1	0.470	9.11	9.04	950.06	$2.700*10^{-3}$	-2.569	-2.567
2	0.511	9.93	10.22	948.88	$2.697*10^{-3}$	-2.569	-2.570
4	0.272 (1:3)	15.49	18.21	940 89	$2.674*10^{-3}$	-2.573	-2.575
6	0.460 (1:3)	26.74	34.43	924.67	$2.628*10^{-3}$	-2.580	-2.580
8	0.573 (1:3)	33.51	44.17	914.93	$2.600*10^{-3}$	-2.585	-2.585

Figure 3.2.2.2 Graphical presentation for calculated log(y-x) values vs time for samples A and B of (49a)

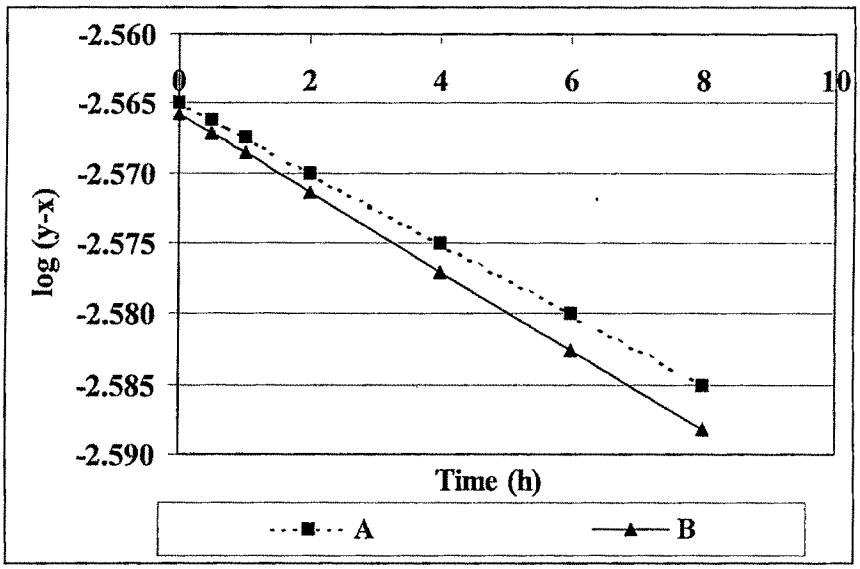

Table 3.2.2.4 The absorbance readings of (49) for the studies of (49b) in buffers

Time	pH 2.0	Sample A pH 7.4	Sample B pH 7.4	Sample C pH 7.4
(h)	Absorbance			
0.0	0.216	0.265	0.291	0.367
0.5	0.219	0.345	0.382	0.501
1.0	0.317	0.476	0.490	0.614
2.0	0.253	0.751	0.755	0.722
4.0	0.196	0.927	0.857	0.881
6.0	0 204	0.295 (1:3)	0.269 (1:3)	0.298 (1:3)
8.0	0.216	0.326 (1:3)	0.338 (1:3)	0.387 (1:3)

Table 3.2.2.5 Data presentation for set A (49b) for calculation of the rate constant k

Time (h)	Absorb-ance	Conc. of (49) (ug/ml)	x (ug/ml)	(y-x) (ug/ml)	(y-x) (mol/litre)	Log(y-x)	Calculated Log(y-x)
0	0.265	4.35	0	932.35	$2.454*10^{-3}$	-2.610	-2.612
0.5	0 345	6.62	3.53	928.82	$2.445*10^{-3}$	-2.612	-2 613
1	0.476	9.23	7.60	924.75	$2.434*10^{-3}$	-2.614	-2 614
2	0.751	14.72	16.13	916.22	$2.412*10^{-3}$	-2.618	-2.616
4	0.927	18.24	21.60	910.75	$2.397*10^{-3}$	-2.620	-2.619
6	0.295 (1:3)	22.48	28.20	904.15	$2.380*10^{-3}$	-2.623	-2.623
8	0.326 (1:3)	24.96	32.05	900.30	$2.370*10^{-3}$	-2.625	-2.627

Figure 3.2.2.3 Graphical presentation for calculated log(y-x) values vs time for samples A, B and C of (49b)

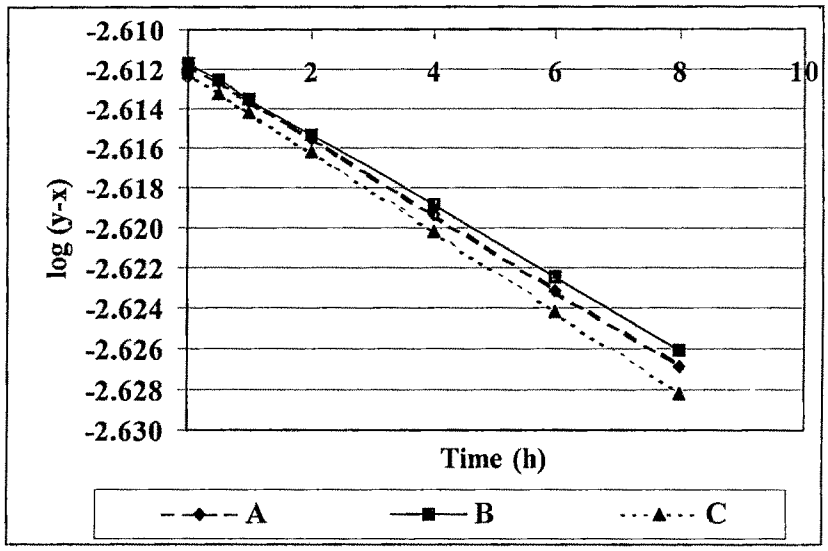

Table 3.2.2.6 The absorbance readings of (49) for the studies of (49c) in buffers

Time	pH 2.0	Sample A pH 7.4	Sample B pH 7.4
(h)	Absorbance		
0.0	0.056	0.099	0.106
0.5	0.091	0.110	0.140
1.0	0.067	0.110	0.151
2.0	0.069	0.230	0.235
4.0	0.105	0.268	0.239
6.0	0.077	0.270	0.241
8.0	0.095	0.412	0.520

Table 3.2.2.7 Data presentation for set A (49c) for calculation of the rate constant k

Time (h)	Absorb-ance	Conc. of (49) (ug/ml)	x (ug/ml)	(y-x) (ug/ml)	(y-x) (mol/litre)	Log(y-x)	Calculated Log(y-x)
0	0.099	1.33	0	978.82	$2.498*10^{-3}$	-2.602	-2.6027
0.5	0.11	1.93	0.96	977.86	$2.495*10^{-3}$	-2.603	-2.6030
1	0.118	2.09	1.22	977.60	$2.494*10^{-3}$	-2.603	-2.6032
2	0.230	4.32	4.80	974.02	$2.485*10^{-3}$	-2.605	-2.6037
4	0.256	4.84	5.64	973.18	$2.483*10^{-3}$	-2.605	-2.6047
6	0.260	4.92	5.76	973.06	$2.483*10^{-3}$	-2.605	-2.6057
8	0.412	7.96	10.63	968.19	$2.470*10^{-3}$	-2.607	-2.6067

Figure 3.2.2.4 Graphical presentation for calculated log(y-x) values vs time for samples A and B of (49c)

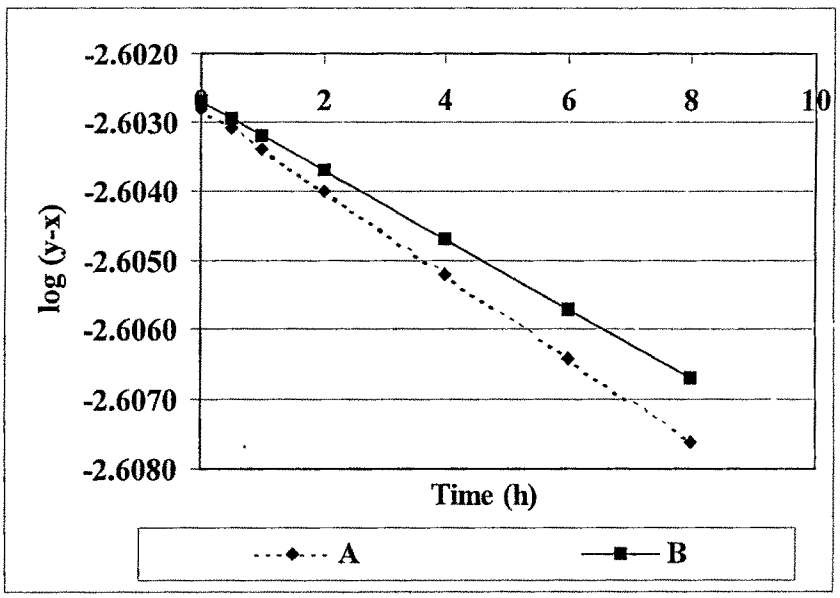

Table 3.2.2.8 The absorbance readings of (49) for the studies of (49d) in buffers

Time	pH 2.0	Sample A pH 7.4	Sample B pH 7.4	Sample C pH 7.4
(h)	Absorbance			
0.0	0.165	0.278	0.369	0.228
0.5	0.216	0.352	0.450	0.298
1.0	0.198	0.350	0.480	0.321
2.0	0.168	0.540	0.563	0.419
4.0	0.171	0.716	0.669	0.665
6.0	0.153	0.314 (1:2)	0.295 (1:2)	0.735 (1:2)
8.0	0.151	0.386 (1:2)	0.318 (1:2)	0.890 (1:2)

Table 3.2.2.9 Data presentation for set A (49d) for calculation of the rate constant k

Time (h)	Absorb-ance	Conc. of (49) (ug/ml)	x (ug/ml)	(y-x) (ug/ml)	(y-x) (mol/litre)	Log(y-x)	Calculated Log(y-x)
0	0.278	3.22	0	950.18	$2.515*10^{-3}$	-2.600	-2.6007
0.5	0.352	6.76	5.47	944.71	$2.500*10^{-3}$	-2.602	-2.6015
1	0.358	6.88	5.66	944.52	$2.500*10^{-3}$	-2.602	-2.6023
2	0.54	10.51	11.28	938.90	$2.485*10^{-3}$	-2.605	-2.6039
4	0.716	14.02	16.71	933.47	$2.470*10^{-3}$	-2.607	-2.6071
6	0.314 (1:2)	18.00	22.86	927.32	$2.454*10^{-3}$	-2.610	-2.6103
8	0.386 (1:2)	22.31	29.53	920.65	$2.436*10^{-3}$	-2.613	-2.6135

Figure 3.2.2.5 Graphical presentation for calculated log(y-x) values vs time for samples A, B and C of (49d)

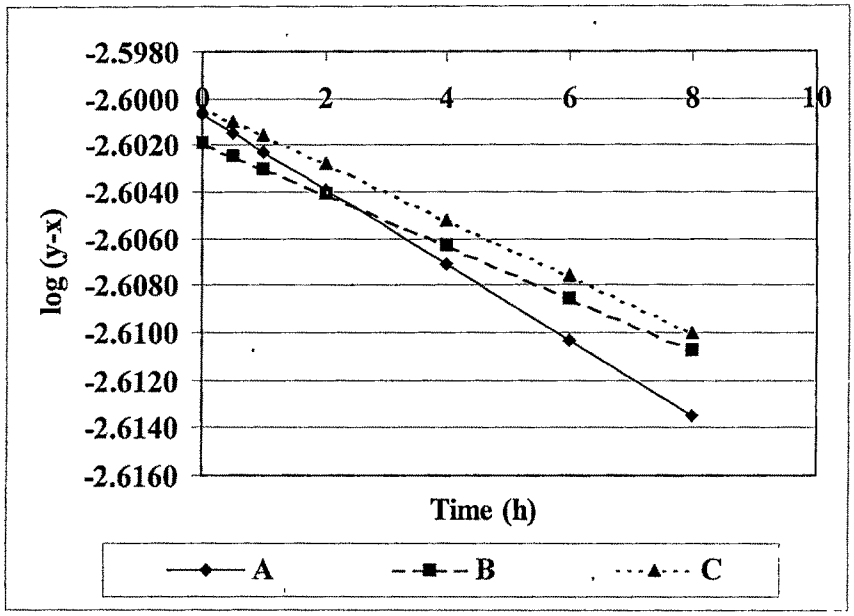

Table 3.2.2.10 The absorbance readings of (49) for the studies of (49e) in buffers

Time	pH 2.0	Sample A pH 7.4	Sample B pH 7.4
(h)	Absorbance		
0.0	0.041	0.104	0.081
0.5	0.067	0.215	0.131
1.0	0.071	0.326	0.277
2.0	0.027	0.361	0.326
4.0	0.095	0.409	0.389
6.0	0.063	0.427	0.413
8.0	0.081	0.511	0.463

Table 3.2.2.11 Data presentation for set A (49e) for calculation of rate constant, k

Time (h)	Absorb-ance	Conc. of (49) (ug/ml)	x (ug/ml)	(y-x) (ug/ml)	(y-x) (mol/litre)	Log(y-x)	Calculated Log(y-x)
0	0.104	1.04	0	983.23	$2.496*10^{-3}$	-2.603	-2.6046
0.5	0.215	4.02	4.81	978.42	$2.484*10^{-3}$	-2.605	-2.6049
1	0.326	6.24	8.38	974.85	$2.475*10^{-3}$	-2.606	-2.6052
2	0.361	6.94	9.51	973.72	$2.472*10^{-3}$	-2.607	-2.6058
4	0.409	7.90	11.06	972.17	$2.468*10^{-3}$	-2.608	-2.6070
6	0.427	8.26	11.63	971.60	$2.467*10^{-3}$	-2.608	-2.6082
8	0.511	9.93	14.34	968.89	$2.460*10^{-3}$	-2.609	-2.6094

Figure 3.2.2.6 Graphical presentation for calculated log(y-x) values vs time for samples A and B of (49e)

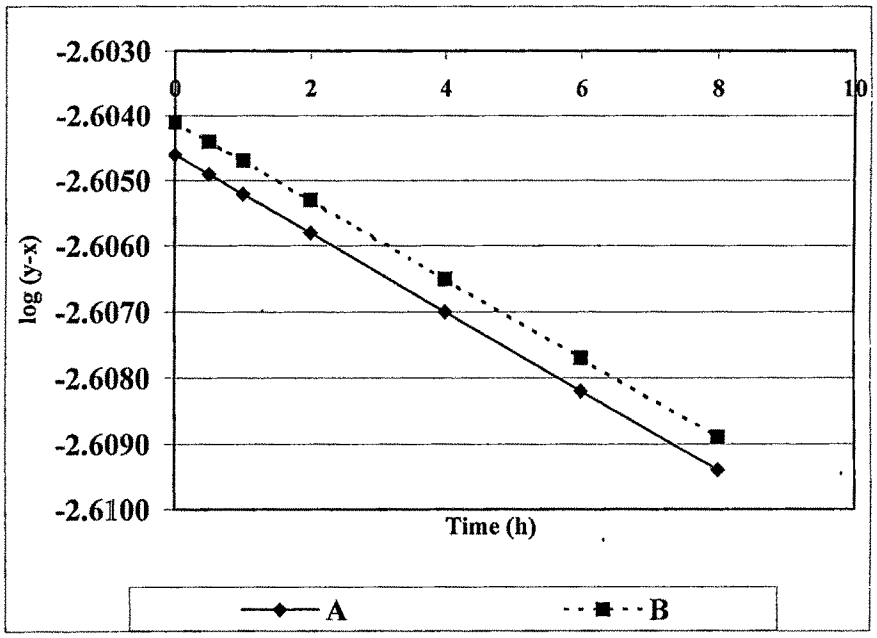

Table 3.2.2.12 The absorbance readings of (49) for the studies of (49f) in buffers

Time (h)	pH 2.0	Sample A pH 7.4	Sample B pH 7.4
	Absorb.	Absorb.	Absorb.
0.0	0.099	0.072	0.096
0.5	0.078	0.096	0.114
1.0	0.039	0.086	0.104
2.0	0.030	0.075	0.090
4.0	0.131	0.083	0.107
6.0	0.029	0.101	0.115
8.0	0.061	0.065	0.081

Table 3.2.2.13 Chemical Hydrolyses of Derivatives (49a-e)

Compound	t ½ (h) pH7.4 Buffer
49a	121
49b	153
49c	505
49d	250
49e	491

No observable hydrolysis was observed for all the derivatives of flurbiprofen (**49**) in buffer of pH 2.0. The tropinol derivative (**49f**) did not show any hydrolysis even in buffer (pH 7.4) till 8 hours as was observed earlier for the derivative (**45f**). The long half-lives (121-505 h) observed for these derivatives (**49a-e**) in buffer (pH 7.4) clearly indicate that they would be stable for sufficient period of time to be absorbed intact from the GIT and would successfully block the direct contact effect of flubiprofen (**49**).

3.2.2.2 Hydrolyses studies in serum

The basic principle underlying the evaluation of the derivatives (**49a-f**) for their *in vitro* enzymatic susceptibility in pooled human serum was similar to that described for the study of the compounds (**45a-f**) in human serum. A test solution of concentration (1.0 mg/ml) was maintained in human serum at 37±1°C. Aliquots (0.5 ml) upon withdrawal were treated with TCA (to arrest chemical and enzymatic hydrolyses) and the protein-precipitated solution was extracted with n-hexane, dried and the absorbance measured at 237 nm against a blank obtained by giving similar treatment without the derivative solution. Here, absorbance were directly measured for the n-hexane extracts because unlike chloroform, no emulsification was observed in case of n-hexane with the serum proteins giving a clear separate organic layer. The concentration of the parent drug (**49**) was calculated using Equation-4. The percent release of the parent NSAID from **49a** was determined as described for **45a,** from the absorbance readings given in Table 3.2.2 14. The absorbance data for studies of (**49b-c**) and (**49d-f**) are given in Tables 3.2.2.14 and 3.2.2.15 respectively. The percent release of parent drug (**49**) from the derivatives (**49a-e**) are tabulated in Table 3.2.2.16.

Table 3.2.2.14 The absorbance data for studies of (49a-c) in human serum 80%)

Time (min)	49a (Sample A and B) Absorbance		49b (Sample A and B) Absorbance		49c (Sample A and B) Absorbance	
	A	B	A	B	A	B
15	0.341	0.280	0.667	0.559	0.186	0.151
30	0.481	0.408	0.750	0.595	0.188 (1:2)	0.201 (1:2)
60	0.398 (1:3)	0.367 (1:3)	0.753	0.690	0.209 (1:2)	0.216 (1:2)
120	0.456 (1:3)	0.505 (1:3)	0.412 (1:3)	0.378 (1:3)	0.268 (1 2)	0.228 (1 2)

Table 3.2.2.15 The absorbance data for studies of (49d-f) in human serum (80%)

Time (min)	49d (Sample A and B) Absorbance		49e (Sample A and B) Absorbance		49f (Sample A and B) Absorbance	
	A	B	A	B	A	B
15	0.233	0.241	0.160	0.124	0.071	0.059
30	0.248	0.322	0.159 (1:1)	0.139 (1:1)	0.060	0.065
60	0.273 (1:1)	0.316 (1:1)	0.192 (1:1)	0.187 (1:1)	0.059	0.067
120	0.374 (1:1)	0.434 (1:1)	0.265 (1:1)	0.226 (1:1)	0.083	0.052

Table 3.2.2.16 Enzymatic Hydrolyses of Derivatives (49a-e)

Compound	% Release of parent NSAID 49) (80% human serum)		
	½ h	1 h	2h
49a	13.3	41.9	51.0
49b	17.1	17.2	43.9
49c	15.2	19.6	31.9
49d	11.9	15.4	29.9
49e	4.5	8.0	17.9
49f	0.0	0.0	0.0

It can be seen from the contents of Table 3.2.2.16 that the compound (**49f**) did not show any enzymatic hydrolysis in serum whereas rest of the derivatives (**49a-e**) were observed to liberate the parent drug. These results suggest that except for **49f** all the other derivatives would undergo enzymatic cleavage in the circulation following absorption from GIT, to liberate the parent drug for eliciting the desired anti-inflammatory activity.

3.2.3. HYDROLYSES STUDIES OF DERIVATIVES OF DICLOFENAC (51a-e)

3.2.3.1 Hydrolyses studies in buffers

The derivatives (**51a-e**) were evaluated for their stability in buffers (pH 2.0 and 7.4). The calibration curve was prepared for estimating diclofenac (**51**) released and was based on

the principle discussed for the estimation of biphenylacetic acid (**45**) in buffers (pH 2.0 and 7.4). Solutions of diclofenac were prepared in alkaline medium and partitioned into chloroform in acidic medium followed by extraction into sodium hydroxide solution (0 1 N), heating of the aqueous extract (to remove the traces of chloroform) and measuring the absorbance at λ_{max} (274 nm) of diclofenac (**51**). Three sets of determinations were made and regressed to give Equation-5. The absorbance data for the calibration curve and the graphical presentation of the regressed line obtained, proving the linearity of the data has been given in Table 3.2.3.1 and Figure 3.2.3.1. Beer-Lambert law was observed to follow in the range of 5-40 ug/ml.

Table 3.2.3.1 Calibration curve data for estimating diclofenac (51) in buffers

Sr. No	Concentration ug/ml	Absorbance		Regressed values
		A	B	C
1	5.0	0.222	0.175	0.178
2	10.0	0.312	0.276	0.322
3	15.0	0.471	0.471	0.467
4	20.0	0.614	0.605	0.611
5	25.0	0.760	0.751	0.755
6	30.0	0.909	0.889	0.899
7	35.0	1.026	1.078	1.044
8	40.0	1.193	1.175	1.188

$A = 0.0289*C - 0.0337$ Equation-5

$r = 0.998$, $s = 0.0203$

[A = absorbance, C = concentration (ug/ml)]

Figure 3.2.3.1 Calibration plot for estimating diclofenac (51) in buffers

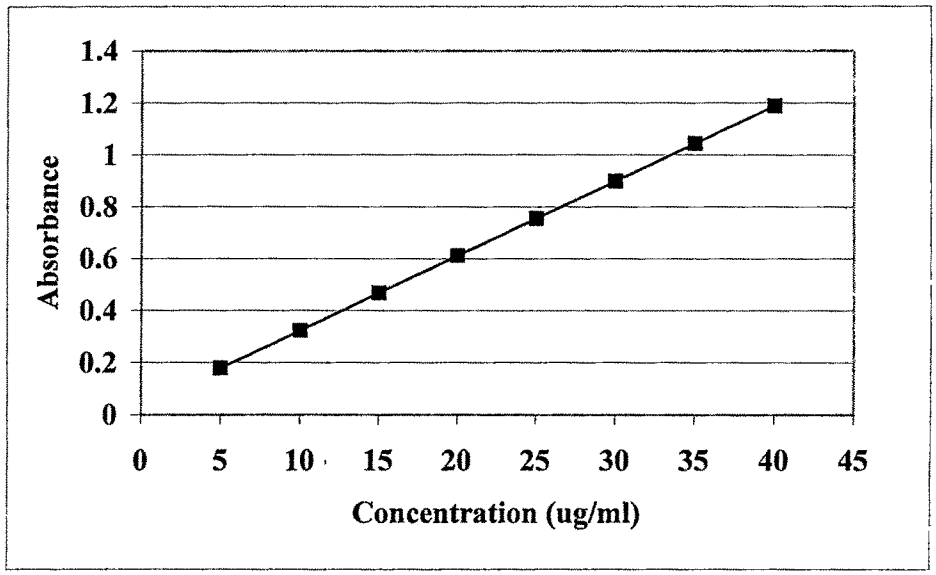

Solution of the derivative (**51a**) (1 mg/ml) was maintained at 37 ± 1°C. Aliquots (1.0 ml) were withdrawn at different time intervals and after bringing the pH to acidic side (~2), the aliquots were extracted into chloroform followed by further reextraction of organic layer into sodium hydroxide solution, heating the aqueous solution to expel off traces of chloroform and measuring the absorbance at 274nm. The absorbance data was given mathematical treatment to give the rate constant as described for compound (**45a**). The absorbance readings are given in Table 3.2.3.2 for derivative (**51a**) followed by the data for calculating the rate constant in Table 3.2.3.3. The plots proving that the hydrolysis of **51a** follows psuedo-first order kinetics has been presented graphically in figure 3.2.3.2.

Kinetic studies in buffer solutions (pH 2.0 and 7.4) were performed for rest of the other derivatives (**51b-e**) exactly in the same way as described above for derivative (**51a**) The absorbance and rate constant calculation data are shown in Tables 3.2.3.4 to 3.2.3.11, and the graphical representations are shown in Figures 3.2.3.3 to 3.2.3.6 Half-lives of all the derivatives (**51a-e**) have been shown in Table 3.2.3.12 in buffer solution (pH 7.4).

Table 3.2.3.2 The absorbance readings of (51) for the studies of (51a) in buffers

Time	pH 2.0	Sample A pH 7.4	Sample B pH 7.4	Sample C pH 7.4
(h)	Absorbance			
0.0	0.22	0.029	0.045	0.057
0.5	0.36	0.154	0.159	0.131
1.0	0.33	0.214	0.240	0.217
2.0	0.27	0.339	0.356	0.314
4.0	0.26	0.457	0.463	0.432
6.0	0.27	0.474	0.561	0.439
8.0	0.32	0.684	0.650	0.639

Table 3.2.3.3 Data presentation for set A (51a) for calculation of the rate constant k

Time (h)	Absorb-ance	Conc. of (51) (ug/ml)	x (ug/ml)	(y-x) (ug/ml)	(y-x) (mol/litre)	Log(y-x)	Calculated Log(y-x)
0	0.029	0.67	0	999.08	$2.474*10^{-3}$	-2.607	-2.608
0.5	0.154	4.16	4.78	994.30	$2.462*10^{-3}$	-2.609	-2.609
1	0.214	6.24	7.62	991.46	$2.455*10^{-3}$	-2.610	-2.610
2	0.339	10.56	13.54	985.54	$2.440*10^{-3}$	-2.613	-2 611
4	0.457	14.65	19.13	979.95	$2.426*10^{-3}$	-2.615	-2.614
6	0.474	15.24	19.93	979.15	$2.424*10^{-3}$	-2.615	-2.617
8	0.684	22.50	29.87	969.21	$2.400*10^{-3}$	-2.620	-2.619

Figure 3.2.3.2 Graphical presentation for calculated log(y-x) values vs time for samples A and B (51a)

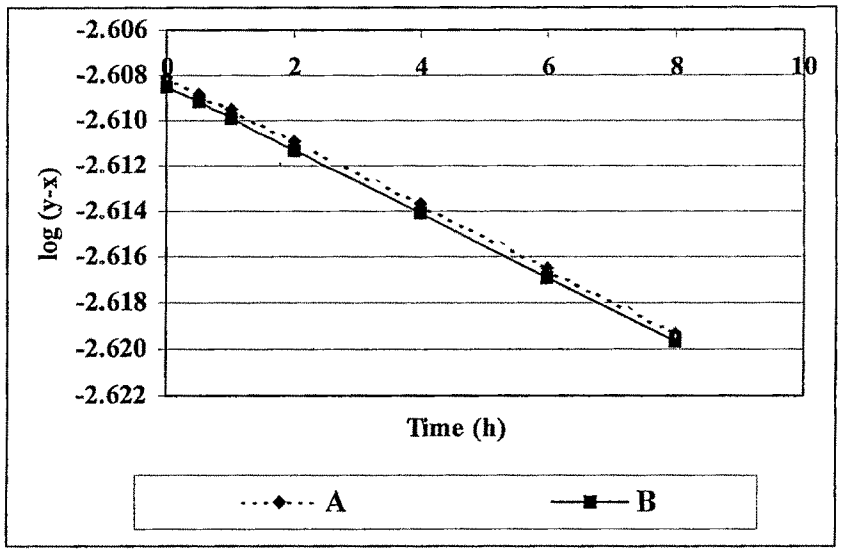

Table 3.2.3.4 The absorbance readings of (51) for the studies of (51b) in buffers

Time	pH 2.0	Sample A pH 7.4	Sample B pH 7.4	Sample C pH 7.4
(h)	Absorbance			
0.0	0.048	0.034	0.045	0.078
0.5	0.054	0.062	0.081	0.083
1.0	0.065	0.071	0.104	0.106
2.0	0.076	0.098	0.192	0.139
4.0	0.087	0.176	0.226	0.178
6.0	0.039	0.301	0.286	0.292
8.0	0.045	0.394	0.331	0.401

Table 3.2.3.5 Data presentation for set A (51b) for calculation of the rate constant k

Time (h)	Absorb-ance	Conc. of (51) (ug/ml)	x (ug/ml)	(y-x) (ug/ml)	(y-x) (mol/litre)	Log(y-x)	Calculated Log(y-x)
0	0.034	0.82	0	998.94	$2.313*10^{-3}$	-2.636	-2.6350
0.5	0.062	0.98	0.23	998.71	$2.312*10^{-3}$	-2.636	-2.6355
1	0.071	1.29	0.69	998.25	$2.311*10^{-3}$	-2.636	-2.6360
2	0.098	2.22	2.06	996.88	$2.308*10^{-3}$	-2.637	-2.6370
4	0.176	4.92	6.01	992.93	$2.299*10^{-3}$	-2 638	-2.6390
6	0.301	9.25	12.34	986.60	$2.284*10^{-3}$	-2.641	-2.6410
8	0.394	12.47	17.05	981.89	$2.273*10^{-3}$	-2.643	-2.6430

Figure 3.2.3.3 Graphical presentation for calculated log(y-x) values vs time for samples A and B of (51b)

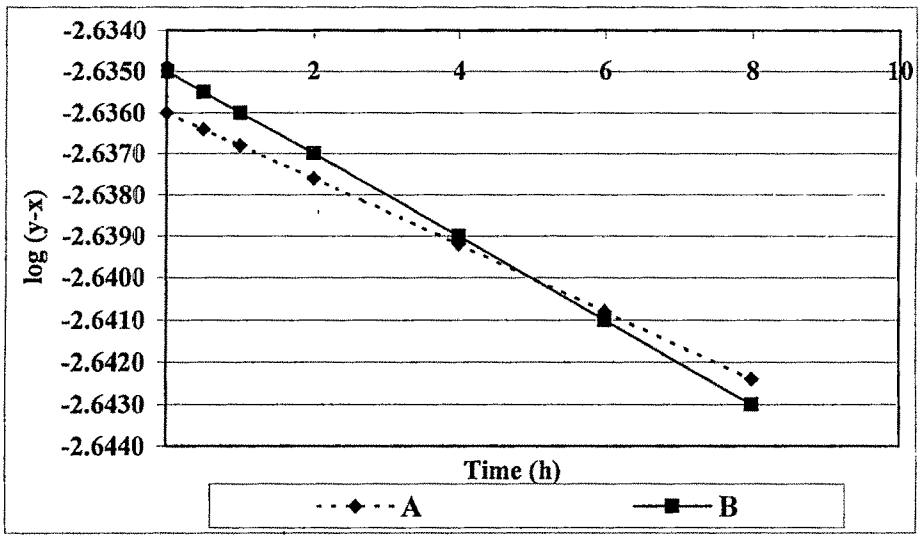

Table 3.2.3.6 The absorbance readings of (51) for the studies of (51c) in buffers

Time	pH 2.0	Sample A pH 7.4	Sample B pH 7.4	Sample C pH 7.4
(h)	Absorbance			
0.0	0.022	0.011	0.039	0.022
0.5	0.045	0.046	0.059	0.044
1.0	0.061	0.058	0.079	0.047
2.0	0.035	0.078	0.126	0.09
4.0	0.039	0.139	0.143	0.146
6.0	0.047	0.185	0.173	0.198
8.0	0.054	0.194	0.228	0 210

Table 3.2.3.7 Data presentation for set A (51c) for calculation of the rate constant k

Time (h)	Absorb-ance	Conc. of (51) (ug/ml)	x (ug/ml)	(y-x) (ug/ml)	(y-x) (mol/litre)	Log(y-x)	Calculated Log(y-x)
0	0.011	0.26	0	999.79	$2.253*10^{-3}$	-2.647	-2.6472
0.5	0.046	0.43	0.25	999.54	$2.252*10^{-3}$	-2 647	-2.6475
1	0.058	0.84	0.87	998.92	$2.251*10^{-3}$	-2.648	-2.6477
2	0.078	1.53	1.91	997.88	$2.249*10^{-3}$	-2.648	-2.6482
4	0.139	3.64	5.09	994.70	$2.241*10^{-3}$	-2.649	-2.6492
6	0.185	5.24	7.48	992.31	$2.236*10^{-3}$	-2.651	-2.6502
8	0.194	5.55	7.95	991.84	$2.235*10^{-3}$	-2.651	-2.6512

Figure 3.2.3.4 Graphical presentation for calculated log(y-x) values vs time for samples A and B of (51c)

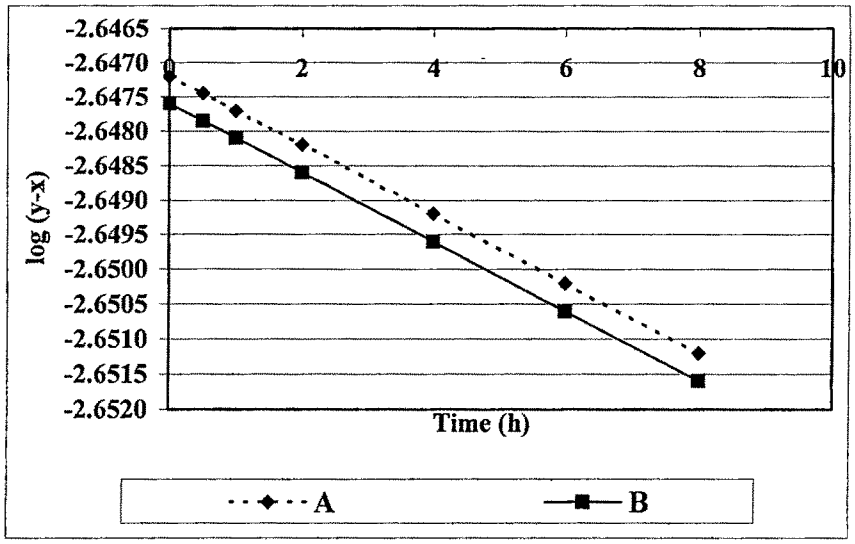

Table 3.2.3.8 The absorbance readings of (51) for the studies of (51d) in buffers

Time	pH 2.0	Sample A pH 7.4	Sample B pH 7.4	Sample C pH 7.4
(h)	Absorbance			
0.0	0.037	0.037	0.033	0.052
0.5	0.048	0.091	0.084	0.108
1.0	0.055	0.143	0.133	0.162
2.0	0.067	0.220	0.205	0.225
4.0	0.071	0.304	0.302	0.323
6.0	0.068	0.347	.0352	0.356
8.0	0.059	0.419	0.438	0.390

Table 3.2.3.9 Data presentation for set A (51d) for calculation of the rate constant k

Time (h)	Absorb-ance	Conc. of (51) (ug/ml)	x (ug/ml)	(y-x) (ug/ml)	(y-x) (mol/litre)	Log(y-x)	Calculated Log(y-x)
0	0.037	0.26	0	999.62	$2.326*10^{-3}$	-2.633	-2.6344
0.5	0.091	1.98	2.51	997.11	$2.320*10^{-3}$	-2.634	-2.6349
1	0.143	3.78	5.13	994.49	$2.314*10^{-3}$	-2.636	-2.6354
2	0.22	6.45	9.01	990.61	$2.305*10^{-3}$	-2.637	-2.6364
4	0.304	9.35	13.24	986.38	$2.295*10^{-3}$	-2.639	-2.6384
6	0.347	10.84	15.41	984.21	$2.290*10^{-3}$	-2.640	-2.6404
8	0.419	13.33	19.03	980.59	$2.282*10^{-3}$	-2.642	-2.6424

Figure 3.2.3.5 Graphical presentation for calculated log(y-x) values vs time for samples A ,B and C of (51d)

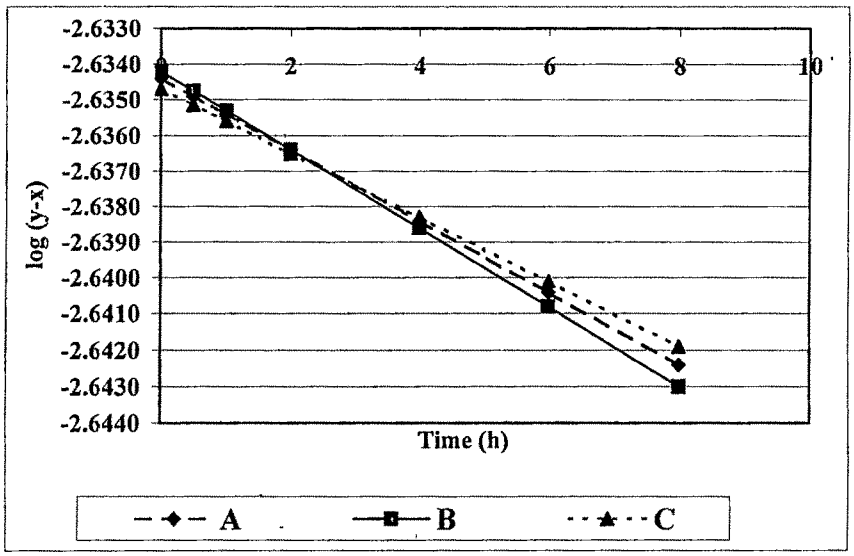

Table 3.2.3.10 The absorbance readings of (51) for the studies of (51e) in buffers

Time	pH 2.0	Sample A pH 7.4	Sample B pH 7.4
(h)	Absorbance		
0.0	0.030	0.036	0.037
0.5	0.057	0.120	0.053
1.0	0.045	0.169	0.254
2.0	0.065	0.236	0.365
4.0	0.075	0.356	0.370
6.0	0.039	0.412	0.420
8.0	0.065	0.439	0.465

Table 3.2.3.11 Data presentation for set A (51e) for calculation of rate constant k

Time (h)	Absorb-ance	Conc. of (51) (ug/ml)	x (ug/ml)	(y-x) (ug/ml)	(y-x) (mol/litre)	Log(y-x)	Calculated Log(y-x)
0	0.036	0.31	0	999.69	$2.242*10^{-3}$	-2.649	-2.6508
0.5	0.12	2.99	4.04	995.65	$2.233*10^{-3}$	-2.651	-2.6514
1	0.169	4.68	6.60	993.09	$2.227*10^{-3}$	-2.652	-2.6519
2	0.236	7.00	10.11	989.58	$2.219*10^{-3}$	-2.654	-2.6530
4	0.356	11.15	16.38	983.31	$2.205*10^{-3}$	-2.657	-2.6552
6	0.412	13.09	19.31	980.38	$2.199*10^{-3}$	-2.658	-2.6574
8	0.439	14.02	20.72	978.97	$2.196*10^{-3}$	-2.658	-2.6596

Figure 3.2.3.6 Graphical presentation for calculated log(y-x) values vs time for samples A and B (51e)

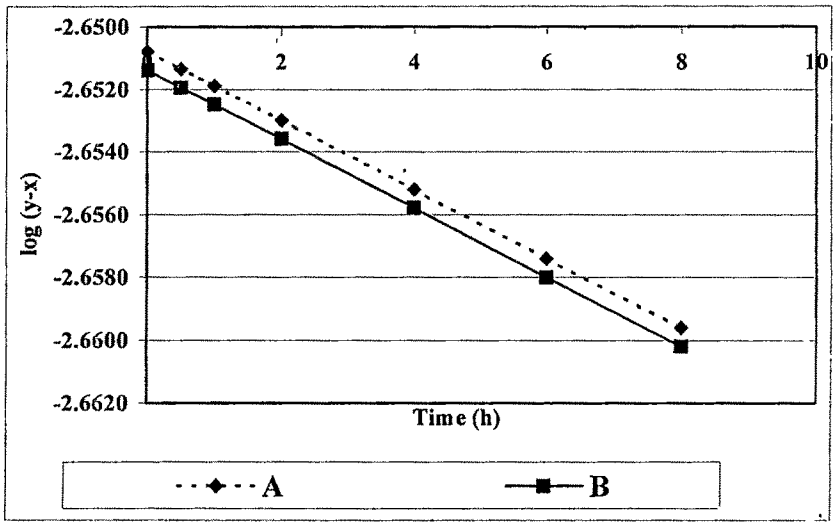

3.2.3.12 Chemical Hydrolyses of Derivatives (51a-e)

Compound	$t_{½}$ (h) pH7.4 Buffer
51a	208
51b	369
51c	317
51d	295
51e	271

The derivatives (**51a-e**) showed no noticeable hydrolysis in buffer (pH 2.0) till 8 hours. However, the half-lives ranging from 208-369 hours was observed for these derivatives in buffer pH 7.4. Looking at the high stability of these derivatives in both the buffers it can be expected that they would be stable for sufficient time period in GIT so as to allow their absorption in the intact form and thereby prevent the local GI irrtaition of the parent compound (**51**) by successfully blocking the acidic carboxyl group.

3.2.3.2 Hydrolyses studies in human serum (80%)

Calibration curve for estimating diclofenac (**51**) upon hydrolysis of derivatives (**51a-e**) in human serum was prepared based upon the principle described for estimating

4-biphenylacetic acid (**45**) in the studies for derivatives (**45a-f**) performed in human serum. Solutions of diclofenac (**51**) with varying concentrations were prepared in sodium hydroxide solution (0.1 N) and the same sequence of extraction and reextraction was carried out as described in case of **45** before taking the absorbance readings on the UV spectrophotometer at the UV maximum (274 nm) of diclofenac. Beer-Lambert law was followed in the range of 5-40 ug/ml. Two closest observations were regressed to give Equation-6 and the regressed values are given in Table 3.2.3.13 and represented by graph in Figure 3.2.3.7.

Table 3.2.3.13 Calibration curve data for estimating diclofenac (51) in serum

Sr. No	Concentration ug/ml	Absorbance		Regressed values
		A	B	C
1	5.0	0.244	0.256	0.198
2	10.0	0.412	0.329	0.369
3	20.0	0.633	0.686	0.710
4	30.0	0.943	1.074	1.051
5	40.0	1.503	1.373	1.392

A = 0.0341*C - 0.0283 Equation-6

r = 0.992, s = 0.0582

[A = absorbance, C = concentration (ug/ml)]

Figure 3.2.3.7 Calibration plot for estimating diclofenac (51) in serum

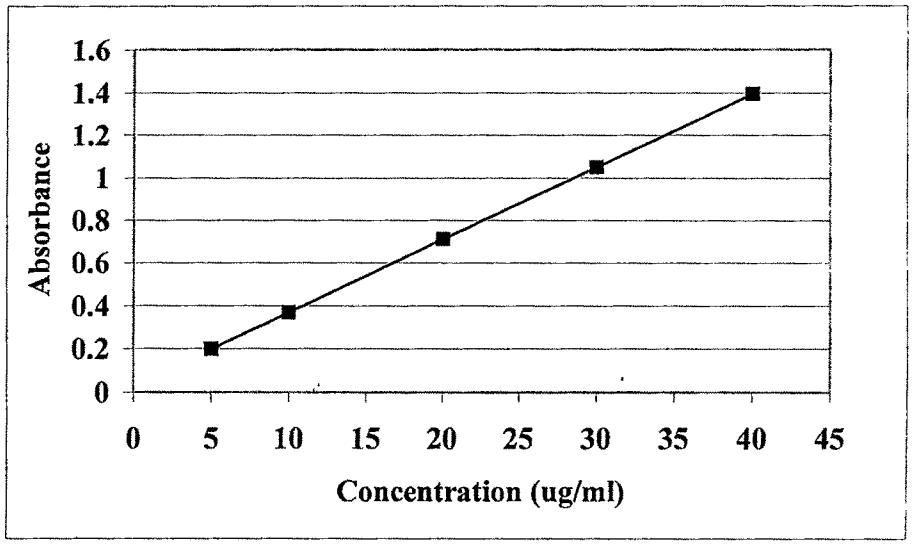

The UV spectrophotometric method adopted for evaluation of the enzymatic susceptibility of the derivatives (**51a-e**) to release the parent drug (**51**) was based on the same principle as discussed for estimating 4-biphenylacetic acid (**45**) in the study of compounds (**45a-f**) in serum. A stock solution of **51a** (1 mg/ml) in human serum was maintained at 37±1°C. Aliquots (0.5 ml) were treated with trichloroacetic acid (TCA, 10%, 1.0 ml) to arrest further (chemical and enzymatic) hydrolysis by deactivating the serum proteins (enzymes) as well as bringing the pH to acidic side. The acidified solution was extracted into isopropyl ether. The organic extract was further extracted with sodium hydroxide solution (0.1 N), heated on a water bath and the absorbance was measured at 274 nm. Concentration of the parent drug (**51**) was calculated using the Equation-6. Samples were analysed in duplicate and the average percent release of diclofenac was determined. The absorbance data for compounds (**51a-c**) and (**51d-e**) are given in Tables 3.2.3.14 – 3.2.3.15. The percent release of diclofenac from each derivative has been given in Table 3.2.3.16.

Table 3.2.3.14 The absorbance data for the studies of (51a-c) in human serum (80%)

Time (min)	51a (Sample A and B) Absorbance		51b (Sample A and B) Absorbance		51c (Sample A and B) Absorbance	
	A	B	A	B	A	B
15	0.421	0.479	0.387	0.349	0.162	0.189
30	0.533	0.583	0.518	0.410	0.193	0.245
60	0.495 (1:1)	0.600 (1:1)	0.717	0.611	0.208	0.275
120	0.371 (1:2)	0.292 (1:2)	0.909	0.854	0.326	0.315

Table 3.2.3.15 The absorbance data for studies of (51d-e) in human serum (80%)

Time (min)	51d (Sample A and B) Absorbance		51e (Sample A and B) Absorbance	
	A	B	A	B
15	0.181	0.156	0.243	0.198
30	0.192	0.195	0.272	0.252
60	0.254	0.275	0.346	0.317
120	0.260	0.283	0.666	0.579

Table 3.2.3.16 Enzymatic Hydrolyses of Derivatives (51a-e)

Compound	% Release of parent NSAID 51) (80% human serum)		
	½ h	1 h	2h
51a	38.6	72.9	80.5
51b	39.6	56.6	73.1
51c	13.7	15.0	23.1
51d	11.7	20.2	26.4
51e	20.9	22.9	55.7

The results of Table 3.2.1.16 for the derivatives (**51a-e**), show a good enzymatic susceptibility for all these compounds towards esterases liberating the parent drug diclofenac (**51**) at different rates. These results confirm that after absorption from GIT all the derivatives (**51a-e**) would successfully cleave off to release the parent drug, which would then elicit the desired pharmacological activity.

3.2.4. HYDROLYSES STUDIES OF DERIVATIVES OF INDOMETHACIN(54a-e)

3.2.4.1 Hydrolyses studies in buffers

The derivatives (**54a-e**) were studied for their stability in buffers (pH 2.0 and 7.4). Indomethacin has been reported[110] to be unstable in strongly alkaline medium so for preparing the calibration curve for estimating indomethacin, its stock solution was prepared in methanol and dilutions were made with buffer pH 7.4. However, the method using n-hexane as described for compound (**49**) could not be applied in case of indomethacin due to the lesser solubility of indomethacin in this solvent.

Attempt was made to prepare the calibration curve based on the principle as described for studies carried in buffers for the derivatives of 4-biphenylacetic acid (**45**). The stock solution of indomethacin (**54**) was prepared in methanol followed by dilutions in buffer (pH 7.4). The aliquots were acidified and extracted into chloroform, further reextracted with sodium hydroxide solution, heated the aqueous extract and cooled to room temperature. But during the absorbance measurements it was found that the aqueous extracts showed no absorbances in the whole UV range indicating the degradation of indomethacin under these conditions. Such a conclusion was made since, solutions of indomethacin in sodium hydroxide were found to be stable by us, upto a period of 2 hours only, at room temperature with UV maximum at 229nm (reported[110] is 227 nm in methanol). Degradation took place upon heating the solutions for 10 minutes in water bath which was indicated by the absence of UV maximum at 229 nm for these solutions. Hence, this method was found unsuitable for preparing the calibration curve.

It was thought of removing chloroform from the chloroform extracts obtained in the above said method and then dissolving the residue in methanol followed by measurement of the absorbance. This would have avoided the steps of partitioning of indomethacin

(**54**) present in chloroform into sodium hydroxide solution but, as discussed in case of derivatives (**45** and **51**), the problem posed by chloroform with the studies to be done in serum was known to us. So, it was thought of replacing chloroform with a suitable solvent, which would not pose emulsification problem while using it for extracting indomethacin from the serum solutions.

We had a choice between isopropyl ether or diethyl ether, both of which show good solubility for indomethacin (**54**). Diethyl ether was selected for extraction purpose due to its lower boiling point compared to that of isopropyl ether allowing a faster removal of the organic solvent. The stock solution of indomethacin (**54**) was prepared in methanol followed by dilutions in buffer of pH 7.4. The aliquots were acidified and extracted into solvent ether, the solvent removed under vacuum and the residue dissolved in methanol. The absorbance of the methanolic solution was measured at 227 nm. The experiment was repeated in triplicate and regression analysis performed to give Equation-7. Beer-Lambert law was followed in the range of 2-14 ug/ml. The regressed values are given in Table 3.2.4.1 and represented by a graph in Figure 3.2.4.1.

Table 3.2.4.1 Calibration curve data for estimating indomethacin (54) in buffers and pooled human serum (80%)

Sr. No	Concentration ug/ml	Absorbance			Regressed values
		A	B	C	D
1	2.0	0.159	0.183	0.176	0.154
2	4.0	0.291	0.285	0.300	0.288
3	6.0	0.416	0.396	0.423	0.421
4	8.0	0.549	0.535	0.541	0.555
5	10.0	0.685	0.652	0.647	0.689
6	12.0	0.785	0.842	0.835	0.823
7	14.0	0.971	0.993	0.996	0.957

$A = 0.0669*C + 0.0197$ Equation-7

$r = 0.996$ $s = 0.053$

[A = absorbance, C = concentration (ug/ml)]

Figure 3.2.4.1 Calibration plot for estimating indomethacin (54) in buffers and pooled 80% human serum

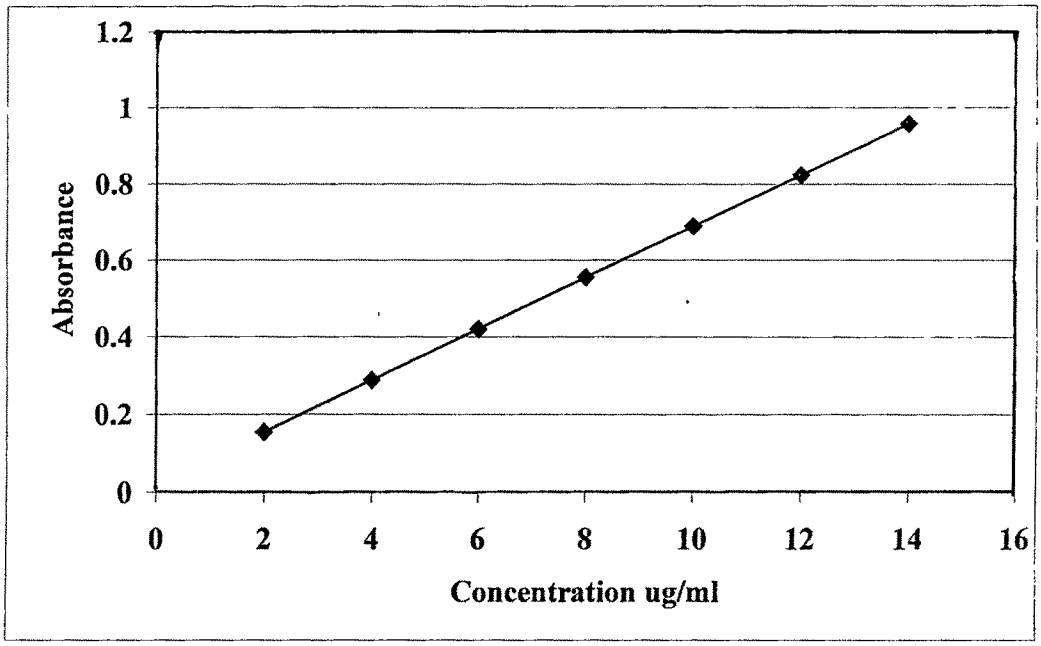

Solution of the derivative (**54a**) (1 mg/ml) was maintained at 37 ± 1°C. Aliquots (1.0 ml) were withdrawn at different time intervals and after bringing the pH to acidic side (~2), the aliquots were extracted into solvent ether, the solvent removed under vacuum and the residue dissolved in methanol. The absorbance of the methanolic solution was measured at 227 nm. The absorbance data was given mathematical treatment to give the rate constant as described for compound (**45a**). The absorbance readings are given in Table 3.2.4.2 for derivative (**54a**) followed by the data for calculating the rate constant in Table 3.2.4.3. The plots proving that the hydrolysis of **54a** follows psuedo-first order kinetics has been presented graphically in figure 3.2.4.2.

Kinetic studies in buffer solutions (pH 2.0 and 7.4) were performed for rest of the other derivatives (**54b-e**) exactly in the same way as described above for derivative (**54a**). The absorbance and rate constant calculation data are shown in Tables 3.2.4.4 to 3.2.4.11, and the graphical representations are shown in Figures 3.2.4.3 to 3.2.4.6. Half-lives of all the derivatives (**54a-e**) have been shown in Table 3.2.4.12 in buffer solution (pH 7.4).

Table 3.2.4.2 The absorbance readings of (54) for the studies of (54a) in buffers

Time	pH 2.0	Sample A pH 7.4	Sample B pH 7.4
(h)	Absorbance		
0.0	0.210 (1:9)	0.613 (1:6)	0.539 (1.6)
0.5	0.219 (1:9)	0.791 (1:6)	0.685 (1:6)
1.0	0.218 (1:9)	0.857 (1:6)	0.812 (1:6)
2.0	0.198 (1:9)	0.87 (1:6)	0.739 (1:6)
4.0	0.173 (1:9)	0.961 (1:6)	0.862 (1:6)
6.0	0.210 (1:9)	0.887 (1:7)	0.785 (1:7)

Table 3.2.4.3 Data presentation for set A (54a) for calculation of the rate constant k

Time (h)	Absorb-ance	Conc. of (54) (ug/ml)	x (ug/ml)	(y-x) (ug/ml)	(y-x) (mol/litre)	Log(y-x)	Calculated Log(y-x)
0	0.613 (1:6)	27.65	0	667.72	0.0016	-2.808	-2.838
0.5	0.791 (1:6)	80.70	63.76	603.96	0.0014	-2.851	-2.841
1	0.857 (1:6)	87.61	72.06	595.66	0.0014	-2.857	-2.845
2	0.870 (1:6)	88.97	73.69	594.03	0.0014	-2.859	-2.852
4	0.961 (1:6)	98.49	85.13	582.59	0.0014	-2.867	-2.867
6	0.887 (1:7)	103.71	91.41	576.31	0.0013	-2.872	-2.881

Figure 3.2.4.2 Graphical presentation for calculated log(y-x) values vs time for samples A and B of (54a)

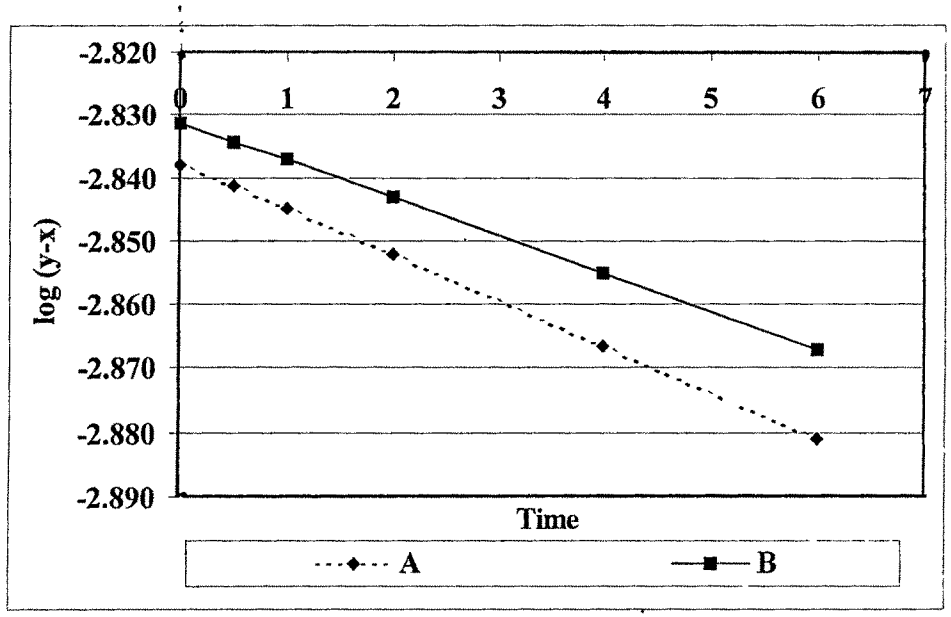

Table 3.2.4.4 The absorbance readings of (54) for the studies of (54b) in buffers

Time	pH 2.0	Sample A pH 7.4	Sample B pH 7.4
(h)	Absorbance		
0.0	0.162 (1:8)	0.519 (1:6)	0.487 (1:6)
0.5	0.166 (1:8)	0.614 (1:6)	0.621 (1:6)
1.0	0.16 (1:8)	0.693 (1:6)	0.726 (1:6)
2.0	0.173 (1:8)	0.737 (1:6)	0.801 (1:6)
4.0	0.147 (1:8)	0.859 (1:6)	0.865 (1:6)
6.0	0.169 (1:8)	0.916 (1:6)	0.937 (1:6)

Table 3.2.4.5 Data presentation for set A (54b) for calculation of the rate constant k

Time (h)	Absorb-ance	Conc. of (54) (ug/ml)	x (ug/ml)	(y-x) (ug/ml)	(y-x) (mol/litre)	Log(y-x)	Calculated Log(y-x)
0	0.519 (1:6)	21.39	0	726.14	$1.589*10^{-3}$	-2.799	-2 821
0.5	0.614 (1:6)	62.18	54.96	671.18	$1.469*10^{-3}$	-2.833	-2.825
1	0.693 (1:6)	70.45	65.54	660.60	$1.446*10^{-3}$	-2.840	-2.829
2	0.737 (1:6)	75.05	71.43	654.71	$1.433*10^{-3}$	-2.844	-2.837
4	0.859 (1:6)	87.82	87.78	638.36	$1.397*10^{-3}$	-2.855	-2.852
6	0.916 (1:6)	93.78	95.41	630.73	$1.380*10^{-3}$	-2.860	-2.867

Figure 3.2.4.3 Graphical presentation for calculated log(y-x) values vs time for samples A and B of (54b)

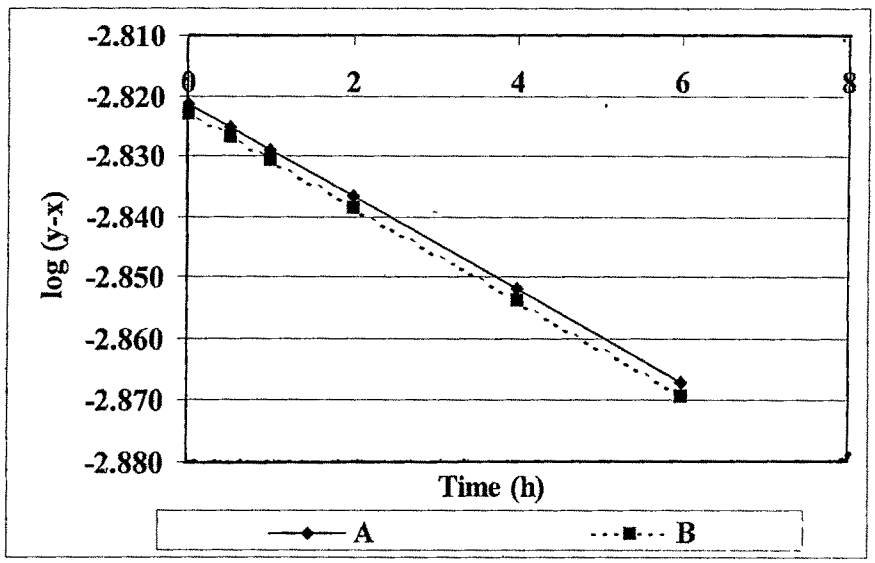

Table 3.2.4.6 The absorbance readings of (54) for the studies of (54c) in buffers

Time	pH 2.0	Sample A pH 7.4	Sample B pH 7.4	Sample C pH 7.4
(h)	Absorbance			
0.0	0.326 (1:5)	0.472 (1:5)	0.365 (1:5)	0.375
0.5	0.361 (1:5)	0.557 (1:5)	0.479 (1:5)	0.541
1.0	0.369 (1:5)	0.61 (1:5)	0.593 (1:5)	0.657 (1:4)
2.0	0.343 (1:5)	0.637 (1:5)	0.646 (1:5)	0.813 (1.4)
4.0	0.417 (1:5)	0.689 (1:5)	0.708 (1:5)	0.875 (1:4)
6.0	0.371 (1:5)	0.743 (1:5)	0.739 (1:5)	0.912 (1:4)

Table 3.2.4.7 Data presentation for set A (54c) for calculation of the rate constant k

Time (h)	Absorb-ance	Conc. of (54) (ug/ml)	x (ug/ml)	(y-x) (ug/ml)	(y-x) (mol/litre)	Log(y-x)	Calculated Log(y-x)
0	0.472 (1:5)	30.81	0	595.16	$1.269*10^{-3}$	-2.897	-2.908
0.5	0.557 (1:5)	48.19	22.84	572.32	$1.220*10^{-3}$	-2.914	-2.910
1	0.610 (1:5)	52.94	29.08	566.08	$1.207*10^{-3}$	-2.918	-2.912
2	0.637 (1:5)	55.36	32.26	562.90	$1.200*10^{-3}$	-2.921	-2.916
4	0.689 (1:5)	60.03	38.39	556.77	$1.187*10^{-3}$	-2.925	-2.925
6	0.743 (1:5)	64.87	44.75	550.41	$1.174*10^{-3}$	-2.930	-2.934

Figure 3.2.4.4 Graphical presentation for calculated log(y-x) values vs time for samples A and B of (54c)

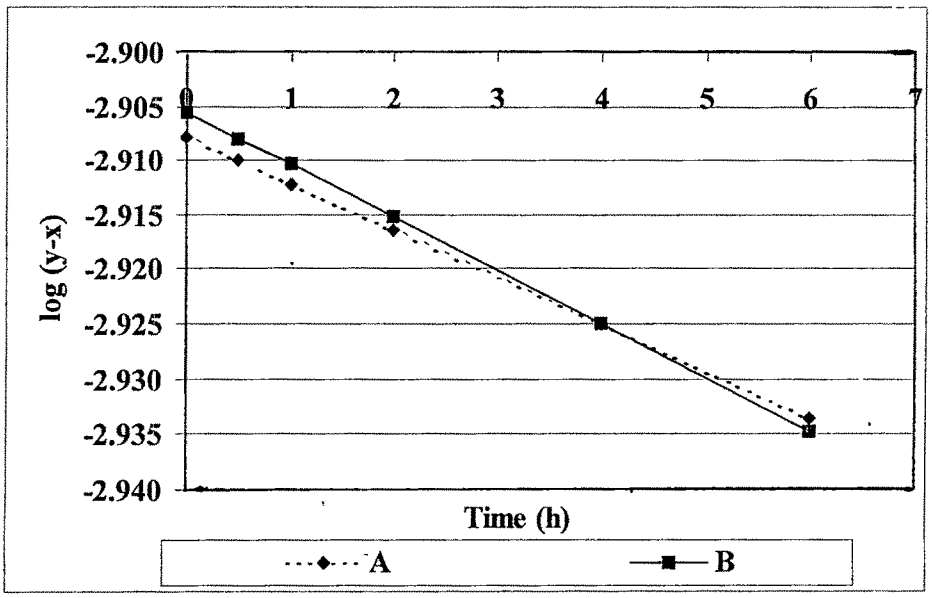

Table 3.2.4.8 The absorbance readings of (54) for the studies of (54d) in buffers

Time	pH 2.0	Sample A pH 7.4	Sample B pH 7.4
(h)	Absorbance		
0.0	0.269 (1:5)	0.352 (1:5)	0.413 (1:5)
0.5	0.284 (1:5)	0.41 (1:5)	0.436 (1:5)
1.0	0.323 (1:5)	0.487 (1:5)	0.479 (1:5)
2.0	0.296 (1:5)	0.52 (1:5)	0.531 (1:5)
4.0	0.335 (1:5)	0.543 (1:5)	0.562 (1:5)
6.0	0.269 (1:5)	0.592 (1:5)	0.613 (1:5)

Table 3.2.4.9 Data presentation for set A (54d) for calculation of the rate constant k

Time (h)	Absorb-ance	Conc. of (54) (ug/ml)	x (ug/ml)	(y-x) (ug/ml)	(y-x) (mol/litre)	Log(y-x)	Calculated Log(y-x)
0	0.352 (1:5)	25.26	0	678.02	$1.490*10^{-3}$	-2.827	-2.833
0.5	0.41 (1:5)	35.00	12.42	665.60	$1.463*10^{-3}$	-2 835	-2.835
1	0.487 (1:5)	41.91	21.22	656.80	$1.444*10^{-3}$	-2.841	-2.836
2	0.52 (1:5)	44.87	25.00	653.02	$1.435*10^{-3}$	-2.843	-2.839
4	0.543 (1:5)	46.93	27.63	650.39	$1.430*10^{-3}$	-2.845	-2.845
6	0.592 (1:5)	51.33	33.23	644.79	$1.417*10^{-3}$	-2.849	-2.851

Figure 3.2.4.5 Graphical presentation for calculated log(y-x) values vs time for samples A and B of (54d)

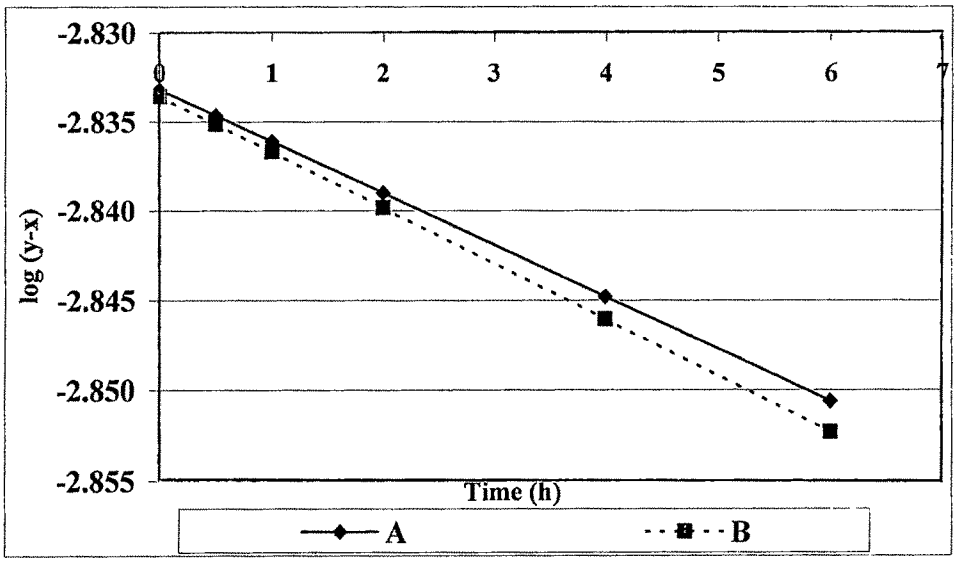

Table 3.2.4.10 The absorbance readings of (54) for the studies of (54e) in buffers

Time	pH 2.0	Sample A pH 7.4	Sample B pH 7.4
(h)	Absorbance		
0.0	0.256 (1:7)	0.317 (1:7)	0.289 (1·7)
0.5	0.289 (1:7)	0.365 (1:7)	0.317 (1:7)
1.0	0.312 (1:7)	0.413 (1:7)	0.365 (1:7)
2.0	0.291 (1:7)	0.435 (1:7)	0.419 (1:7)
4.0	0.265 (1:7)	0.517 (1:7)	0.467 (1:7)
6.0	0.275 (1:7)	0.620 (1:7)	0.570 (1:7)

Table 3.2.4.11 Data presentation for set A (54e) for calculation of rate constant k

Time (h)	Absorb-ance	Conc. of (54) (ug/ml)	x (ug/ml)	(y-x) (ug/ml)	(y-x) (mol/litre)	Log(y-x)	Calculated Log(y-x)
0	0.317 (1:7)	31.44	0	585.15	$1.243*10^{-3}$	-2.906	-2.911
0.5	0.365 (1:7)	41.29	13.00	572.15	$1.215*10^{-3}$	-2.915	-2.914
1	0.413 (1:7)	47.03	20.57	564.58	$1.199*10^{-3}$	-2.921	-2.917
2	0.435 (1.7)	49.66	24.04	561.11	$1.191*10^{-3}$	-2.924	-2.923
4	0.517 (1:7)	59.47	36.98	548.17	$1.164*10^{-3}$	-2.934	-2.935
6	0.620 (1:7)	71.78	53.23	531.92	$1.129*10^{-3}$	-2.947	-2.947

Figure 3.2.4.6 Graphical presentation for calculated log(y-x) values vs time for samples A and B of (54e)

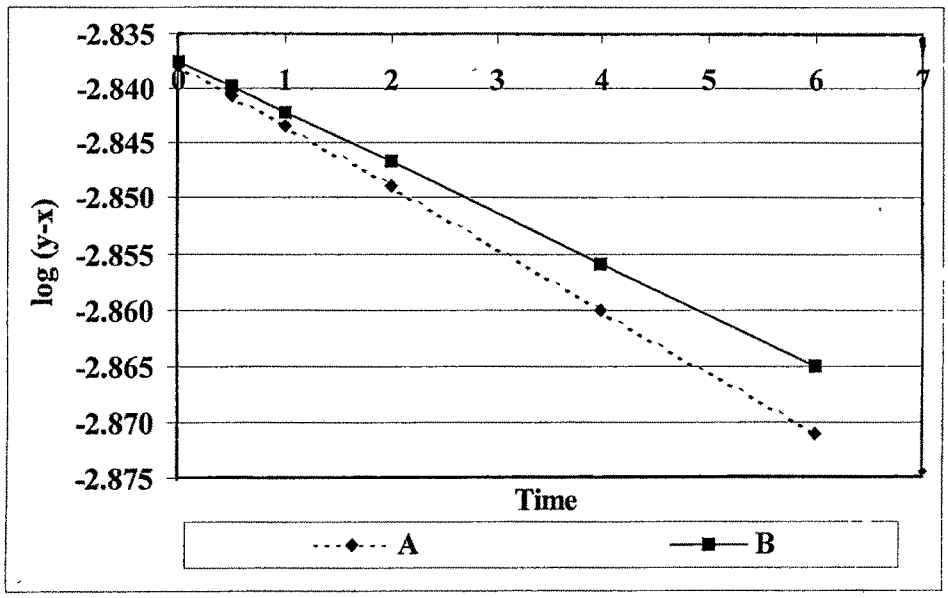

Table 3.2.4.12 Chemical Hydrolyses of Derivatives (54a-e)

Compound	$t_{½}$ (h) pH7.4 Buffer
54a	46
54b	39
54c	66
54d	99
54e	52

The aminoalcohol ester derivatives of indomethacin (**54**) did not show any hydrolysis till a period of 6 hours in buffer pH 2.0. The half-lives ranged from 39 hours to 99 hours for these derivatives (**54a-e**) in buffer (pH 7.4) as shown in Table 3.2.4.12 assuring that these compounds would be absorbed intact from the GIT and would prevent the local GI irritation of the parent drug indomethacin (**54**).

3.2.4.2 Hydrolyses studies in serum

The UV spectrophotometric method adopted for evaluation of the enzymatic susceptibility of the derivatives (**54a-e**) to release the parent drug (**54**) was based on the same principle as discussed for estimating indomethacin (**54**) in the study of compounds (**54a-e**) in buffers. A stock solution of (**54a**) (1 mg/ml) in human serum was maintained at 37±1°C. Aliquots (0.5 ml) were treated with trichloroacetic acid (TCA, 10%, 1.0 ml) to arrest further (chemical and enzymatic) hydrolysis by deactivating the serum proteins (enzymes) as well as bringing the pH to acidic side. The acidified solution was extracted into solvent ether, vacuum dried and the residue dissolved in methanol. The absorbance was measured at 227 nm. Concentration of the parent drug was calculated using Equation-7. Samples were analyzed in duplicate and the average percent release of the parent drug determined are given in Table 3.2.4.15.

Table 3.2.4.13 The absorbance data for studies of (54a-c) in human serum (80%)

Time (min)	54a (Sample A and B) Absorbance		54b (Sample A and B) Absorbance		54c (Sample A and B) Absorbance	
	A	B	A	B	A	B
15	0.683(0.5:2)	0.613(0.5:3)	0.991 (1:1)	0.967 (1:2)	0.783 (0.5·3)	0.637 (0.5:3)
30	0.713(0.5.3)	0.737(0.5:3)	0.771 (1:2)	0.713 (1:2)	0.826 (0.5:3)	0.686 (0.5:3)
60	0.786(0.5:3)	0.803(0.5:3)	0.800 (1:2)	0.816 (1:2)	0.865 (0.5:3)	0.776 (0.5:3)
120	0.791(0.5:3)	0.713(0.5:3)	0.869 (1:2)	0.851 (1:2)	0.906 (0.5.3)	0.817 (0.5:3)

Table 3.2.4.14 The absorbance data for studies of (54d-e) in human serum (80%)

Time (min)	54d (Sample A and B) Absorbance		54e (Sample A and B) Absorbance	
	A	B	A	B
15	0.907 (1:1)	0.483 (1:3)	0.504 (0.5:4)	0.513 (0.5:4)
30	0.623 (1:3)	0.573 (1:3)	0.579 (0.5:4)	0.567 (0.5:4)
60	0.631 (1:3)	0.619 (1:3)	0.609 (0.5:4)	0.631 (0.5:4)
120	0.680 (1:3)	0.645 (1:3)	0.637 (0.5:4)	0.651 (0.5:4)

Table 3.2.4.15 Enzymatic Hydrolyses of Derivatives (54a-e)

Compound	% Release of parent NSAID 54) (80% human serum)		
	½ h	1 h	2h
54a	35.5	47.8	49.6
54b	54.4	59.3	70.9
54c	50.1	59.1	65.0
54d	40.6	42.1	53.3
54e	27.8	36.9	45.4

As was observed in case of derivatives of diclofenac (**51**), the derivatives (**54a-e**) of indomethacin (**54**) also showed a high enzymatic susceptibility towards esterases to liberate the parent drug indomethacin (**54**) as indicated by the results in Table 3.2.4 15. These results indicate that the derivatives (**54a-e**) would be releasing the parent drug indomethacin (**54**) by the action of esterases which, would then exhibit the normal pharmacological activity.

3.2.5. HYDROLYSES STUDIES OF DERIVATIVES OF ASPIRIN (56a-e)

Presence of two ester linkages (I and II) in these derivatives (**56a-e**) posed a different type of problem in establishing a quantitative method for their estimations. These deriva-

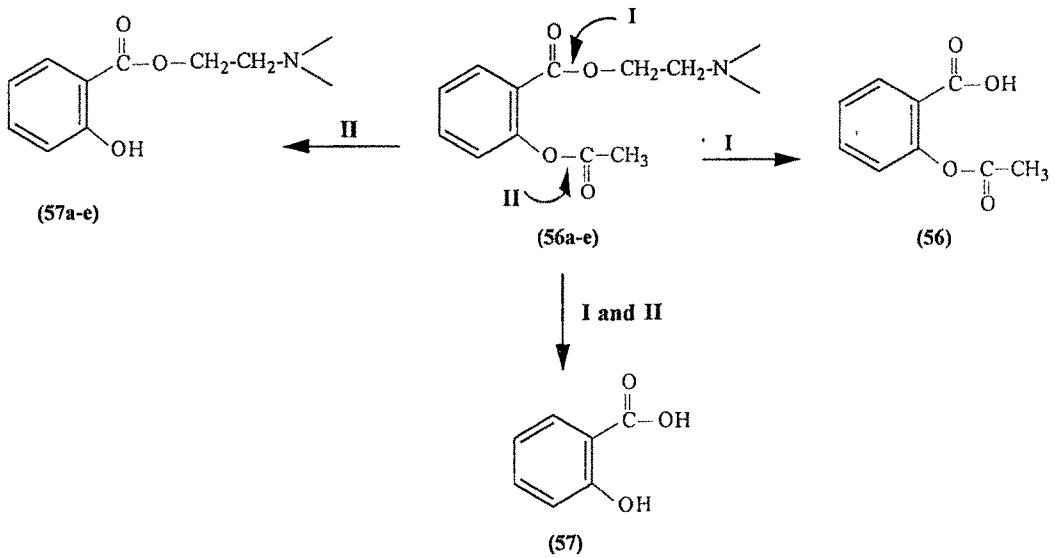

tives (**56a-e**) may cleave at site-I to afford the desired drug, aspirin (**56**), at site-II to offer

the deacetylated products (**57a-e**) or at both the sites (I and II) to give free salicylic acid (**57**). It was not known in advance which way hydrolysis reaction would proceed in buffers (pH 2.0 and 7.4) and in the serum. So, methods were to be established for the estimations of all of these species (**56, 57, 57a-e**). Advantage was taken of the existence of differences in their absorption maxima in UV spectrophotometry and the difference in physicochemical properties of the free acids (**56** and **57**) and their esters (**56a-e** and **57a-e**). Deacetylated products (**57** and **57a-e**) showed absorption maxima at 305 nm while both the acetylated products (**56** and **56a-e**) showed the maxima at 279 nm.

3.2.5.1 Hydrolyses studies in buffers

Expecting that the derivatives (**56a-e**) would cleave at site-I a standard curve was prepared for the estimation of liberated aspirin (**56**). A stock solution of aspirin was prepared in methanol and various dilutions were prepared from it. Aliquots from each dilutions were withdrawn, acidified with buffer solution of pH 2.0, extracted with isopropyl ether, dried and absorbance measured at 279 nm. The experiment was repeated in triplicate and the closest two sets were regressed to afford Equation-8. It was found that Beer-Lambert law was observed in the range of 20-180 ug/ml. Calibration curve data and the plot are shown in Table 3.2.5.1 and Figure 3.2.5.1, repectively.

Table 3.2.5.1 Calibration curve data for estimating aspirin (56) in buffers and pooled human serum (80%)

Sr. No	Concentration ug/ml	Absorbance		Regressed values
		A	B	C
1	20.0	0.147	0.129	0 136
2	40.0	0.266	0.248	0.264
3	60.0	0.401	0.390	0.391
4	80.0	0.504	0.513	0 519
5	100.0	0.653	0.643	0 647
6	120.0	0.813	0.779	0.775
7	140.0	0.917	0.886	0.903
8	160.0	1.061	1.034	1.031
9	180.0	1.118	1.159	1.158

$A = 0.0064*C - 0.0084$ Equation-8

$r = 0.927$ $s = 0.339$

[A = absorbance, C = concentration (ug/ml)]

Figure 3.2.5.2 Calibration plot for estimating aspirin (56) in buffers and pooled 80% human serum

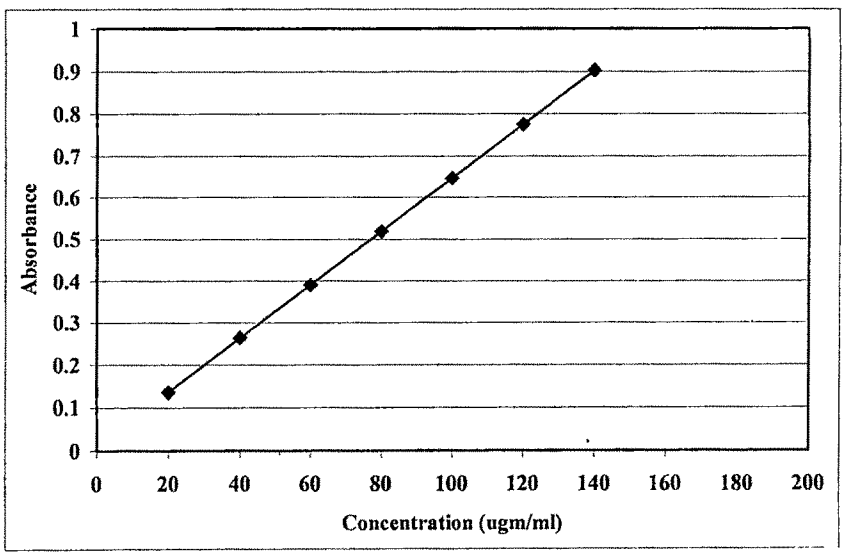

In vitro studies were performed by maintaining a test solution of **56a** in buffers (pH 2.0 and 7.4) at 37 ± 1°C. Aliquots (1.0 ml) were withdrawn at regular time intervals of 0,0.5, 1.0, 2.0, 4.0 and 6.0 hours, acidified with buffer (pH 2.0) and extracted into isopropyl ether. The organic extract was dried and absorbance measured at 279 nm. But, to our surprise no absorbance was observed at 279 nm for the derivative (**56a**) in buffers (pH 2.0 and 7.4) indicating that no hydrolysis occurred for this derivative till a period of six hours in either of these buffers.

Another possibility was that there might be formation of the deacetylated product (**57a**). If this product was formed then it would remain in the aqueous phase in the protonated form with a UV maximum of 305 nm as described in the discussion part of synthesis of (**56a-e**) (Chapter 3 3.1.7). To check this possibility the acidified aqueous layers for all the aliquots were scanned for any absorbance at 305 nm but no absorbance was observed at this wavelengths. Strong bands appeared at 279 nm, which corresponded for the intact derivative (**56a**). The organic layer was also checked for any absorbance at 305 nm, for presence of liberated salicylic acid if formed during the hydrolysis. But no absorbance was observed for the organic extract at 305 nm. Hence, it was concluded that the derivative (**56a**) remains intact in the buffers till a period of 6 hours. The observations were similar for other derivatives (**56b-e**).

3.2.5.2 Hydrolyses studies in serum

For evaluation of the enzymatic susceptibility of the derivatives (**56a-e**) of aspirin it was decided to make a calibration curve for salicylic acid also besides the curve prepared for aspirin (as described above) since aspirin has been reported[111] to hydrolyze to salicylic acid (**57**) by action of esterases. Stock solution of salicylic acid was prepared in sodium hydroxide solution (0.1 N). Aliquots (0.5 ml) were withdrawn, treated with TCA, acidified with buffer (pH 2.0), extracted into isopropyl ether, dried and absorbance measured at 305 nm. Three determinations were made and regression analysis of the data was performed to give Equation-9. Beer-Lambert law was followed in the range of 5-35 ug/ml (Table 3.2.5.2 and Figure 3.2.5.2).

Table 3.2.5.2 Calibration curve data for estimating salicylic acid (57) in buffers and pooled human serum (80%)

Sr. No	Concentration ug/ml	Absorbance		Regressed values
		A	B	C
1	5.0	0.156	0.171	0.163
2	10.0	0.307	0.349	0.326
3	15.0	0.477	0.512	0.489
4	20.0	0.635	0.663	0.652
5	25.0	0.796	0.815	0.815
6	30.0	0.976	0.991	0.978
7	35.0	1.160	1.143	1.141

$A = 0.0326*C - 0.00043$ Equation-9

$r = 0.999$ $s = 0.386$

[A = absorbance, C = concentration (ug/ml)]

Figure 3.2.5.2 Calibration plot for estimating salicylic acid (57) in buffers and pooled 80% human serum

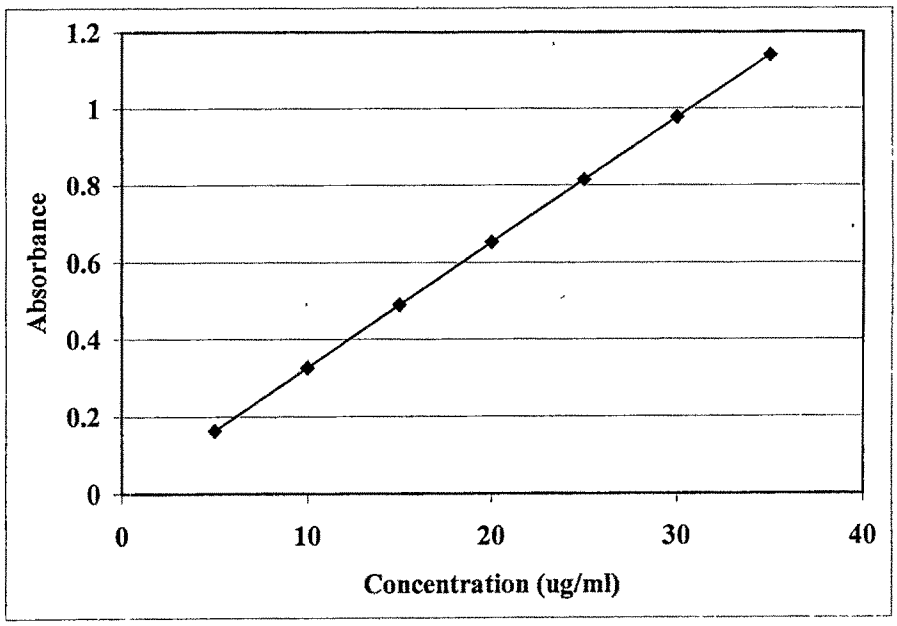

The derivative (**56a**) solution (1 mg/ml) was maintained at 37±1°C in human serum (80%). Aliquots (0.5 ml) were withdrawn at different time intervals, treated with TCA (to precipitate the serum proteins), extracted into isopropyl ether, dried and absorbance measured at 279 nm and 305 nm. For all the aliquots absorbance was observed only at 305 nm with no absorbance at 279 nm. This confirmed the formation of salicylic acid (**57**) upon hydrolysis of (**56a**) with no formation of aspirin (**56**). Further, the precipitated aqueous solution in each case was filtered through whatman filter paper checked for absorbance at 305 nm to observe the formation of deacetylated product (**57a**) but, no absorbance was observed at this wavelength. This confirmed that the derivative (**56a**) is getting hydrolyzed in serum to liberate free salicylic acid (**57**) which in acidic pH (~2.0) got extracted into the organic layer giving absorbance at 305 nm. The concentration of salicylic acid (**57**) was determined using Equation-9. The experiment was repeated with other derivatives (**56b-e**) and the data are presented in Tables 3.2.5.3 and 3.2.5.4. Percent release of salicylic acid was determined for each derivative and is tabulated in Table 3.2.5.5.

Table 3.2.5.3 The absorbance data for studies of (56a-c) in human serum (80%)

Time (min)	56a (Sample A and B) Absorbance		56b (Sample A and B) Absorbance		56c (Sample A and B) Absorbance	
	A	B	A	B	A	B
15	0 431	0.369	0.223	0.312	0.037	0.062
30	0.593	0.551	0.378	0.435	0.092	0.117
60	0.629	0.613	0.566	0.641	0.128	0.149
120	0.721	0.703	0.729	0.817	0.241	0.295

Table 3.2.5.4 The absorbance data for studies of (56d-e) in human serum (80%)

Time (min)	56d (Sample A and B) Absorbance		56e (Sample A and B) Absorbance	
	A	B	A	B
15	0.079	0.089	0.105	0.112
30	0.130	0.147	0.170	0.216
60	0.157	0.179	0.252	0.275
120	0.208	0.228	0.610	0.574

Table 3.2.5.5 Enzymatic Hydrolyses of Derivatives (56a-e)

Compound	% Release of salicylic acid (57) (80% human serum)		
	½ h	1 h	2h
56a	48.36	72.39	93.22
56b	75.84	80.44	92.21
56c	11.81	16.41	30.85
56d	16.67	20.12	26.64
56e	21.78	32.26	78.02

The hydrolyses studies in buffers clearly indicate that all the derivatives (**56a-e**) are stable enough (at least for six hours) to be absorbed intact form in the GIT. But, after entering systemic circulation, the serum esterases would not only remove the aminoalcohols but would also deacetylate the derivatives (**56a-e**) to liberate free salicylic acid instead of the parent drug aspirin (**56**). So, these derivatives (**56a-e**) may not prove to be better substitutes for aspirin as non-steroidal anti-inflammatory agents.

3.2.6. HYDROLYSES STUDIES OF DERIVATIVES OF KETOROLAC (58a-e)

3.2.6.1 Hydrolyses studies in buffers

The derivatives (**58a-e**) were studied for their stability in both the buffers (pH 2 0 and 7.4). The procedure for preparing the calibration curve for the estimation of ketorolac released during these studies was based on the principle as discussed for compound (**49**) except for change of solvent n-hexane to isopropyl ether. Isopropyl ether was preferred over n-hexane because it exhibited a better solubility for ketorolac (**58**) than n-hexane For preparing the calibration curve ketorolac was dissolved in alkaline solution and dilutions were made to give different concentrations. Aliquots were withdrawn from each of the dilutions, acidified with buffer (pH 2.0), extracted with isopropyl ether, dried and absorbance of the ether extract measured at UV maximum (307 nm) of ketorolac. Another advantage of choosing isopropyl ether as partitioning solvent was its non-interference in the measurement of absorbance of the solution at this wavelength i.e. 307 nm. The experiment was repeated in triplicate. Regression analysis was performed for the absorbance data (two closest observations) to give Equation-10. Beer Lambert law

was obeyed in the concentration range of 2-16 ug/ml. The calibration curve data and the graphical presentation are given in Table 3.2.6.1 and Figure 3.2.6.1, respectively.

Table 3.2.6.1 Calibration curve data for estimating ketorolac (58) in buffers and human serum (80%)

Sr. No	Concentration ug/ml	Absorbance		Regressed values
		A	B	C
1	2.0	0.175	0.134	0.141
2	4.0	0.327	0.281	0.305
3	6.0	0.484	0.444	0.469
4	8.0	0.661	0.591	0.633
5	10.0	0.825	0.779	0.797
6	12.0	0.972	0.898	0.961
7	14.0	1.182	1.079	1.125
8	16.0	1.338	1.271	1.289

A = 0.0820*C + 0.0227 Equation-10

r = 0.9958, s = 0.0562

A = absorbance, C = concentration (ug/ml)]

Figure 3.2.6.1 Calibration plot for estimating ketorolac(58) in buffers and human serum (80%)

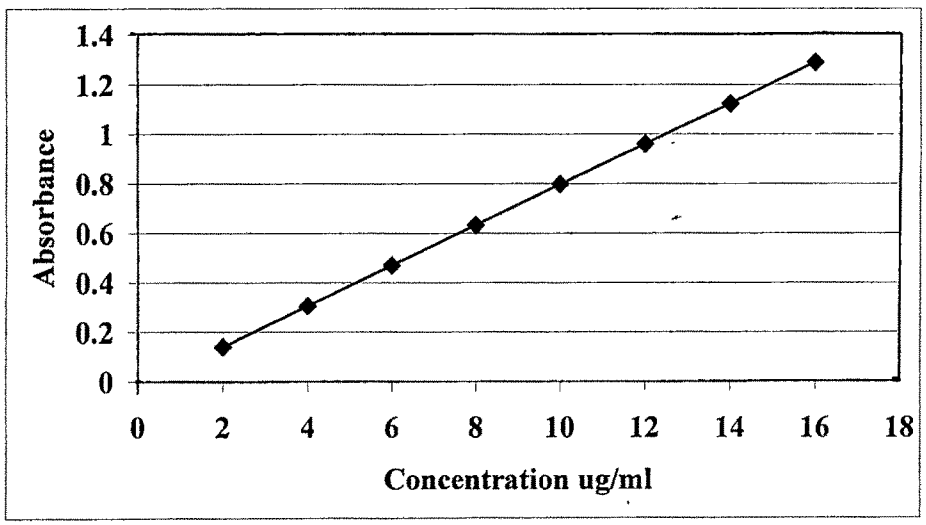

The UV spectrophotometric method developed for estimating the derivatives (**58a-e**) was same as described for the studies carried out for the derivatives (**49a-f**) of flurbiprofen (**49**).

Solution of the derivative (**58a**) (1 mg/ml) was maintained at 37 ± 1°C. Aliquots (1.0 ml) were withdrawn at different time intervals and after bringing the pH to acidic side (~2), the acidified aliquots were extracted into isopropyl ether so that the released parent drug (non-ionic form) would be extracted leaving the (ionic) intact derivative in the aqueous solution without partitioning into the organic layer. The pooled organic extract was dried and absorbance measured at 307 nm. Equation-10 was used for calculating the concentration of the parent drug. The absorbance data was given mathematical treatment to give the rate constant as described for compound (**45a**). The absorbance readings are given in Table 3.2.6.2 for derivative (**54a**) followed by the data for calculating the rate constant in Table 3.2.6.3. The plots proving that the hydrolysis of **58a** follows psuedo-first order kinetics has been presented graphically in figure 3.2.6.2.

Kinetic studies in buffer solutions (pH 2.0 and 7.4) were performed for rest of the other derivatives (**58b-e**) exactly in the same way as described above for derivative (**58a**). The absorbance and rate constant calculation data are shown in Tables 3.2.6.4 to 3.2.6.11, and the graphical representations are shown in Figures 3.2.6.3 to 3.2.6.6. Half-lives of all the derivatives (**58a-e**) have been shown in Table 3.2.6.12 in buffer solution (pH 7.4).

Table 3.2.6.2 The absorbance readings of (58) for the studies of (58a) in buffers

Time	pH 2.0	Sample A pH 7.4	Sample B pH 7.4
(h)	Absorbance		
0.0	0.431 (1:4)	0.502 (1:4)	0.486 (1:4)
0.5	0.406 (1:4)	0.728 (1:4)	0 746 (1:4)
1.0	0.427 (1:4)	0.599 (1:6)	0.604 (1:6)
2.0	0.429 (1:4)	0.672 (1:6)	0.677 (1:6)
4.0	0.427 (1:4)	0.707 (1:6)	0.694 (1:6)
6.0	0.395 (1:4)	0.688 (1:7)	0.707 (1:6)
8.0	0.432 (1:4)	0.712 (1:7)	0.632 (1:7)

Table 3.2.6.3 Data presentation for set A (58a) for calculation of the rate constant k

Time (h)	Absorb-ance	Conc. of (45) (ug/ml)	x (ug/ml)	(y-x) (ug/ml)	(y-x) (mol/litre)	Log(y-x)	Calculated Log(y-x)
0	0.502 (1:4)	27.24	0	651.33	$1.996*10^{-3}$	-2.700	-2.713
0.5	0.728 (1:4)	45.77	23.95	627.38	$1.922*10^{-3}$	-2.716	-2.716
1	0.599 (1:6)	53.07	33.38	617.95	$1.893*10^{-3}$	-2.723	-2.718
2	0.672 (1:6)	59.30	41.43	609.90	$1.869*10^{-3}$	-2.728	-2.723
4	0.707 (1:6)	62.29	45.29	606.04	$1.857*10^{-3}$	-2.731	-2.733
6	0.688 (1:7)	69.34	54.40	596.93	$1.829*10^{-3}$	-2.738	-2.742
8	0.712 (1:7)	71.68	57.42	593.91	$1.820*10^{-3}$	-2.740	-2.752

Figure 3.2.6.2 Graphical presentation for calculated log(y-x) values vs time for samples A and B of 58a

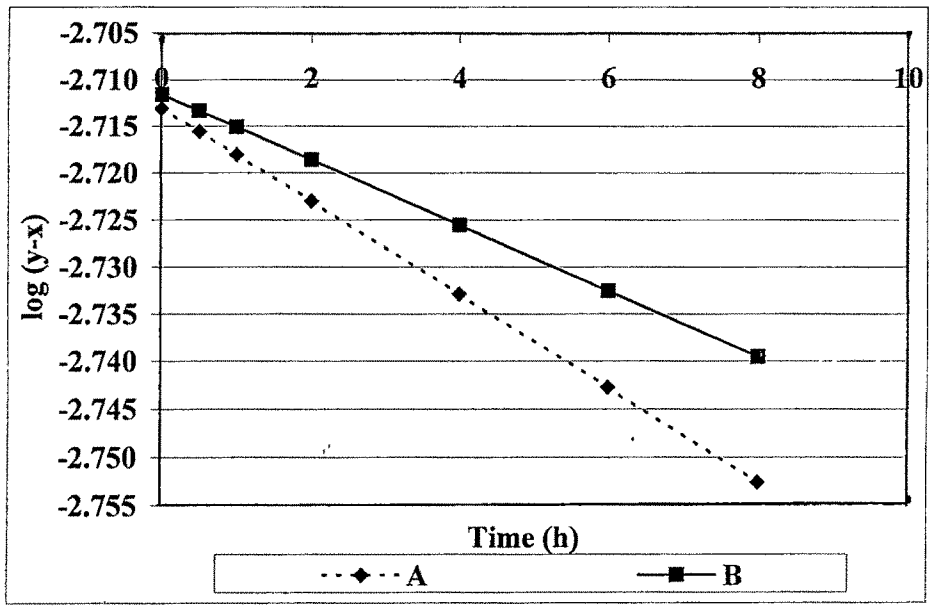

Table 3.2.6.4 The absorbance readings of (58) for the studies of (58b) in buffers

Time	pH 2.0	Sample A pH 7.4	Sample B pH 7.4	Sample C pH 7.4
(h)	Absorbance			
0.0	0.221 (1:4)	0.365 (1:4)	0.355 (1:4)	0.380 (1:4)
0.5	0.220 (1:4)	0.481 (1:4)	0.473 (1:4)	0.495 (1:4)
1.0	0.237 (1:4)	0.309 (1:6)	0.326 (1:6)	0.316 (1:6)
2.0	0.226 (1:4)	0.348 (1:6)	0.345 (1:6)	0.339 (1:6)
4.0	0.239 (1:4)	0.351 (1:6)	0.369 (1:6)	0.372 (1:6)
6.0	0.249 (1:4)	0.383 (1:6)	0.397 (1:6)	0.388 (1:6)
8.0	0.238 (1:4)	0.413 (1:6)	0.429 (1:6)	0.437 (1:6)

Table 3.2.6.5 Data presentation for set A (58b) for calculation of the rate constant k

Time (h)	Absorb-ance	Conc. of (58) (ug/ml)	x (ug/ml)	(y-x) (ug/ml)	(y-x) (mol/litre)	Log(y-x)	Calculated Log(y-x)
0	0.365 (1:4)	15.32	0	787.06	$2.221*10^{-3}$	-2.654	-2.6604
0.5	0.481 (1:4)	30.71	22.42	764.64	$2.171*10^{-3}$	-2.666	-2.6612
1	0.309 (1.6)	28.32	18.93	768.13	$2.167*10^{-3}$	-2.664	-2 6620
2	0.348 (1:6)	31.65	23.78	763.28	$2.153*10^{-3}$	-2.667	-2.6635
4	0.351 (1:6)	31.90	24.16	762.90	$2.149*10^{-3}$	-2.667	-2.6667
6	0.383 (1:6)	34.63	28.13	758.93	$2.141*10^{-3}$	-2.669	-2.6698
8	0.413 (1:6)	37.19	31.87	755.19	$2.131*10^{-3}$	-2.671	-2 6730

Figure 3.2.6.3 Graphical presentation for calculated log(y-x) values vs time for Samples A and B of 58b

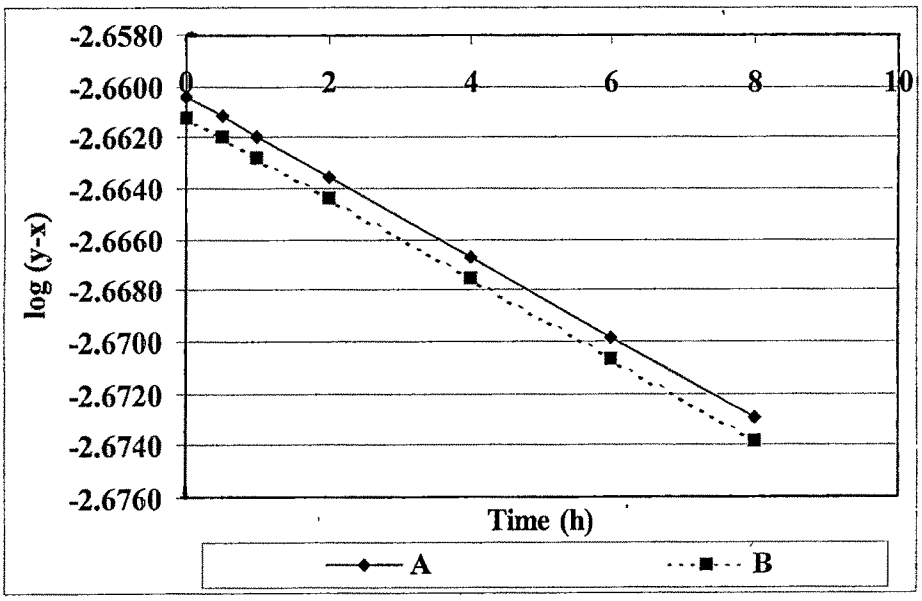

Table 3.2.6.6 The absorbance readings of (58) for the studies of (58c) in buffers

Time	pH 2.0	Sample A pH 7.4	Sample B pH 7.4
(h)	Absorbance		
0.0	0.553 (1:4)	0.713 (1:4)	0.736 (1:4)
0.5	0.578 (1:4)	0.748 (1:4)	0.769 (1:4)
1.0	0.514 (1:4)	0.810 (1:4)	0.826 (1:4)
2.0	0.558 (1:4)	0.851 (1:4)	0.842 (1:4)
4.0	0.517 (1:4)	0.916 (1:4)	0.927 (1:4)
6.0	0.528 (1:4)	0.616 (1:8)	0.637 (1:8)
8.0	0.561 (1:4)	0.631 (1:8)	0.658 (1:8)

Table 3.2.6.7 Data presentation for set A (58c) for calculation of the rate constant k

Time (h)	Absorb-ance	Conc. of (58) (ug/ml)	x (ug/ml)	(y-x) (ug/ml)	(y-x) (mol/litre)	Log(y-x)	Calculated Log(y-x)
0	0.713 (1:4)	34.55	0	503.49	$1.374*10^{-3}$	-2.862	-2.872
0.5	0.748 (1:4)	46.99	17.88	485.61	$1.325*10^{-3}$	-2.878	-2.875
1	0.810 (1:4)	50.77	23.32	480.17	$1.310*10^{-3}$	-2.883	-2.877
2	0.851 (1:4)	53.27	26.91	476.58	$1.300*10^{-3}$	-2.886	-2.883
4	0.916 (1:4)	57.24	32.60	470.89	$1.285*10^{-3}$	-2.891	-2.894
6	0.616 (1:8)	70.10	51.09	452.40	$1.234*10^{-3}$	-2.909	-2.904
8	0.631 (1:8)	71.75	53.46	450.03	$1.228*10^{-3}$	-2.911	-2.915

Figure 3.2.6.4 Graphical presentation for calculated log(y-x) values vs time for Samples A and B of 58c

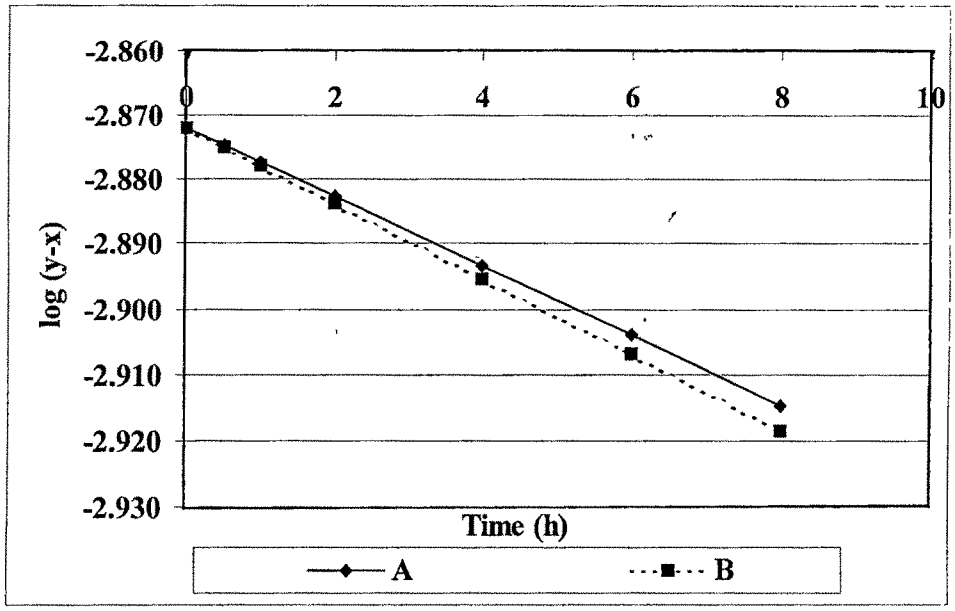

Table 3.2.6.8 The absorbance readings of (58) for the studies of (58d) in buffers

Time	pH 2.0	Sample A pH 7.4	Sample B pH 7.4	Sample C pH 7.4
(h)	Absorbance			
0.0	0.267	0.413 (1:7)	0.326 (1:7)	0.335 (1:7)
0.5	0.249	0.536 (1:7)	0.449 (1:7)	0.456 (1:7)
1.0	0.275	0.571 (1:7)	0.586 (1:7)	0.594 (1:7)
2.0	0.265	0.681 (1:7)	0.710 (1:7)	0.695 (1:7)
4.0	0.219	0.723 (1:7)	0.806 (1:7)	0.797 (1:7)
6.0	0.237	0.861 (1:7)	0.913 (1:7)	0. 883 (1:7)

Table 3.2.6.9 Data presentation for set A (58d) for calculation of the rate constant k

Time (h)	Absorb-ance	Conc. of (58) (ug/ml)	x (ug/ml)	(y-x) (ug/ml)	(y-x) (mol/litre)	Log(y-x)	Calculated Log(y-x)
0	0.413 (1:7)	20.1	0	722.21	$2.049*10^{-3}$	-2.688	-2.712
0.5	0.536 (1:7)	54.51	60.14	662.07	$1.879*10^{-3}$	-2.726	-2.716
1	0.571 (1:7)	57.92	64.85	657.36	$1.865*10^{-3}$	-2.729	-2.720
2	0.681 (1:7)	68.65	79.67	642.54	$1.823*10^{-3}$	-2.739	-2.728
4	0.723 (1:7)	72.75	85.32	636.89	$1.807*10^{-3}$	-2.743	-2.744
6	0.861 (1:7)	86.21	103.91	618 30	$1.754*10^{-3}$	-2.756	-2.761

Figure 3.2.6.5 Graphical presentation for calculated log(y-x) values vs time for Samples A, B and C of 58d

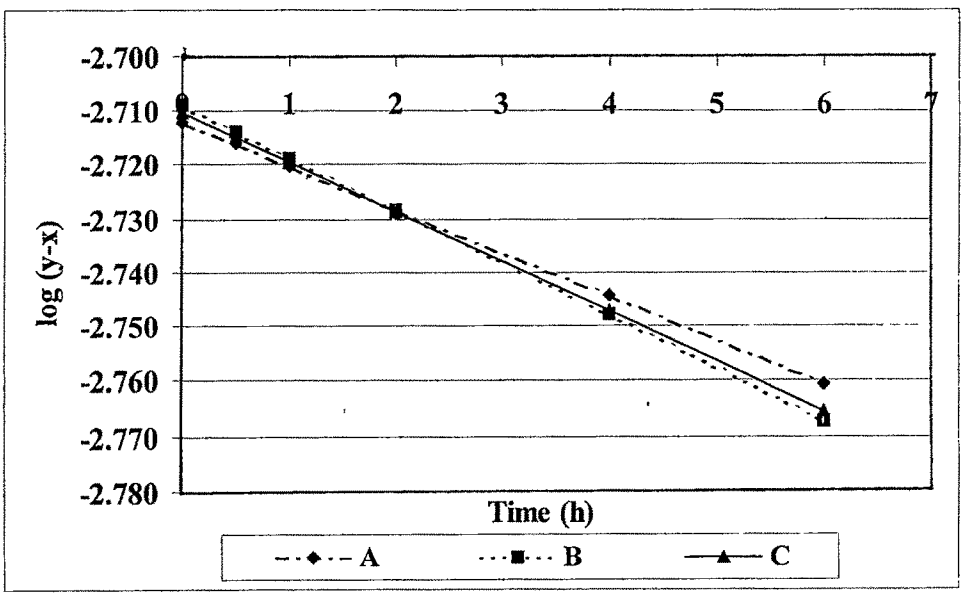

Table 3.2.6.10 The absorbance readings of (58) for the studies of (58e) in buffers

Time	pH 2.0	Sample A pH 7.4	Sample B pH 7.4	Sample C pH 7.4
(h)	Absorbance			
0.0	0.227 (1:2)	0.583	0.392	0.427
0.5	0.285 (1:2)	0.972	0.267 (1:5)	0.279 (1:5)
1.0	0.285 (1:2)	0.231 (1:5)	0.282 (1:5)	0.316 (1:5)
2.0	0.265 (1:2)	0.327 (1:5)	0.308 (1:5)	0.327 (1:5)
4.0	0.268 (1:2)	0.528 (1:5)	0.457 (1:5)	0.430 (1:5)
6.0	0.276 (1:2)	0.673 (1:5)	0.679 (1:5)	0.610 (1:5)
8.0	0.258 (1:2)	0.790 (1:5)	0.713 (1:5)	0.697 (1:5)

3.2.6.11 Data presentation for set A (58e) for calculation of the rate constant k

Time (h)	Absorb-ance	Conc. of (58) (ug/ml)	x (ug/ml)	(y-x) (ug/ml)	(y-x) (mol/litre)	Log(y-x)	Calculated Log(y-x)
0	0.583	10.94	0	841.94	$2.285*10^{-3}$	-2.641	-2.642
0.5	0.972	12.13	1.718	840.22	$2.281*10^{-3}$	-2.642	-2.644
1	0.231 (1:5)	18.56	11.002	830.94	$2.255*10^{-3}$	-2.647	-2.646
2	0.327 (1:5)	25.59	21.139	820.80	$2.228*10^{-3}$	-2.652	-2.651
4	0.528 (1:5)	40.30	42.363	799.58	$2.170*10^{-3}$	-2.663	-2.661
6	0.673 (1:5)	50.90	57.675	784.27	$2.129*10^{-3}$	-2.672	-2.671
8	0.790 (1:5)	59.47	70.029	771.91	$2.095*10^{-3}$	-2.679	-2.681

Figure 3.2.6.6 Graphical presentation for calculated log(y-x) values vs time for Samples A, B and C of 58e

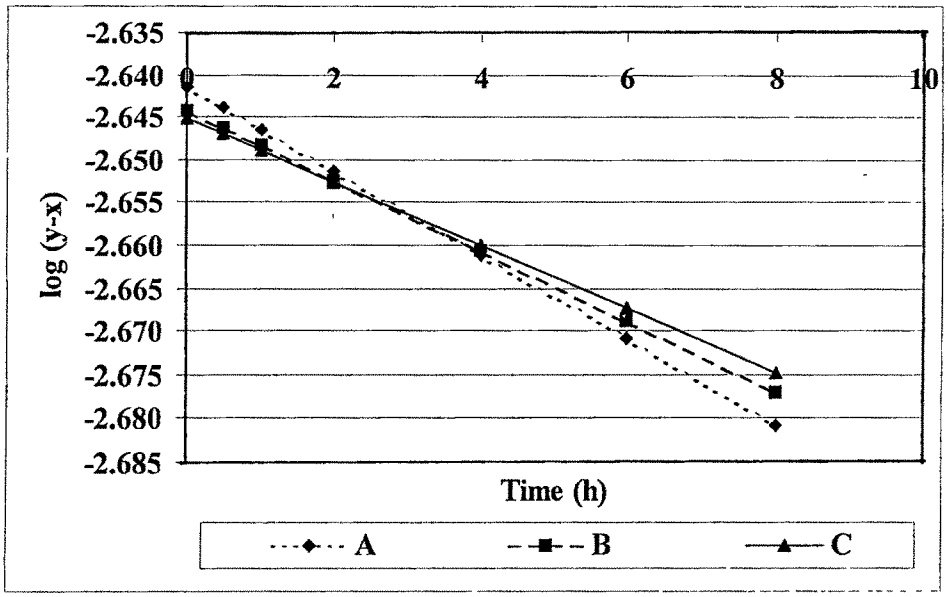

3.2.6.12 Chemical Hydrolyses of Derivatives (58a-e)

Compound	t ½ (h) pH7.4 Buffer
58a	83
58b	191
58c	53
58d	32
58e	68

No observable hydrolysis occurred for the compounds (**58a-e**) till 8 hours in buffer (pH 2.0) indicating them to be highly stable in the acidic environment of the stomach. The long half-lives (32 to 191 hours) observed (Table 3.2.6.12) for these compounds indicate them to be stable for sufficient time period to be absorbed intact from the GIT and prevent the direct contact effect of the parent drug, ketorolac (**58**).

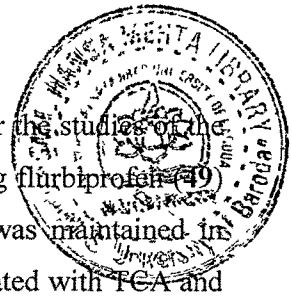

3.2.6.2 Hydrolyses studies in serum

The basic principle for the UV spectrophotometric method adopted for the studies of the derivatives (**58a-e**) in serum was similar to as discussed for estimating flurbiprofen (**49**) from its derivatives. A test solution of concentration (1.0 mg/ml) was maintained in human serum at 37 ±1°C. Aliquots (0.5 ml) upon withdrawal were treated with TCA and the protein-precipitated solution was extracted with isopropyl ether, dried and the absorbance measured at 307 nm against a blank obtained by giving similar treatment without the derivative solution. Here absorbance were directly measured for the isopropyl ether extracts since unlike chloroform no emulsification was observed in case of isopropyl ether with the serum proteins giving a clear separate organic layer and no solvent interference occurred at 307 nm. The concentration of the parent drug (**58**) was calculated using Equation-10. The percent release of the parent NSAID **58** from **58a** was determined as described for **45a**. The absorbance data for compounds (**58a-c**) and (**58d-e**) are given in Tables 3.2.6.13 and 3.2.6.14 respectively. The percent release data of the parent drug (**58**) from (**58a-e**) is tabulated in Table 3.2.2.15.

Table 3.2.6.13 The absorbance data for studies of (58a-c) in human serum (80%)

Time (min)	58a (Sample A and B) Absorbance		58b (Sample A and B) Absorbance		58c (Sample A and B) Absorbance	
	A	B	A	B	A	B
15	0.683(0.5:2)	0.613(0.5.3)	0.991 (1:1)	0.967 (1:2)	0.783 (0 5:3)	0 637 (0 5:3)
30	0.713(0.5:3)	0.737(0.5:3)	0.771 (1:2)	0.713 (1 2)	0.826 (0.5:3)	0.686 (0.5:3)
60	0.786(0.5:3)	0.803(0.5.3)	0.800 (1:2)	0.816 (1:2)	0.865 (0.5:3)	0.776 (0.5·3)
120	0.791(0.5:3)	0.713(0.5:3)	0.869 (1:2)	0.851 (1:2)	0.906 (0.5:3)	0.817 (0.5 3)

Table 3.2.6.14 The absorbance data for studies of (58d-e) in human serum (80%)

Time (min)	58d (Sample) Absorbance		58e (Sample) Absorbance	
	A	B	A	B
15	0.907 (1:1)	0.483 (1:3)	0.504 (0.5:4)	0.513 (0.5:4)
30	0.623 (1:3)	0.573 (1:3)	0.579 (0.5:4)	0.567 (0.5:4)
60	0.631 (1:3)	0.619 (1:3)	0.609 (0.5:4)	0.631 (0.5.4)
120	0.680 (1:3)	0.645 (1:3)	0.637 (0.5:4)	0.651 (0.5:4)

Table 3.2.6.15 Enzymatic Hydrolyses of Derivatives (58a-e)

Compound	% Release of parent NSAID 58) (80% human serum)		
	½ h	1 h	2h
58a	41.9	66.9	71.4
58b	52.2	54.3	61.4
58c	30.3	59.9	76.9
58d	16.1	16.8	19.2
58e	12.41	22.45	44.01

The results in Table 3.2.6.15 indicate high enzymatic susceptibility for these derivatives (**58a-e**) in serum towards esterases. These results suggest that all the derivatives after absorption from the GIT would cleave to liberate the parent drug ketorolac (**58**) for eliciting the desired activity.

3.3. BIOLOGICAL EVALUATION

The synthesized aminoalcohol ester derivatives were evaluated for the various biological activites as discussed under the following headings:

3.3.1. Anticholinergic Activity

3.3.2. Antiinflammatory Activity

3.3.3. Analgesic Activity

3.3.4. Ulcerogenic Potential

3.3.1. ANTICHOLINERGIC ACTIVITY

The aminoalcohol ester derivatives synthesized for the present work were expected to exhibit anticholinergic activity due to their structural resemblance with the aminoalcohol ester class of anticholinergics. Hence, all the synthesized ester derivatives were evaluated for their anticholinergic acitivity on isolated tissue[112] (rat ileum) preparation

3.3.1.1. Anticholinergic activity of compounds (45a-f)

For the evaluation of each individual derivative, the dose response curve (DRC) for acetylcholine (Ach) was recorded till maximum response was obtained and the DRC was repeated again for Ach in presence of the test solution (**45d**), after allowing the tissue to be in contact with the test solution (5 ug/ml) for a period of half an hour in the organ bath. The height for each response (recorded for 30 sec) was converted to percent response considering the maximum height as 100 percent. The two set of percent responses obtained in presence and absence of the drug derivative (**45d**) were plotted (Figure 3.3.1.1) against the log molar concentration of the Ach used and EC_{50} (concentration required for obtaining 50% of the maximum response) was found from the plot and pA_2 value was calculated using the formula given below.

$$pA_2 = \log[M] + \log(x-1)$$

The data for calculations for the derivative (**45d**) has been shown in Tables 3.3.1.1. The parameters used for the calculation of pA_2 values and the calculated pA_2 values for the derivatives (**45a-f**) are given in Table 3.3.1.2. The pA_2 value for atropine sulphate was calculated to be 8.02.

Table 3.3.1.1 Data for calculation of pA_2 value for derivative (45d)

Ach (ug in 30 ml)	log [m] of Ach	Response in absence of antagonist (mm)	% Response (Ach)	Response in presence of antagonist (mm)	% Response (Ach+45d)
0.3	-7.25	3.0	3.41	-	-
1.0	-6.73	29.0	32.9	-	-
3.0	-6.25	62.0	70.5	24.0	32.0
10.0	-5.73	81.0	92.04	58.0	77.3
30.0	-5.25	88.0	100.0	69.0	92 0
100.0	-4.73	-	-	73.0	97.3
300.0	-4.25	-	-	75.0	100.0

Table 3.3.1.2. Data and pA_2 values of derivatives of the drugs (45a-f)

Deriva-tive No	Conc. of Deriva-tive (ug/ml)	-log[M]	EC_{50} in presence of antagonist (P)	EC_{50} in absence of antagonist (A)	x = P/A	log (x-1)	pA_2
45a	5.0	4.806	$1.25*10^{-7}$	$7.00*10^{-8}$	1.786	-0.105	4.70
45b	10.0	4.541	$1.12*10^{-6}$	$3.54*10^{-7}$	3.169	0.336	4.88
45c	5.0	4.857	$1.00*10^{-6}$	$2.23*10^{-7}$	4.484	0.542	5.39
45d	10.0	4.539	$8.91*10^{-7}$	$2.98*10^{-7}$	2.991	0.299	4.80
45e	20.0	4.257	$5.31*10^{-6}$	$5.31*10^{-7}$	10.00	0.954	5.21
45f	2.5	5.127	$5.31*10^{-6}$	$5.31*10^{-7}$	10.00	0.954	6 08

Figure 3.3.1.1 Standard curves for Acetylcholine and derivative (45d)

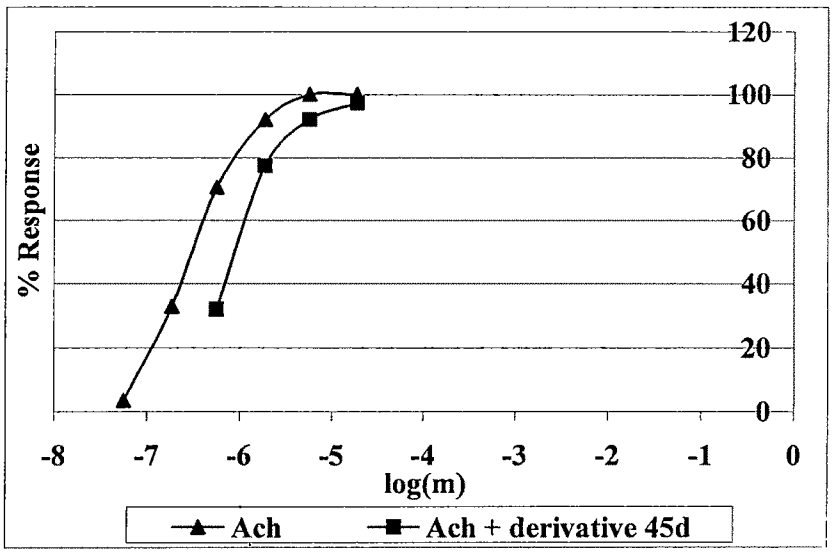

3.3.1.2. Anticholinergic activity of compounds (49a-f)

The compounds (**49a-f**) also were evaluated for their anticholinergic potency as described for compound (**45d**). The data for calculation of pA_2 for **49e** with its graphical presentation has been shown in Table 3.3.1.3. and Figure 3.3.1.2, respectively. The parameters used for the calculation of pA_2 values and the calculated pA_2 values for all the derivatives of **49** are given in Table 3.3.1.4

Table 3.3.1.3. Data for calculation of pA_2 value for derivative (49e)

Ach (ug in 30 ml)	log [m] of Ach	Response in absence of antagonist (mm)	% Response (Ach)	Response in presence of antagonist (mm)	% Response (Ach+49e)
1.0	-6.73	22.0	22.2	-	-
3.0	-6.25	44.0	44.4	9.0	9.09
10.0	-5.73	76.0	76.7	28.0	28.28
30.0	-5.25	94.0	94.9	47.0	47.47
100.0	-4.73	96.0	96.9	73.0	73.7
300.0	-4.25	99.0	100.0	95.0	95.95
1000.0	-3.73	-	-	99.0	100.0

Figure 3.3.1.2 Standard curves for Acetylcholine and derivative (49e)

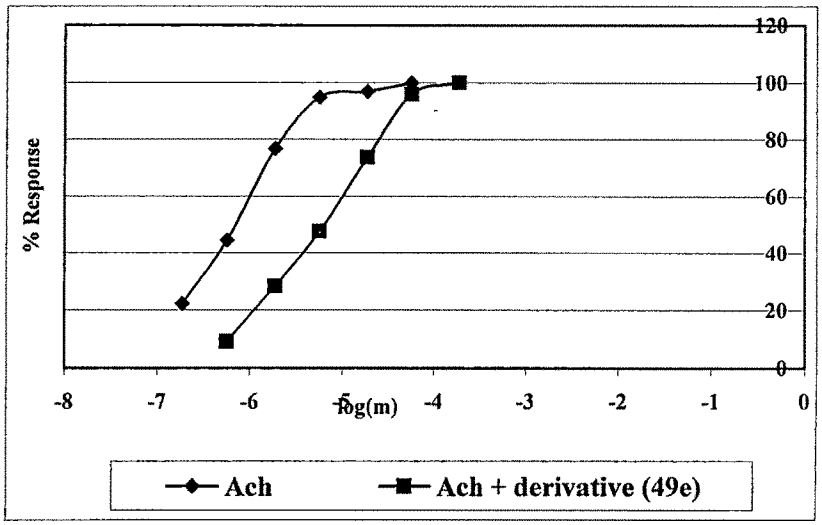

Table 3.3.1.4. Data and pA_2 values of derivatives (49a-f).

Derivative No.	Conc. of Derivative (ug/ml)	-log[M]	EC_{50} in presence of antagonist (P)	EC_{50} in absence of antagonist (A)	x = P/A	log (x-1)	pA_2
49a	10.0	4.847	$7.94*10^{-7}$	$3.54*10^{-7}$	2.240	0.095	4.94
49b	10.0	4.579	$1.88*10^{-6}$	$9.44*10^{-7}$	1.995	-0.002	4.58
49c	5.0	4.894	$8.91*10^{-6}$	$1.06*10^{-6}$	8.415	0.870	5.76
49d	5.0	4.878	$1.78*10^{-6}$	$9.44*10^{-7}$	1.884	-0.054	4.82
49e	5.0	4.896	$5.96*10^{-6}$	$6.68*10^{-7}$	8.912	0.898	5.79
49f	2.5	5.168	$3.76*10^{-7}$	$2.51*10^{-7}$	14.96	1.145	6.31

3.3.1.3. Anticholinergic activity of compounds (51a-e)

The compounds (**51a-e**) were evaluated for their anticholinergic potency as described for compound (**45d**). The data for calculation of pA_2 for compound (**51e**) with its graphical presentation has been shown in Table 3.3.1.5. and Figure 3.3.1.3. The parameters used for the calculation of pA_2 values and the calculated pA_2 values for the derivatives (**51a-e**) of diclofenac are given in Table 3.3.1.6.

Table 3.3.1.5. Data for calculation of pA_2 value for derivative (51e)

Ach (ug in 30 ml)	log [m] of Ach	Response in absence of antagonist (mm)	% Response (Ach)	Response in presence of antagonist (mm)	% Response (Ach+51e)
0.5	-5.56	4.0	13.3	-	-
1.5	-5.08	11.0	36.6	4.0	21.3
5.0	-4.56	21.0	70.2	9.0	47.4
15.0	-4.08	25.5	85.0	14.0	73.6
50.0	-3.56	27.0	90.6	16.0	85.0
150.0	-3.08	27.9	93.0	17.0	89.0
500.0	-2.56	30.0	100	19.0	100

Figure 3.3.1.3 Standard curves for Acetylcholine and derivative (51e)

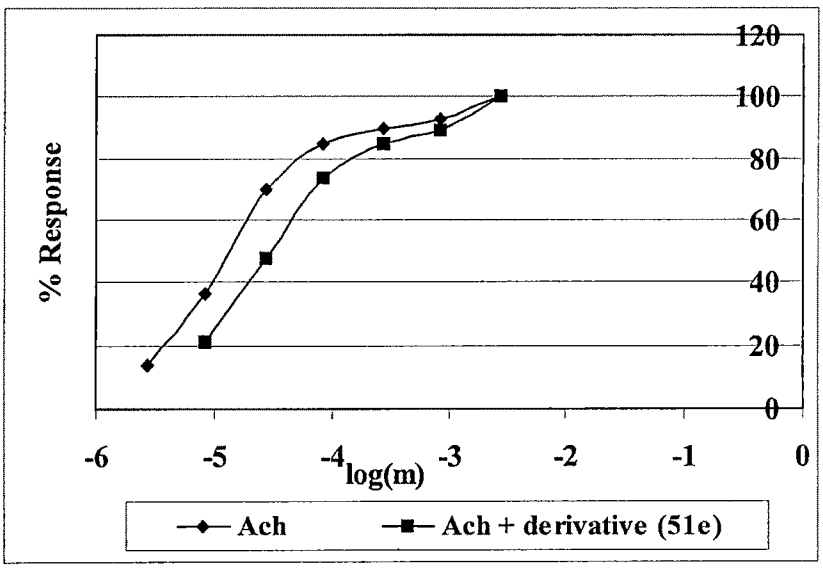

Table 3.3.1.6. Data and pA_2 values of derivatives (51a-e).

Derivative No.	Conc. of Derivative (ug/ml)	-log[M]	EC_{50} in presence of antagonist (P)	EC_{50} in absence of antagonist (A)	x = P/A	log (x-1)	pA_2
51a	5.0	4.907	$1.33*10^{-5}$	$5.31*10^{-6}$	2.511	0 179	5.09
51b	10.0	4.64	$1.46*10^{-6}$	$8.91*10^{-7}$	1.679	-0.168	4 47
51c	5.0	3.471	$5.01*10^{-5}$	$6.68*10^{-6}$	7.499	0.813	4.28
51d	5.0	3.457	$2.51*10^{-5}$	$5.96*10^{-6}$	4.217	0.507	3.96
51e	5.0	3.473	$5.96*10^{-5}$	$1.49*10^{-5}$	3.982	0.475	3.95

3.3.1.4. Anticholinergic activity of compounds (54a-e)

The anticholinergic potency for the compounds (**54a-e**) was evaluated as described for compound (**45d**). The data for calculation of pA_2 for **54a** with its graphical presentation has been shown in Table 3.3.1.7 and Figure 3.3.1.4, respectively. The parameters used for the calculation of pA_2 values and the calculated pA_2 values for the derivatives of indomethacin (**54**) are given in Table 3.3.1.8.

Table 3.3.1.7. Data for calculation of pA_2 value for derivative (54a)

Ach (ug in 30 ml)	log [m] of Ach	Response in absence of antagonist (mm)	% Response (Ach)	Response in presence of antagonist (mm)	% Response (Ach+54a)
0.3	-7.25	3.0	9.09	-	-
1.0	-6.73	5.0	15.2	2.0	10.0
3.0	-6.25	15.0	45.5	6.0	30.0
10.0	-5.73	21.0	63.6	10.0	50.0
30.0	-5.25	28.0	84.6	13.0	65.0
100.0	-4.73	33.0	100.0	16.0	80.0
300.0	-4.25	-	-	20.0	100.0

Figure 3.3.1.4 Standard curves for Acetylcholine and derivative (54a)

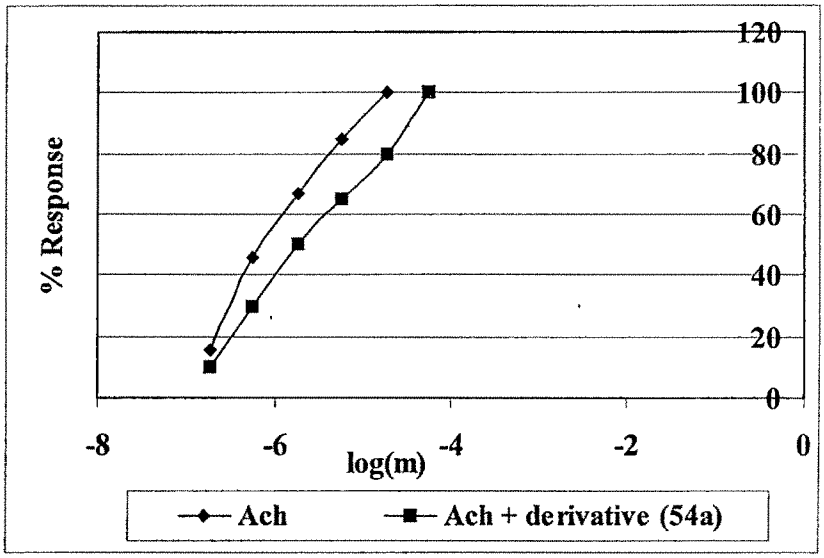

Table 3.3.1.8. Data and pA_2 values of derivatives (54a-e)

Derivative No.	Conc. of Derivative (ug/ml)	-log[M]	EC_{50} in presence of antagonist (P)	EC_{50} in absence of antagonist (A)	x = P/A	log (x-1)	pA_2
54a	5.0	4.93	$1.99*10^{-6}$	$7.07*10^{-7}$	2.815	0.259	5.19
54b	10.0	4.66	$1.49*10^{-6}$	$8.91*10^{-7}$	1.679	-0.168	4.49
54c	5.0	4.972	$1.12*10^{-6}$	$7.49*10^{-7}$	1.499	-0.303	4.67
54d	10.0	4.657	$5.88*10^{-6}$	$1.49*10^{-6}$	3.93	0.466	5 12
54e	5.0	5.071	$2.82*10^{-5}$	$1.12*10^{-5}$	2.52	0.180	5.25

3.3.1.5. Anticholinergic activity of compounds (56a-e)

The anticholinergic acitivity of compounds (**56a-e**) was evaluated as described for compound (**45d**). The data for calculation of pA_2 for (**56a**) with its graphical presentation has been shown in Table 3.3.1.9 and Figure 3.3.1.6. The parameters used for the calculation of pA_2 values and the calculated pA_2 values for the derivatives (**56a-e**) of aspirin (**56**) are given in Table 3.3.1.10.

Table 3.3.1.9. Data for calculation of pA_2 value for derivative (56a)

Ach (ug in 30 ml)	log [m] of Ach	Response in absence of antagonist (mm)	% Response (Ach)	Response in presence of antagonist (mm)	% Response (Ach+56a)
1.0	-6.73	2.0	5.5	-	-
3.0	-6.25	10.0	27.7	2.0	12.5
10.0	-5.73	20.0	55.5	5.0	31.3
30.0	-5.25	27.0	75.0	8.0	50.0
100.0	-4.73	35.0	97.2	11.0	68 8
300.0	-4.25	36.0	100.0	14 0	87.5
1000.0	-3.73	-	100.0	16.0	100.0

Figure 3.3.1.5 Standard curves for Acetylcholine and derivative (56a)

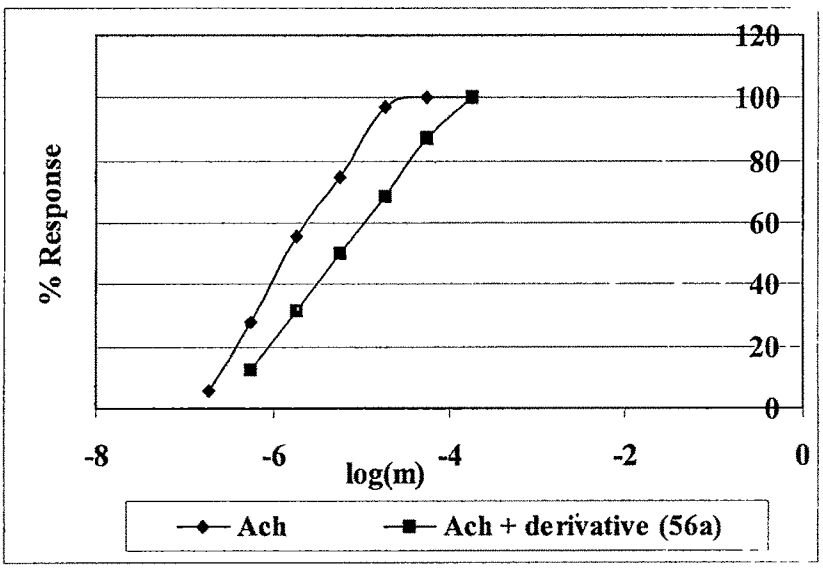

Table 3.3.1.10. Data and pA_2 values of derivatives (56a-e).

Derivative No.	Conc. of Derivative (ug/ml)	-log[M]	EC_{50} in presence of antagonist (P)	EC_{50} in absence of antagonist (A)	x = P/A	log (x-1)	pA_2
56a	10.0	4.458	$5.62*10^{-6}$	$1.67*10^{-6}$	3.36	0.374	4.83
56b	10.0	4.498	$1.86*10^{-6}$	$3.16*10^{-7}$	5.88	0.688	5 18
56c	10.0	4.460	$6.31*10^{-6}$	$1.77*10^{-6}$	3.56	0.409	4.87
56d	40.0	3.842	$1.67*10^{-6}$	$1.05*10^{-7}$	1.596	-0.223	3.62
56e	10.0	4.518	$1.88*10^{-6}$	$2.82*10^{-6}$	6.66	0.753	5 27

3.3.1.6. Anticholinergic activity of compounds (58a-e)

The compounds (**58a-e**) were evaluated for their anticholinergic potency as described for compound (**45d**). The data for calculation of pA_2 for (**58c**) with its graphical presentation has been shown in Table 3.3.1.11 and Figure 3.3.1.6. The parameters used for the calculation of pA_2 values and the calculated pA_2 values for the derivatives (**58a-e**) are given in Table 3.3.1.12.

Table 3.3.1.11. Data for calculation of pA_2 value for derivative (58c)

Ach (ug in 30 ml)	log [m] of Ach	Response in absence of antagonist (mm)	% Response (Ach)	Response in presence of antagonist (mm)	% Response (Ach+58c)
0.1	-7.73	3.0	15.0	1.0	5.5
0.3	-7.25	10.0	50.0	4.0	16.6
1.0	-6.73	14.0	70.0	9.0	38.8
3.0	-6.25	17.0	85.0	13.0	60 0
10.0	-5.73	19.0	95.0	19.0	86.0
30.0	-5.25	20.0	100.0	21.0	95.5
100.0	-4.73	20.0	100	22.0	100.0

Figure 3.3.1.6 Standard curves for Acetylcholine and derivative (58c)

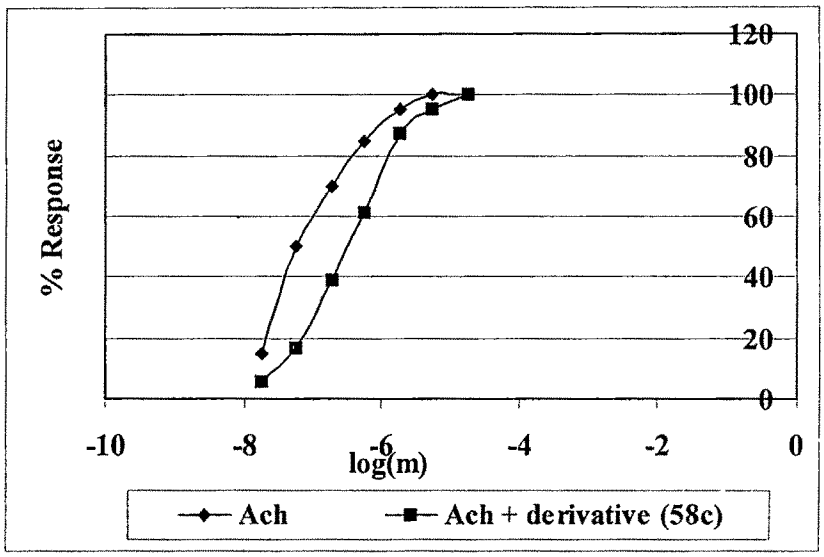

Table 3.3.1.12. Data and pA_2 values of derivatives (58a-e).

Deriva-tive No.	Conc. of Derivative (ug/ml)	-log[M]	EC_{50} in presence of antagonist (P)	EC_{50} in absence of antagonist (A)	x = P/A	log (x-1)	pA_2
58a	10.0	4.513	$2.37*10^{-6}$	$1.41*10^{-6}$	1.679	-0.168	4.35
58b	20.0	4.250	$1.33*10^{-7}$	$2.82*10^{-7}$	4.731	0 571	4 82
58c	20.0	4.260	$6.68*10^{-7}$	$6.68*10^{-7}$	12.59	1 064	5.32
58d	30.0	4.069	$2.66*10^{-7}$	$1.18*10^{-7}$	2.240	0 093	4 16
58e	40.0	3.960	$1.99*10^{-7}$	$9.44*10^{-8}$	2.100	0.045	4.00

As hypothesized all the synthesized esters exhibited anticholinergic activity as expected activity though, much weaker than the standard drug, atropine sulphate. Among all of the esters, the tropinol esters (**45f** and **49f**) were found to be the most potent with the highest pA_2 values. The number of carbon atoms attached to 'N' of the aminoalcohol part seems to have an influence on the anticholinergic potency of the derivatives. The activity was observed to increase with the increase in the number of carbons as the pA_2 values were obtained in the increasing order for the ester derivatives of the parent drugs (**45** and **58**). In case of ester derivatives (**51a-e**) of diclofenac (**51**) maximum anticholinergic potency resided in the dimethylaminoethyl ester derivative (**51a**) having the smallest chain

length. Polar grouping in the aminoester (oxygen of morpholino group) had a varying effect on the anticholinergic potency. The morpholinoethyl ester derivative (**54e** and **56e**) were the most potent among all the derivatives of **54** and **56**. The morpholinoethyl ester derivative (**49e**) was found to be the most potent among all the other esters. The existence of inherent anticholinergic potency in these derivatives would contribute in decreasing the local gastric irritation by decreasing the gastric secretions. Though the derivatives possess weak anticholinergic activity in comparison to atropine, the dose at which they would be required or administered, for the anti-inflammatory effect might be sufficient to exhibit substantial anticholinergic activity, needed for decreasing the gastric secretions to counter the problem of gastric ulceration.

3.3.2. ANTI-INFLAMMATORY ACTIVITY

Sprague-Dawley rats were used in a group of five animals in each group. Carrageenan-induced rat paw edema assay[113] was used for evaluating the anti-inflammatory activity of the derivatives and the respective parent drugs. The parent drugs and their derivatives were administered orally at equimolar doses.

Carrageenan from various sources were evaluated for inducing inflammation into the rat paw. Lambda carrageenan (Type IV) only was found to produce reproducible and substantial inflammation among all the tested samples. 4-Biphenylacetic acid (**45**) (10 mg/kg body weight) was administered orally as suspension (1% w/v carboxymethyl cellulose) to a group of five animals. Another group acting as control was given 1% w/v carboxymethyl cellulose (without drug). Carrageenan (0.1 ml, 1% w/v) was injected into the subplantar region of the left hind paw after one hour of dosing. The paw volume was measured for both the groups immediately after injection and at time intervals of 1, 1.5, 2.0, 2.5, 3.0, 4.0 and 5.0 hours The observations for the paw volume are given in Table 3.3.2.1 and 3.3.2.2 for the control and drug treated rats respectively.

Table 3.3.2.1 Paw volume readings for the control group animals

Animal No.	Paw volume (ml) at different time intervals								Difference (3^{rd} hour)
Time(h)	0.0	1.0	1.5	2.0	2.5	3.0	4.0	5.0	
1	0.68	0.72	0.98	1.13	1.47	1.69	1.69	1.67	1.01
2	0.70	0.78	1.24	1.19	1.43	1.72	1.72	1.72	1.02
3	0.84	0.98	1.06	1.13	1.37	1.86	1.84	1.84	1.02
4	0.76	0.83	0.90	0.98	1.29	1.56	1 54	1.52	0.80
5	0.76	0.86	0.90	1.17	1.32	1.51	1.51	1.51	0.75

Table 3.3.2.2 Paw volume readings for test compound (45) treated group animals

Animal No.	Paw volume (ml) at different time intervals								Difference (3^{rd} hour)
Time(h)	0.0	1.0	1.5	2.0	2.5	3.0	4.0	5.0	
1	0.68	0.68	0.75	0.78	0.92	1.04	1.04	1 04	0.36
2	0.72	0.74	0.80	0.82	0.96	1.26	1.26	1.26	0.54
3	0.74	0.76	0.80	0.80	0.91	0.98	0.98	0.96	0.24
4	0.81	0.81	0.92	0.92	1.18	1.29	1.30	1.30	0.48
5	0.68	0.68	0.74	0.74	0.78	0.82	0.82	0.82	0.14

From the observations given in the above Tables 3.3.2.1 and 3.3.2.2 it was found that the maximum increase in paw volume occurred at third hour. Hence, for rest of the derivatives paw volume was measured at zero and third hour only after the carrageenan injection. The percentage inhibition of swelling was calculated in comparison to the control group by the given formula:

$$\% \text{ Inhibition of paw edema} = (1 - Ed_{drug} / Ed_{control}) \times 100$$

The results for the synthesized derivatives and the respective parent drugs are expressed as edema volume ± S.E.M. and as % inhibition of edema formation (Table 3.3.2.3).

Table 3.3.2.3 Anti-inflammatory activity of the aminoalcohol ester derivatives of the parent drugs (45, 49, 51, 54, 56 and 58).

Compound	Edema volume ± SEM	% Inhibition of edema formation (3^{rd} h)
Control	0.920 ± 0.059	0.00
Biphenylacetic-acid Dose (mg/kg)	0.352 ± 0.073	61.74 **10.0**
45a	0.200 ± 0.035	78.26
45b	0.195 ± 0.074	78.80
45c	0.135 ± 0.033	85.33
45d	0.258 ± 0.088	71.96
45e	0.180 ± 0.050	80.43
45f	0.892 ± 0.021	0.00*
Flurbiprofen Dose (mg/kg)	0.134 ± 0.021	85.43 **8.0**
49a	0.115 ± 0.027	87.50
49b	0.108 ± 0.013	88.32
49c	0.100 ± 0.023	89.13
49d	0.190 ± 0.064	79.35
49e	0.120 ± 0.018	86.96
49f	0.920 ± 0.036	0.00*
Diclofenac Dose (mg/kg)	0.068 ± 0.030	92.60 **20.0**
51a	0.154 ± 0.025	83.26
51b	0.118 ± 0.011	87 17
51c	0.188 ± 0.031	79.56*
51d	0.287 ± 0.039	68.75*
51e	0.14 ± 0.026	84.78

Continued Table 3.3.2.3

Compound	Edema volume ± SEM	% Inhibition of edema formation (3^{rd} h)
Indomethacin **Dose (mg/kg)**	0.502 ± 0.041	45.43 **3.0**
54a	0.490 ± 0.054	46.74
54c	0.768 ± 0.056	16.57*
54d	0.576 ± 0.032	37.50
54e	0.708 ± 0.104	23.09*
Aspirin **Dose (mg/kg)**	0.458 ± 0.055	50 21 **20.0**
56a	0.602 ± 0.115	34.56*
56b	0.684 ± 0.148	25.65*
56c	0.666 ± 0.052	27.61*
56e	0.663 ± 0.060	28.26*
Ketorolac **Dose (mg/kg)**	0.230 ± 0.0.017	75.00 **20.0**
58a	0.284 ± 0.146	69.13
58b	0.295 ± 0 061	73.36
58c	0.243 ± 0.079	73.64
58e	0.336 ± 0.055	72.83

* $p<0.05$ with reference to the respective parent drug. Data are expressed as mean ± S.E.M.

Most of the derivatives were found to possess either an enhanced or comparable anti-inflammatory activity in comparison to their respective parent drugs. The tropinol ester derivatives (**45f** and **49f**) of 4-biphenylacetic acid (**45**) and flurbiprofen (**49**) were devoid of any anti-inflammatory activity in this acute model of inflammation. The absence of the anti-inflammatory activity might be due to the failure of these derivatives to release the respective parent drugs as observed in the hydrolyses studies performed in serum. The graphical presentation for the percent inhibition of the derivatives with their respective parent drugs is shown in Figures 3.3.2.1 to 3.3.2.6.

Figure 3.3.2.1 Antiinflammatory activity of 45 and its derivatives (45a-f)

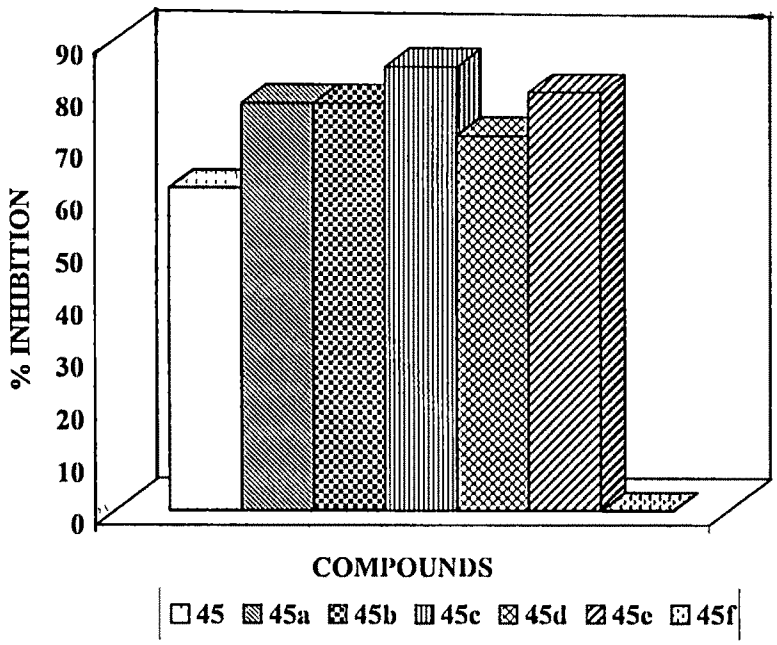

Figure 3.3.2.2 Antiinflammatory activity of 49 and its derivatives (49a-f)

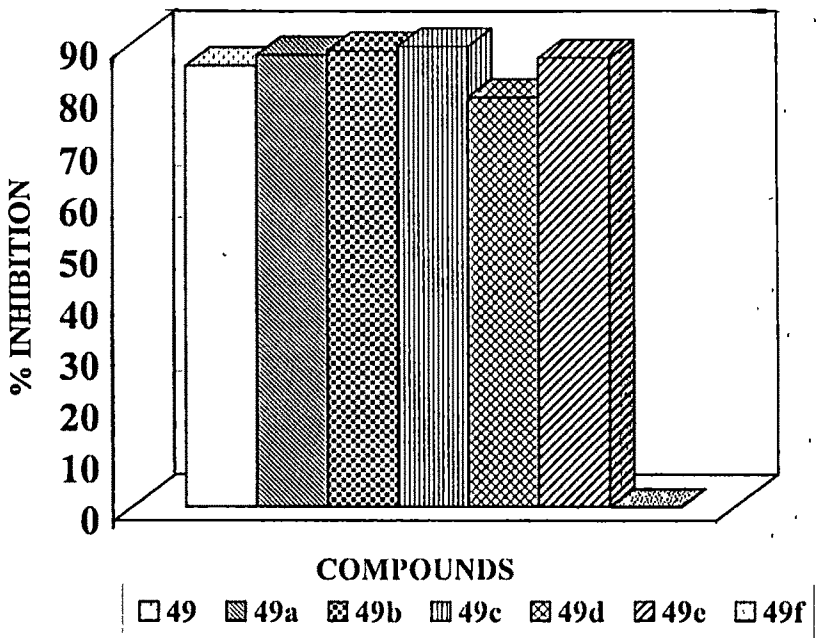

Figure 3.3.2.3 Antiinflammatory activity of 51 and its derivatives (51a-e)

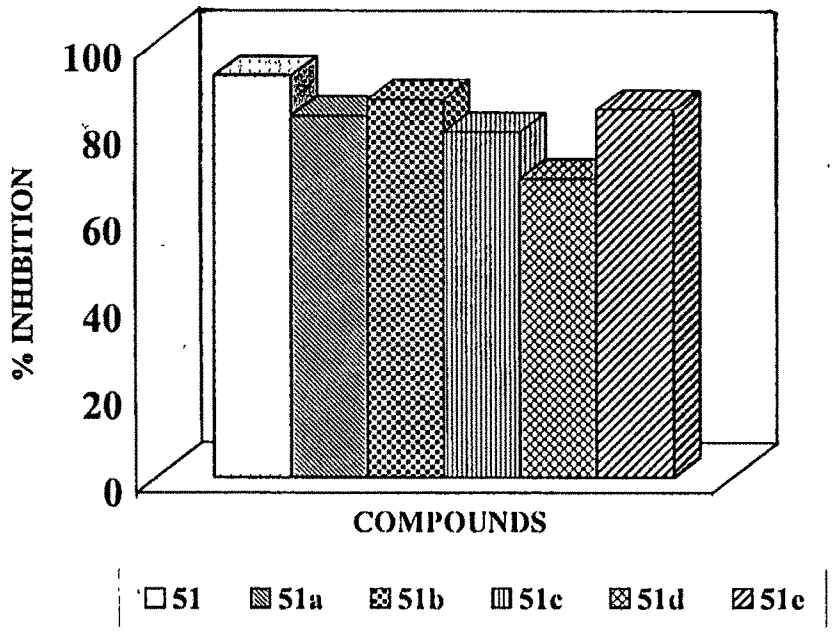

Figure 3.3.2.4 Antiinflammatory activity of 54 and its derivatives

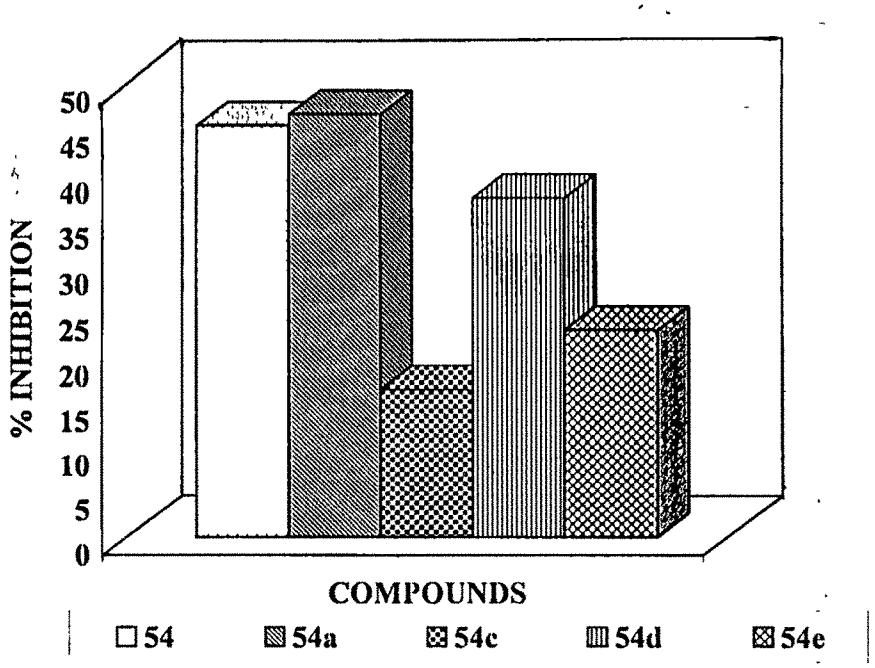

Figure 3.3.2.5 Antiinflammatory activity of 56 and its derivatives

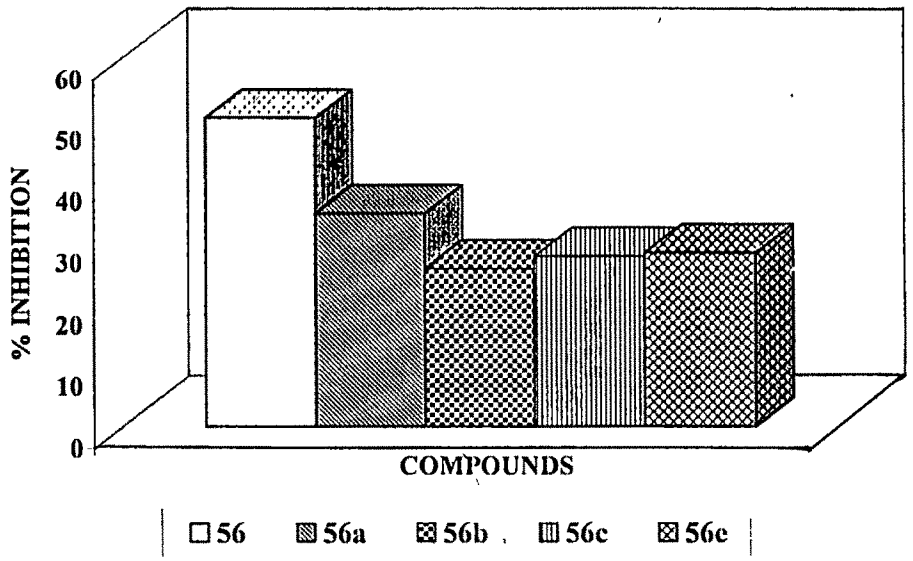

Figure 3.3.2.6 Antiinflammatory activity of 58 and its derivatives

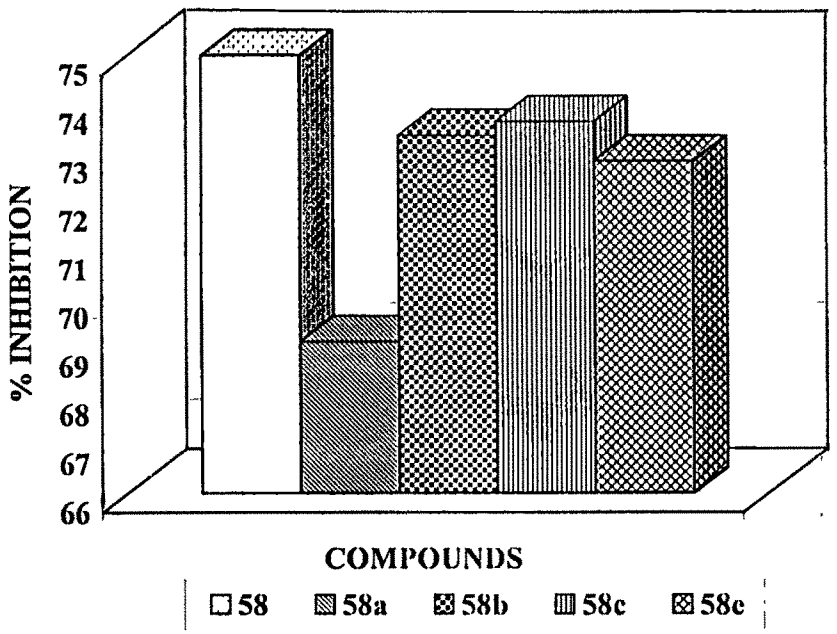

3.3.3. ANALGESIC ACTIVITY

Swiss albino mice in a group of six animals were used for the acitivity. Acetic acid induced writhing model in mouse as described by Koster *et al* [114] was used for evaluating the derivatives and their respective parent drugs for peripheral analgesic activity. The test compounds were administered orally at equimolar doses with respect to their parent drugs Acetic acid (0.6 % v/v) was given intraperitoneally for inducing the writhings response in the test animals.

4-Biphenylacetic acid (**45**) for example, was administered orally as a suspension in carboxymetyl cellulose (1% w/v) to a group of six mice. A control group of six mice received only the vehicle. One hour after oral administration writhing response was induced by injecting acetic acid (10 ml/kg body weight) intraperitoneally to the test animals. Five minutes after the acetic acid injection, the number of writhes were calculated for a period of 20 minutes in both the groups. The percent inhibition of writhing was calculated using the
formula:

$$\% \text{ Inhibition of writhing} = (1\text{-}T/S) \times 100$$

Similarly, the derivatives of compound (**45**) were also evaluated at the same equimolar dose at which 4-biphenylacetic acid (**45**) was evaluated. The results are given in Table-3.3.3.1. Rest of the other derivatives were evaluated in the same way alongwith their respective parent drugs (**49, 51, 54** and **58**). The results are indicated as number of writhes ± SEM and as percentage inhibition of writhing in comparison to the control group in following Table 3.3.3.1.

Table 3.3.3.1 Analgesic activity of derivatives of parent drugs (45,49, 51, 54 and 58)

Compound	No. of writhes ± SEM	% Inhibition of writhing
Control	36.60±1.44	0 00
Biphenylacetic-acid **Dose (mg/kg)**	17 66±3.09	51.73 **25.0**
45a	20.40±2.43	44.26
45c	19.40±1.03	46.99
45e	23.83±1.75	37.16
Flurbiprofen **Dose (mg/kg)**	16.83±0.70	54.01 **10.0**
49b	23.50±1.95	35.79*
49d	22.00±0.71	39.89*
49f	17.80±0.66	51.37
Diclofenac **Dose (mg/kg)**	15.60±1.63	57.38 **45.0**
51a	11.20±3.38	69.40
51b	10.00±1.64	72.68
51c	15.00±1.70	59.02
51d	14.00±2.45	61.75
51e	22.00±3.27	39.89
Indomethacin **Dose (mg/kg)**	21.20 ± 3.14	42.08 **15.0**
54a	22.00 ± 2.19	39.89
54c	23.80 ± 2.52	34.97
54e	23.60 ± 1.50	35.52

Continued Table 3.3.3.1

Compound	No. of writhes ± SEM	% Inhibition of writhing
Ketorolac **Dose (mg/kg)**	16.80 ± 1.59	54.10 **20.0**
58b	21.40 ± 3.26	41.53
58c	28.17 ± 1.58	23.04*
58e	19.40 ± 1.33	46.99

* $p<0.05$ with reference to the respective parent drug. Data are expressed as mean ± S.E.M.

The graphical presentation for the percent inhibition of the number of writhes for the derivatives with their respective parent drugs is given in the Figures 3.3.3.1 to 3.3.3.5.

Figure 3.3.3.1 Analgesic activity of 45 and its derivatives

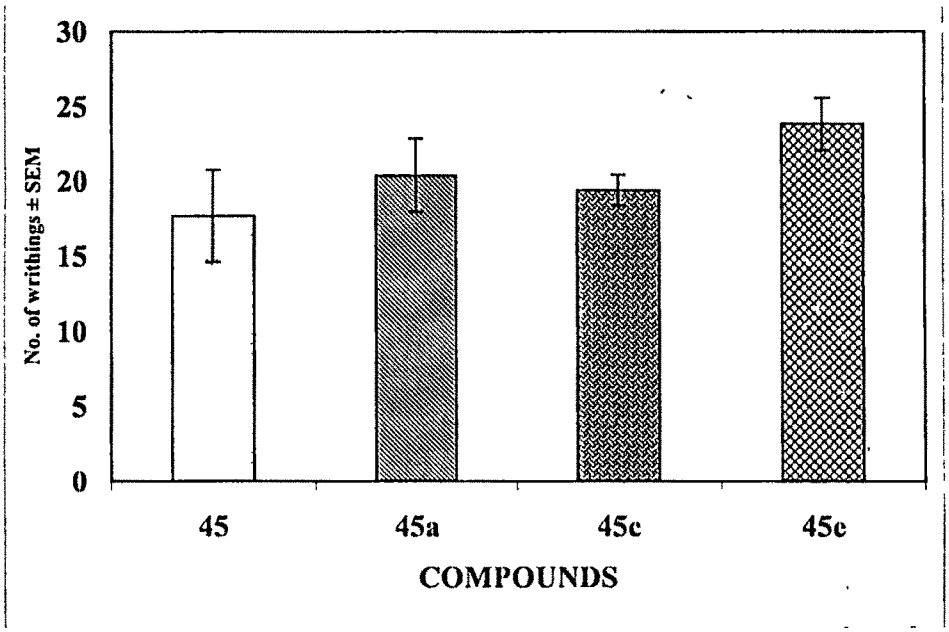

Figure 3.3.3.2 Analgesic activity of 49 and its derivatives

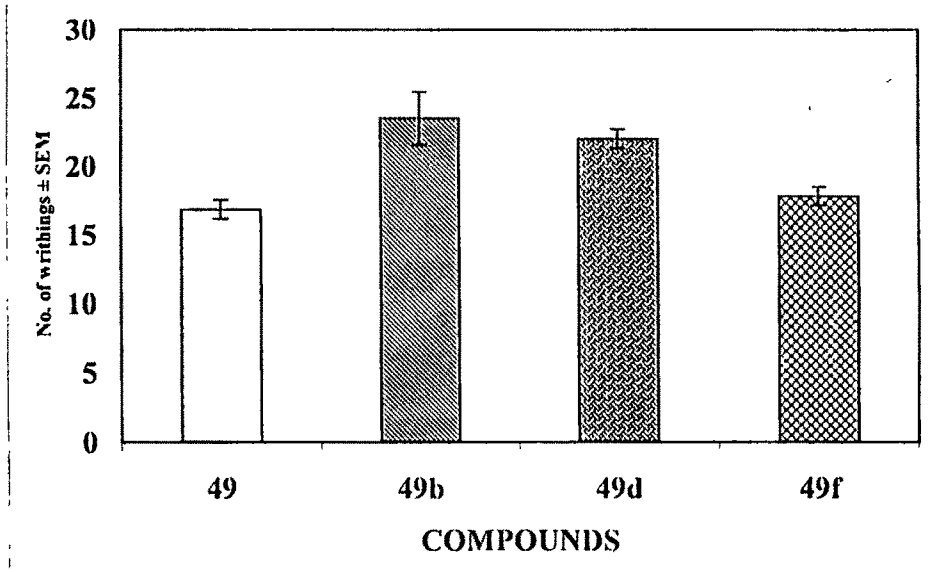

Figure 3.3.3.3 Analgesic activity of 51 and its derivatives

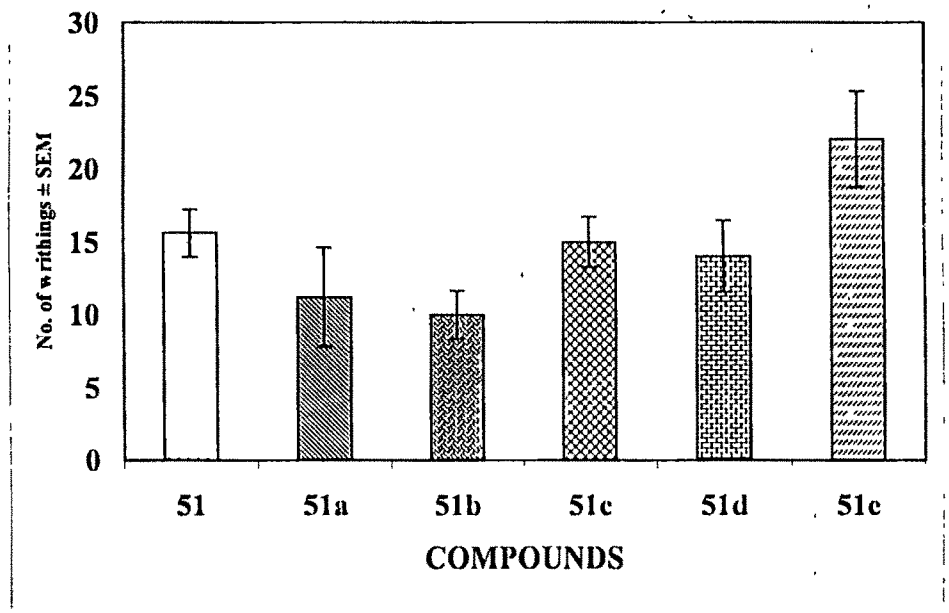

Figure 3.3.3.4 Analgesic activity of 54 and its derivatives

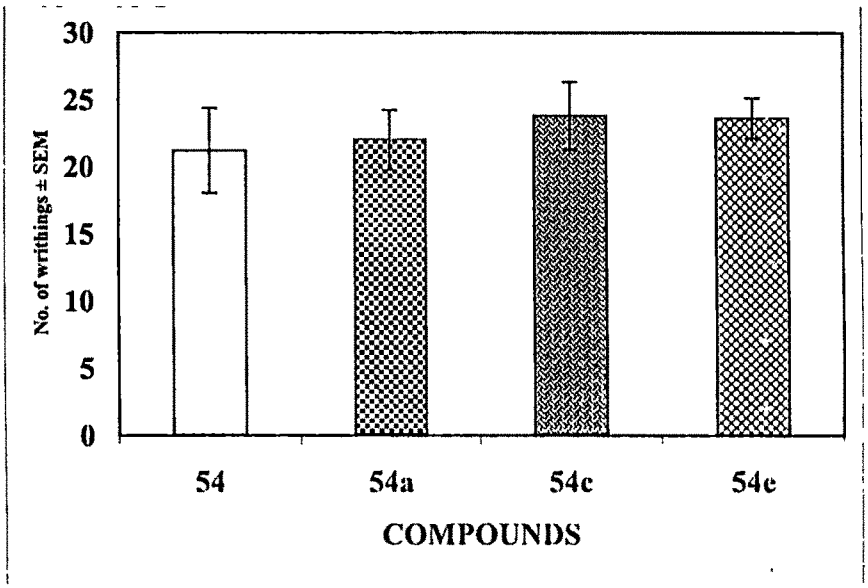

Figure 3.3.3.5 Analgesic activity of 58 and its derivatives

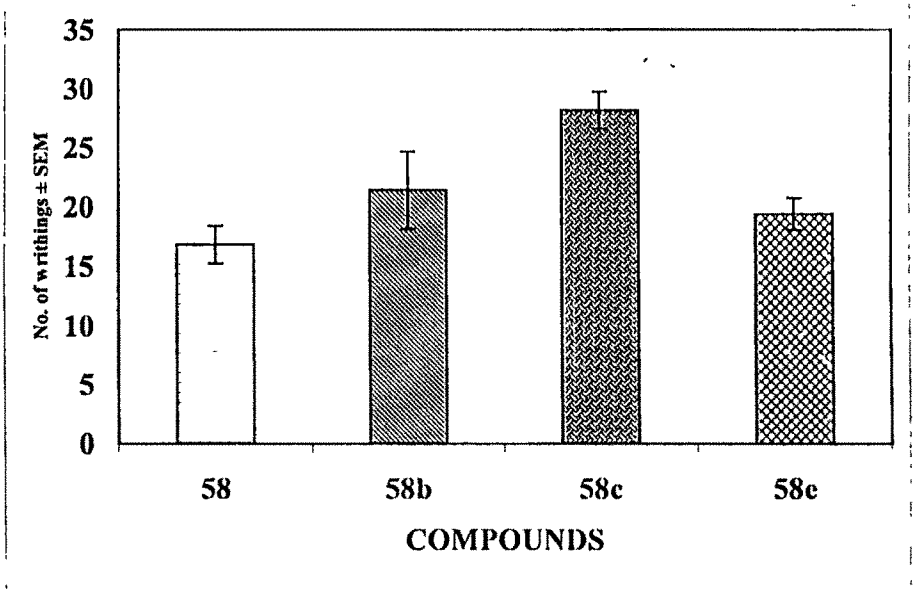

The results of Table 3.3.3.1 indicate that except for the compounds (**49b** and **49d**) all the other aminoester derivatives exhibited an analgesic activity which was not statistically different ($p<0.05$) from their respective parent drugs hence, it can be inferred that the analgesic potency of the parent drugs is retained by these derivatives. Surprisingly, the

tropinol ester (**49f**) exhibited equipotent analgesic activity when compared with the parent drug (**49**). This could not be explained logically because it did not exhibit enzymatic susceptibility for releasing the parent NSAID flurbiprofen (**49**) unlike all the other derivatives of various parent NSAIDs.

3.3.4. ULCEROGENICITY

Sprague-Dawley rats of either sex were used in groups of five and their ulcerogenic potential was determined as described by Parmar *et al* [115]. The derivatives and their respective parent drugs were administered orally at equimolar doses. For evaluating the ulcerogenicity of the derivatives in each case the dose of the parent drug for inducing substantial ulcers was established by trial and error. The derivatives were administered at an equimolar dose to their respective parent drugs.

Animals were fasted for 36 hours and parent drug for example (**45**) was administered orally at a dose of 500 mg/kg as suspension in CMC (1% w/v) and the animals were fasted again for four hours after dosing. The animals were sacrificed and the stomach dissected out, cut along the greater curvature, washed with saline and mounted on a flat surface after fixing in formalin. The diameter of the stomach was measured to provide the total area, which was halved to give the actual mucosal area (Am). The linear and circular ulcers were measured to calculate the ulcerated area. Total petiaches were also counted in the mucosal area. The ulcer index was determined by the following given formula:

$$\text{Ulcer index} = 10 * Au/Am$$

Determinations were carried out for other parent drugs and some of the selected derivatives of these drugs. The results, expresssed as ulcer index ± S.E.M for the derivatives along with their respective parent drugs are given in the Table 3.3.4.1.

Table 3.3.4.1 Ulcerogenicity of the aminoalcohol ester derivatives of the parent drugs (45,49, 51, 54, 56 and 58)

Compound	**Ulcer Index ± SEM**
Control	0.000
Biphenylacetic- acid **Dose (mg/kg)**	0.564±0.069 **500.0**
45a	0.228±0.025*
45d	0.182±0.050*
45e	0.158±0.027*
Flurbiprofen **Dose (mg/kg)**	0.800±0.048 **25.0**
49b	0.135±0.023*
49c	0.256±0.056*
49d	0.157 ± 0.087*
49e	0.126 ± 0.032*
Diclofenac **Dose (mg/kg)**	0.797 ± 0.029 **75.0**
51a	0.522 ± 0.095
51b	0.329 ± 0.074*
51c	0.426 ± 0.119*
51d	0.323 ± 0.051*
51e	0.368 ± 0.054*
Indomethacin **Dose (mg/kg)**	0.547 ± 0.116 **25.0**
54a	0.149 ± 0.044*
54c	0.134 ± 0.042*
54e	0.259 ± 0.031*

Continued Table 3.3.4.1

Compound	Ulcer Index ± SEM
Aspirin	0.738 ± 0.039
Dose (mg/kg)	**100.0**
56a	0.341 ± 0.046*
56c	0.265 ± 0.067*
56e	0.317 ± 0.058*
Ketorolac	0.484 ± 0.030*
Dose (mg/kg)	**75.0**
58a	0.237 ± 0.120*
58c	0.219 ± 0.075*
58d	0.213 ± 0.051*

* $p<0.05$ with reference to the respective parent drug. Data are expressed as mean ± S.E.M.

The graphical presentation for the ulcer index ± S.E.M for the derivatives with their respective parent drugs is given in the Figures 3.3.4.1 to 3.3.4.6.

Figure 3.3.4.1 Ulcerogenicity of 45 and its derivatives

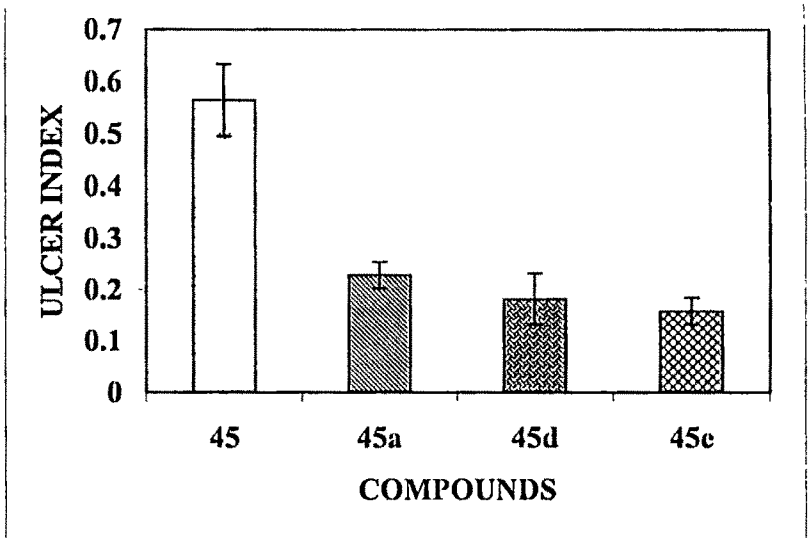

Figure 3.3.4.2 Ulcerogenicity of 49 and its derivatives

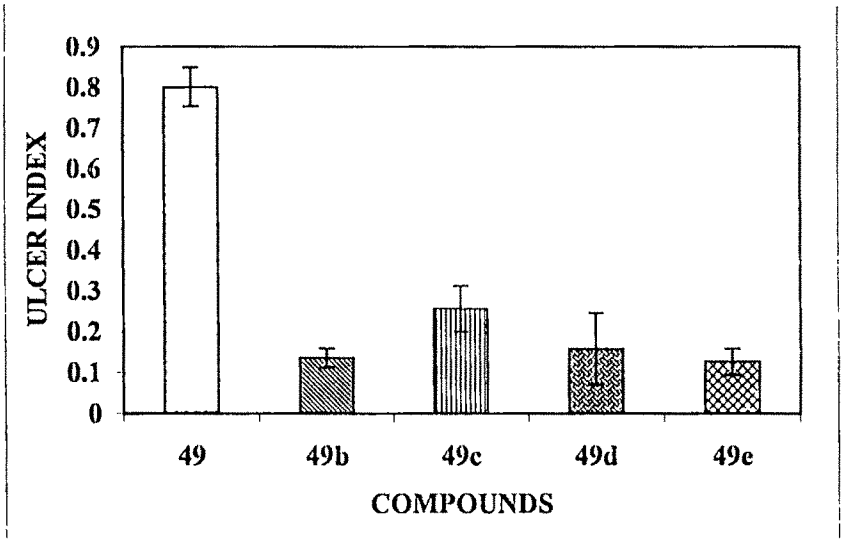

Figure 3.3.4.3 Ulcerogenicity of 51 and its derivatives

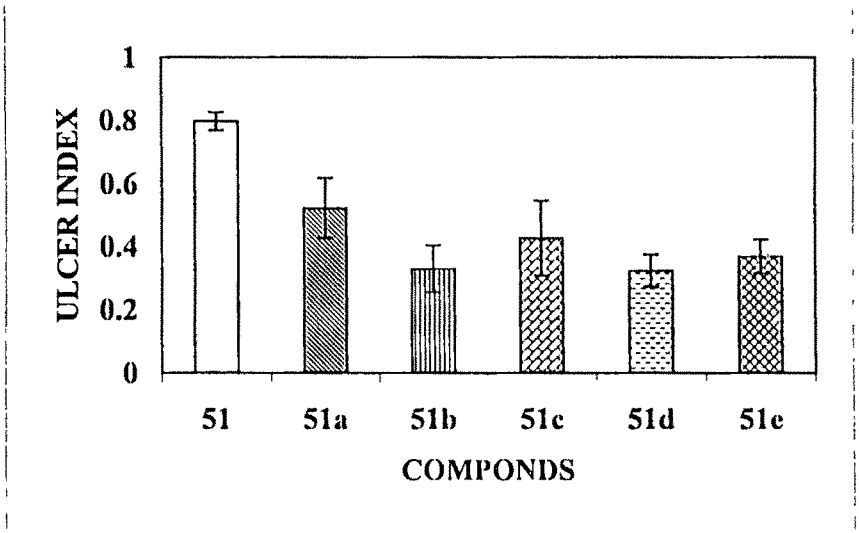

Figure 3.3.4.4 Ulcerogenicity of 54 and its derivatives

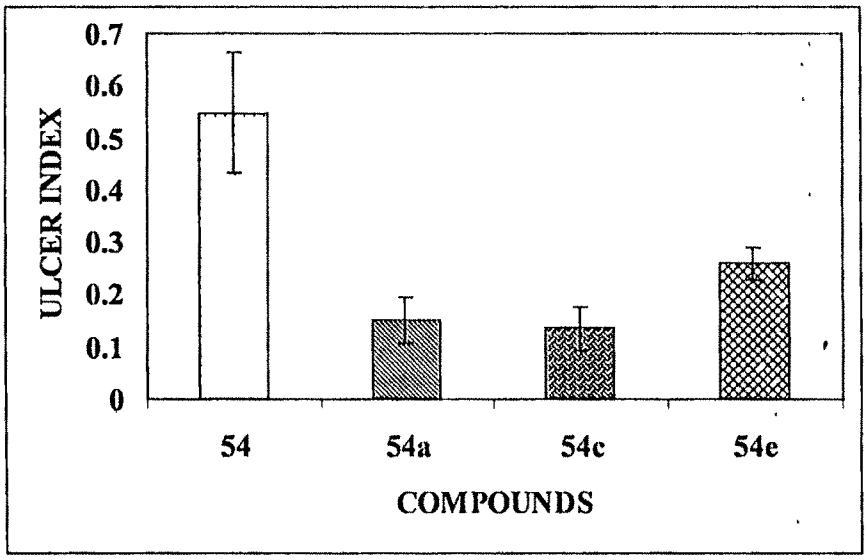

Figure 3.3.4.5 Ulcerogenicity of 56 and its derivatives

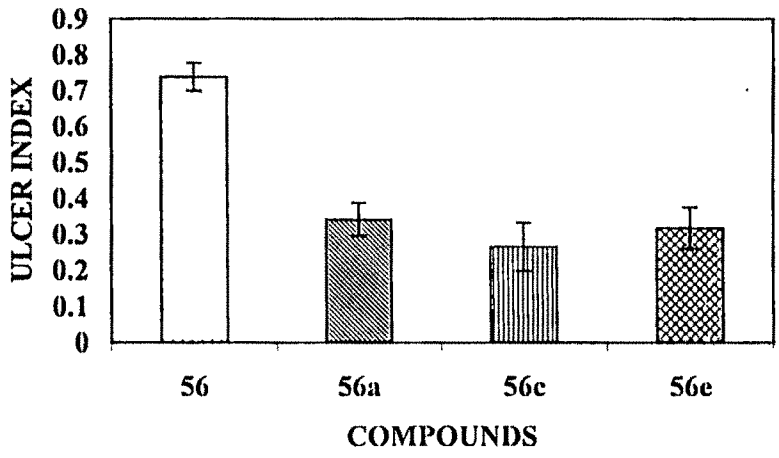

Figure 3.3.4.6 Ulcerogenicity of 58 and its derivatives

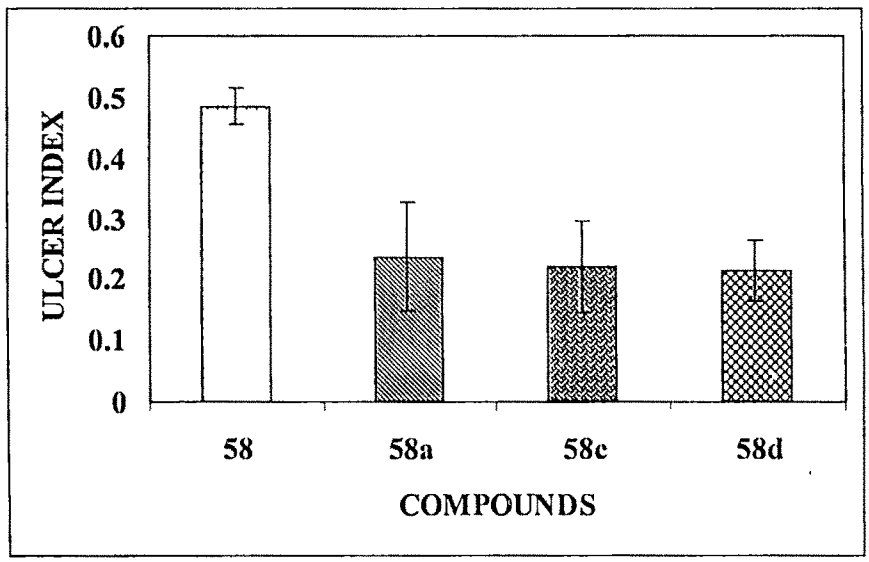

It can be observed that the ulcer index of all the derivatives evaluated for their ulcerogenic potential are significantly ($p<0.05$) less than their corresponding parent drugs. This observation supports the results of the kinetic studies performed for these derivatives in buffers indicating the successful blockade of acidic carboxyl group to prevent local GI irritation. Further, the existence of inherent anticholinergic activity of the derivatives might have also contributed in decreasing the ulcerogenicity by decreasing the gastric acid secretions. The observed residual ulcerogenicity might be due to systemic inhibition of COX-I after liberation of parent drugs in systemic circulation.

3.4. BIODISTRIBUTION AND GAMMA IMAGING STUDIES

The aim of the current study was to optimize the therapeutic efficacy of clinically used NSAIDs, as discussed earlier. Gastrointestinal ulceration is the sole major problem, which limits their (NSAIDs) chronic use in a disease like arthritis. It has been tried in the current work to address this problem, when these NSAIDs are to be given by the oral route for a longer period of time. An alternative to this approach could be site-specific delivery of these NSAIDs to the affected tissues. Reports are available in literature where beginning has already been made in this direction.

It has been reported[116] that quaternary ammonium compounds like hexamethonium and decamethonium accumulated preferentially in certain avascular cartilaginous tissues on intramuscular injection whereas, little has been found in blood rich bone marrow. It has been postulated that these quaternary ammonium compounds are localized in the cartilage tissues, probably by virtue of ionic interactions with the polyanionic acid mucopolysaccharides which have widespread presence in the cartilaginous tissues. These observations have been supported further by other workers[117-122] The authors[117] have emphasized that the localization of these quaternary ammonium compounds in the articular and epiphyseal cartilage and joint spaces might be of significance in relation to the distribution of drugs to inflamed joints and lesions of articular cartilage, and raised the possibility of enhancing the duration and intensity of anti-inflammatory effect by chemically designing a drug combining both the antiarthritic activity and joint localization property. This idea has been further extended to the site specific delivery of antirheumatic agent *D*-glucosamine to the cartilagenous tissues by conjugating it with some quaternary ammonium groups[123].

^{14}C-Labeled quarternary ammonium-glucosamine conjugates (**59** and **60**) were prepared

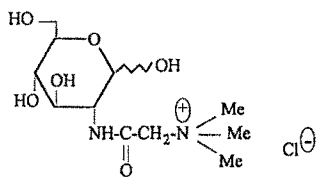

(59)

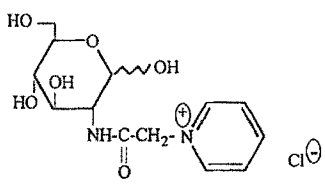

(60)

and their biodistribution in rats were studied. It was reported that introduction of a quaternary ammonium moiety in *D*-glucosamine, a compound which already exhibited a

special tropism for cartilage, allowed the molecule to be carried more selectively to the cartilagenous tissues soon after intravenous injection in rodents. Both the compounds have been reported to have higher affinity for cartilagenous tissues than the unconjugated ^{14}C-*D*-glucosamine.

Nearly 80% of all radiopharmaceuticals, used in nuclear medicine are ^{99m}Tc-labeled compounds. The reason for such a predominant position of ^{99m}Tc in clinical use is its extremely favourable physical and radiation characteristics. It has a 6-hour (approximately) half-life and emits soft monochromatic γ-rays of 140 keV power which do not affect the patient adversely. ^{99m}Tc is readily available in a sterile, pyrogen free and carrier free state from ^{99}Mo-^{99m}Tc generators. Technetium can exist in eight oxidation states namely, -1 to +7, and the stability of these oxidation states depends on the type of ligands and chemical environment. The +7 and +4 states are the most stable states. The lower oxidation states are normally stabilized by complexation with ligands.

Since we have already converted carboxyl group containing NSAIDs into tertiary amines it was thought worthwhile to convert them into quaternary compounds and to study their biodistribution. For such a study to be performed, radiolabeling of the synthesized derivatives was required to be done for their localization/quantification in the body. Any type of radiolabeling of the synthesized compounds was beyond our reach at this department. So, help was taken from Institute of Nuclear Medicine and Allied Sciences (INMAS), New Delhi for this work. In that institute the only type of labeling facility that was available was radiolabeling with ^{99m}Tc, it was planned to go for ^{99m}Tc labeling of the synthesized compounds.

The radioactive form of technetium (^{99m}Tc) is available as sodium pertechnetate salt (^{99m}Tc-$NaTcO_4$). In this salt, technetium is present as a stable state so, it does not easily complex with various ligands. To make a complex, the oxidation state has to be reduced to +5 or less. For this purpose various reducing agents like stannous chloride, stannous citrate, stannous tartrate, sodium borohydride with concentrated hydrochloric acid and ferrous sulphate with dithionite are used. Among these, stannous chloride in acidic medium is the most widely used reducing agent. After reduction of technetium to lower oxidation state, the pH of the medium has to be raised because complexes in general are less stable in acidic media and more stable in neutral/alkaline media. But, the pH of the

medium cannot be raised to a more basic side otherwise the stannic form of tin (which is present in the medium) and the reduced forms of technetium precipitate out. So, a compromise has to be made and a proper pH adjustment of the solution has to be done so that there is no precipitation and the complex also remains stable.

The reduced ^{99m}Tc can combine with different ligands[124] like –COO^--, -OH, -NH_2, -CO-, -COOR and -SH to afford complexes which may be stable depending on the medium and the complexing agent. For a new compound acting as a complexing agent for ^{99m}Tc, its labeling efficiency has to be evaluated. If the new compound is a good complexing agent then it would give a stable complex under the given conditions and the labeling efficiency would be approximately 100 % but, if the complex is not very stable then this efficiency would be much less. To assess the stablility, the solution of the complex is run on ascending instant thin layer chromatography (ITLC) in three different solvent systems separately, as mobile phases i.e. acetone (100%), saline (0.9%) and a mixture of pyridine-acetic acid-water (PAW) (3.5:5:1), and detection is carried out using γ- camera In acetone (100%) and saline (0.9%) solvent systems the ^{99m}Tc-bound complex would remain at the base of application of the spot and the uncomplexed ^{99m}Tc would travel alongwith the solvent front while in the PAW solvent system the complex would travel alongwith the solvent front while the uncomplexed ^{99m}Tc would remain at the base. By substracting the activity obtained from acetone/saline run ITLC from the activity of PAW-run ITLC (activity of the solvent front region) the net amount of activity obtained from the labeled compound could be obtained which in fact, would provide the labeling efficiency. Stability of the labeled complex in human serum could also be determined based on the above said principle. After incubating the labeled complex with serum, samples were withdrawn at different time intervals and run on ITLC using the three mobile phases described earlier, separately. Any increase in reduced/hydrolysed ^{99m}Tc activity is an indication of break down of the complex in human serum.

Compounds (**45f, 49f** and **51d**) were chosen as they were available in slightly higher quantities to perform these studies. For quaternization of the derivatives (**45f, 49f** and **51d**), the aqueous solution of each derivative was treated individually with ammonia followed by extraction with chloroform. Drying and complete removal of the organic solvent in each case yielded oily residues, which were methylated using methyl iodide as methylating agent in methanol. The quaternized derivatives (**45g, 49g** and **51g**) were

prepared (Scheme-VII) instantly before carrying out these studies and were not characterized. All these six compounds were labeled using the above discussed principle. Sodium pertechnetate was reduced using stannous chloride in acidic medium. Optimum quantity of stannous chloride to give highest yield (92-95%) of the complex for all the derivatives was determined to be 100 ug. The labeling efficiency was found to be 80 to

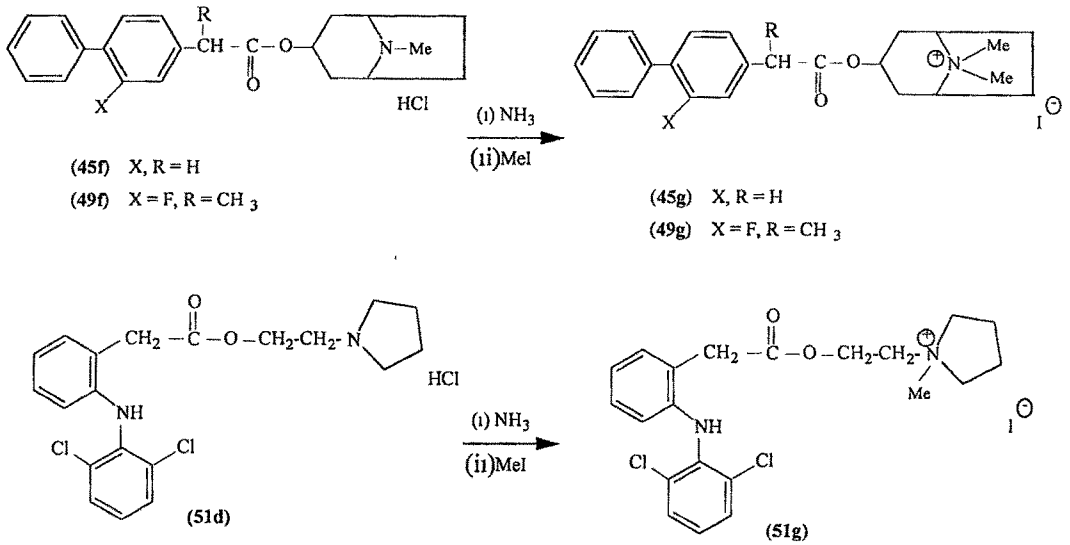

Scheme-VII

85% when 50 ug stannous chloride was used and a slight turbidity was obtained in the final solution when 200 ug of stannous chloride was added. The optimum pH range was found to be 6.5-7.0 since at pH values higher than 7.0, turbidity appeared in the solution. The optimum incubation time was found to be 15 minutes since no increase in the labeling efficiency could be observed by increasing the incubation time to 30 minutes and more. The labeling efficiency for all the six compounds (**45f, 49f, 51d, 45g, 49g** and **51g**) was found to be between 92-95%.

The stability study for each of the labeled complex was performed *in vitro* in normal saline and in human serum by peforming the ITLC as described above. It was observed that in saline, even after a period of 24 hours, the complexes for all the six compounds (**45f, 49f, 51d, 45g, 49g** and **51g**) were highly stable with labeling efficiency of 92-95%. In serum, the complexes for compounds (**45f, 45g, 49f** and **49g**) were stable till a period of 6 hours of incubation with labeling efficiency found to be more than 92% for each compound. However, the complexes for the compounds (**51d** and **51f**) were observed to

degrade within 15 minutes, with the labeling efficiency reducing to less than 50% in each case. Hence, the compounds (**45f, 45g, 49f** and **49g**) only were selected for the biodistribution and gamma imaging studies.

3.4.1. BIODISTRIBUTION STUDIES

Swiss albino mice were used for the biodistribution studies of the ^{99m}Tc-labeled compounds (**45f, 45g, 49f** and **49g**). An injected dose (100 µl) of the ^{99m}Tc- labeled complex was administered through the tail vein of each mouse. Blood was obtained by cardiac puncture at different time intervals, animals (group of three mice for each time interval) were sacrificed, different organs dissected out, washed with normal saline, made free from adhering tissues, weighed, and the radioactivity measured in a shielded-well gamma scintillation counter. The percent radioactivity for each organ was calculated, and considering 7.3% of the total body weight as whole blood, calculations were performed for determining the radioactivity for whole blood (Tables 3.4.1.1 to 3.4.1.4).

Table 3.4.1.1 Biodistribution of compound (45f) in mice

Organ/ Tissue	Percent injected dose / whole organ or tissue (± S.E.M.)				
	0.5 h	1 h	2 h	4h	24 h
Blood	0.45 ± 0.07	0.29 ± 0.03	0.31 ± 0.03	0.20 ± 0.01	0.13 ± 0.01
Heart	0.09 ± 0.02	0.10 ± 0.01	0.06 ± 0.01	0.02 ± .002	0.01 ± 0.001
Lung	1.16 ± 0.04	1.01 ± 0.07	0.80 ± 0.06	0.38 ± 0.01	0.12 ± 0 01
Liver	8.85 ± 0.69	9.79 ± 0.01	9.57 ± 0.44	6.59 ± 0.59	8.03 ± 0.27
Spleen	5.90 ± 1.27	4.88 ± 0.20	4.66 ± 0.12	4.41 ± 0.12	4.41 ± 0.48
Kidney	0.42 ± 0.08	0.49 ± 0.02	0.44 ± 0.01	0.38 ± 0.03	0.35 ± 0.03
Intestine	0.39 ± 0.04	0.61 ± 0.12	0.70 ± 0.04	0.43 ± 0.02	0.33 ± 0.12
Stomach	0.04 ± 0.01	0.04 ± 0.01	0.11 ± 0.01	0.12 ± 0.07	0.03 ± 0.003

Table 3.4.1.2 Biodistribution of compound (45g) in mice

Organ/ Tissue	Percent injected dose / gram of organ or tissue (± S.E.M.)				
	0.5 h	1 h	2 h	4h	24 h
Blood	0.83 ± 0.13	0.61 ± 0.09	0.42 ± 0.02	0.36 ± 0 04	0.02 ± 0.001
Heart	0.22 ± 0.09	0.12 ±0.08	0.25 ± 0.02	0.19 ± 0.001	0.04 ± 0.002
Lung	0.94 ± 0.24	0.57 ± 0.14	0.66 ± 0.04	0.49 ± 0.09	0.18 ± 0 01
Liver	13.71 ± 1.06	13.08 ± 0.35	12.80 ± 0.38	11.88 ± 1.34	14.37 ± 1 01
Spleen	4.75 ± 0.95	2.80 ± 0.41	2.17 ± 0.13	2.02 ± 0.38	1.12 ± 0.04
Kidney	0.44 ± 0.04	0.73 ± 0.13	0.55 ± 0.01	0.45 ± 0.04	0.41 ± 0.05
Intestine	0.37 ± 0.09	0.58 ± 0.10	0.57 ± 0.03	0.44 ± 0.01	0.27 ± 0.07
Stomach	0.04 ± 0.01	0.17 ± 0.19	0.17 ± 0.05	0.19 ± 0.04	0.11 ± 0.03

Table 3.4.1.3 Biodistribution of compound (49f) in mice

Organ/ Tissue	Percent injected dose / whole organ or tissue (± S.E.M.)				
	0.5 h	1 h	2 h	4h	24 h
Blood	1.28 ± 0.13	0.52 ± 0.12	0.51 ± 0.11	0.44 ± 0.04	0.28 ± 0.08
Heart	0.09 ± 0.02	0.06 ± 0.004	0.06 ± 0.01	0.08 ± 0.002	0.002 ± 1.46E-05
Lung	0.44 ± 0.02	0.42 ± 0.05	0.32 ± 0.03	0.51 ± 0.08	0.01 ± 0.001
Liver	7.33 ± 1.47	9.39 ± 0.97	18.03 ± 0.34	16.12 ± 0.25	0.66 ± 0.02
Spleen	1.43 ± 0.22	1.72 ± 0.09	0.83 ± 0.11	1.99 ± 0.54	0.05 ± 0.01
Kidney	0.63 ± 0.30	0.78 ± 0.03	0.64 ± 0.07	1.42 ± 0.14	0.03 ± 0.003
Intestine	0.83 ± 0.15	0.86 ± 0.05	0.95 ± 0.17	0.63 ± 0.20	0.02 ±0.002
Stomach	0.09 ± 0.01	0.09 ± 0.16	0.09 ± 0.03	0.17 ±0.03	0.007 ±0.002

Table 3.4.1.4 Biodistribution of compound (49g) in mice

Organ/ Tissue	Percent injected dose / whole organ or tissue (± S.E.M.)				
	0.5 h	1 h	2 h	4h	24 h
Blood	1.25 ± 0.13	1.01 ± 0.18	0.86 ± 0 45	0.78 ± 0.05	0.35 ± 0.06
Heart	0.08 ± 0.01	0.11 ± 0.02	0.07 ± 0.004	0.08 ± 0.01	0.05 ± 0 01
Lung	1.36 ± 0.19	0.93 ± 0.12	0.80 ± 0.10	0.54 ± 0.07	0.20 ± 0.04
Liver	16.38 ± 0.39	18.66 ± 1.21	18.64 ± 0.42	16.98 ± 0.85	9.10 ± 1 11
Spleen	3.58 ± 0.44	2.55 ± 0.33	2.17 ± 0.31	1.56 ± 0.13	1.80 ± 0.77
Kidney	1.51 ± 0.04	1.08 ± 0.14	0.96 ± 0.26	1.09 ± 0.19	0.73 ± 0.05
Intestine	0.44 ± 0.05	0.82 ± 0.15	0.95 ± 0.17	1.39 ± 0 12	0.31 ± 0.07
Stomach	0.11 ± 0.04	0.06 ± 0.003	0.06 ± 0.02	0.16 ± 0.09	0.06 ± 0.01

Stomach is the target site[125] for free ^{99m}Tc in the body and if the complex degrades the free radioactivity gets accumulated in stomach. The results of the biodistribution studies suggest that the complexes for the compounds (**45f, 45g, 49f** and **49g**) are stable *in vivo* in serum till 24 hours as can be seen from the low percent radioactivity in stomach at the different time intervals. Major fraction of the drugs is metabolized by the liver and the route of elimination is kidney as this can be noted from the higher concentrations of radioactivity in these organs.

3.4.2. GAMMA IMAGING STUDIES

Inflammation was induced in the right hind paw of the rats by injecting carrageenan (0 1 ml, 1% w/v in normal saline) into the subplantar region of the paw and the radiolabeled complex (0.2 ml) of the desired compound (**45f, 45g, 49f** and **49g**) was administered through tail vein to each rat after an interval of 3 hours. The animals were anaesthetized with ketamine/diazepam (i.m.), fixed on a board and images were taken 1 hour after the administration of the radiolabeled complexes. The gamma images obtained are shown in Figures 3.4.2.1 to 3.4.2.4. The arrows in the figures indicate the localization of the radiolabeled complex in the inflamed site (right paw of rat).

Figure 3.4.2.1 Gamma camera image of rats at 1 h after i.v. administration of 99m-Tc-compound 45f

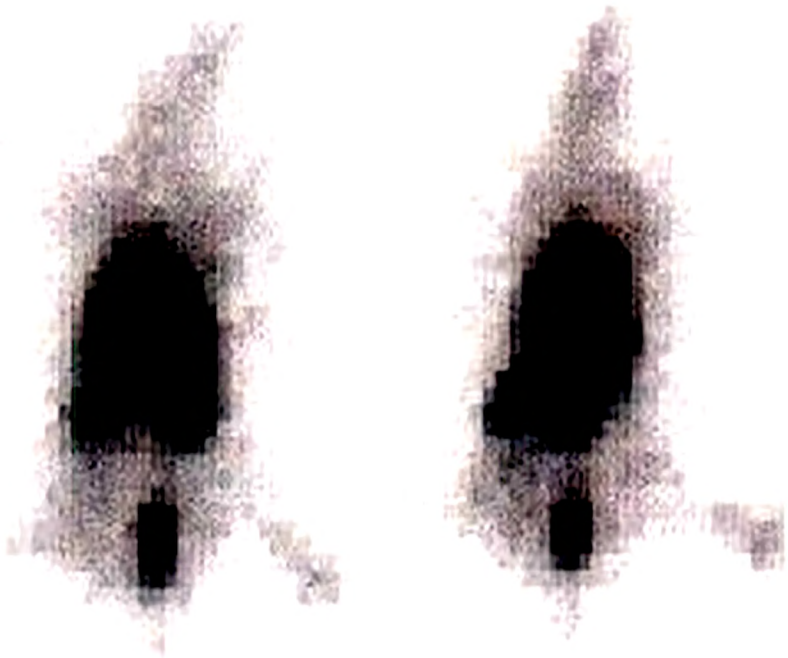

Figure 3.4.2.2 Gamma camera image of rats at 1 h after i.v. administration of 99m-Tc-compound 45g

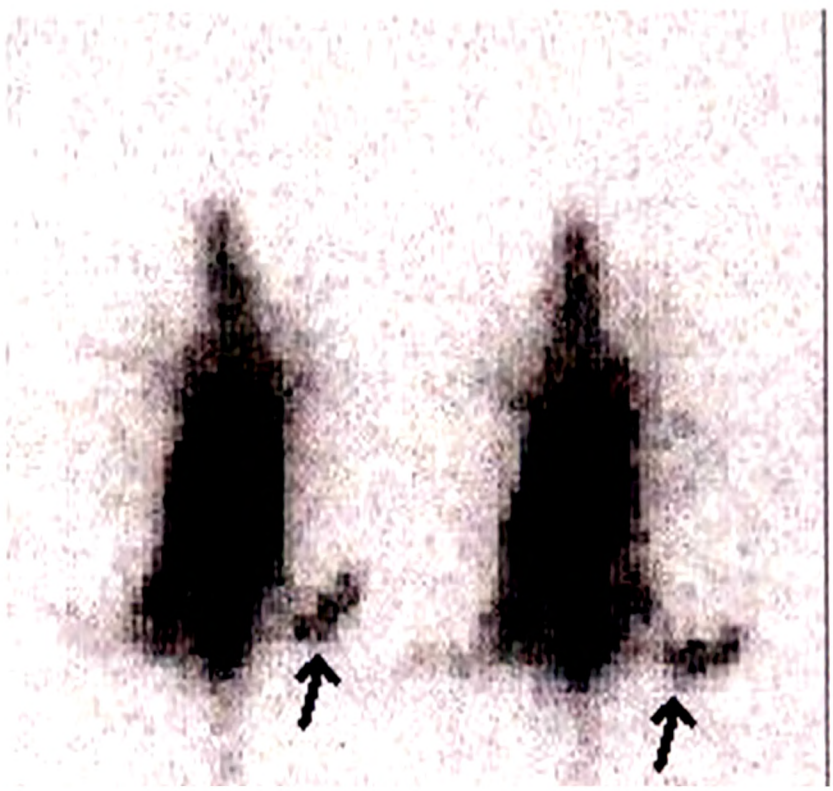

Figure 3.4.2.3 Gamma camera image of rats at 1 h after i.v. administration of 99m-Tc-compound 49f

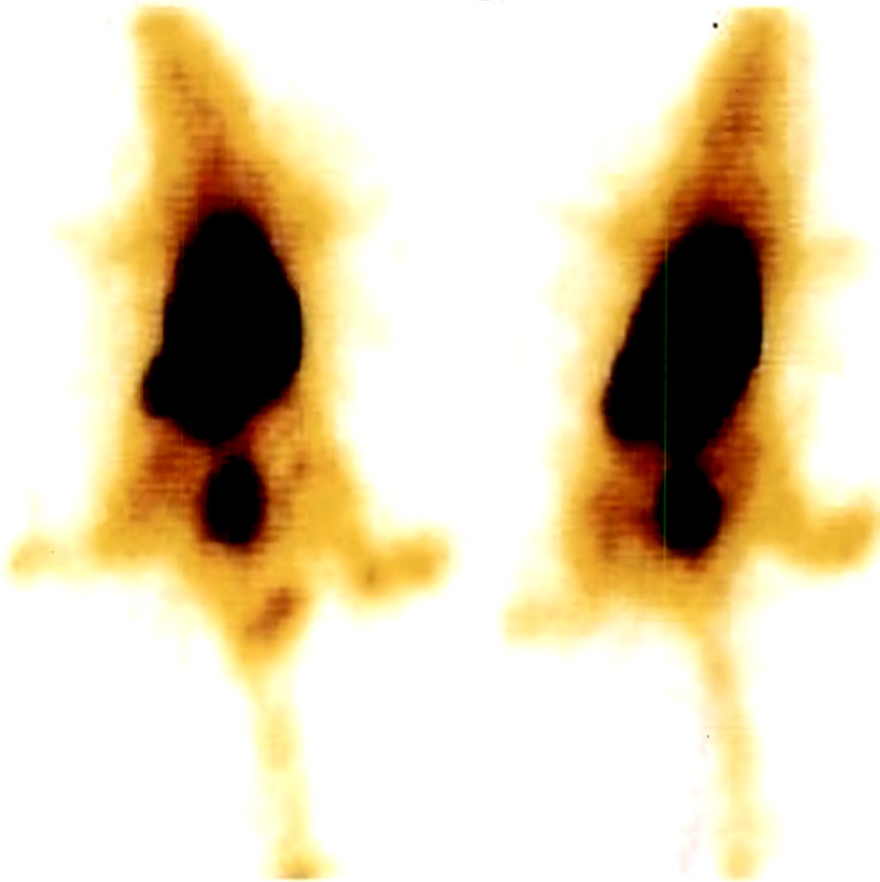

Figure 3.4.2.4 Gamma camera image of rats at 1 h after i.v. administration of 99m-Tc-compound 49g

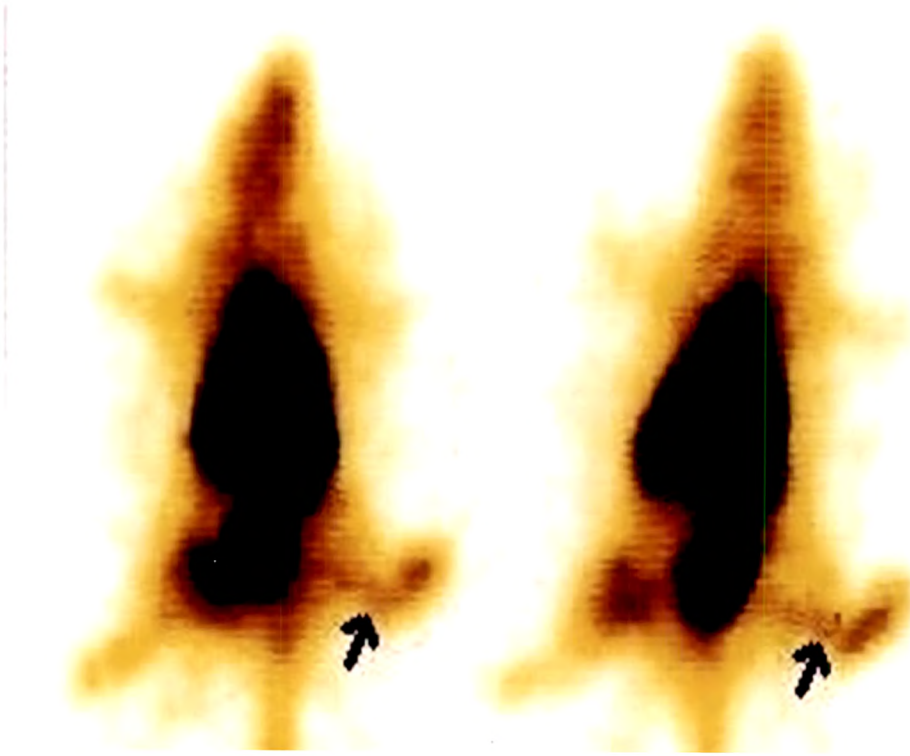

It could be seen from the imaging studies that in comparison to the tertiary compounds (**45f** and **49f**) the quaternized compounds (**45g** and **49g**) showed a higher affinity for the inflamed paw, as expected.

It is pertinent to mention here that the derivatives (**45f** and **49f**) were found to be inactive as anti-inflammatory agents in the acute inflammation model (Section 3.3 2) because they were not getting hydrolysed to liberate the free parent NSAIDs (**45** and **49**) upto three hours But, it could be assumed that once localized in the cartilagenous tissues in arthritis patients they would be hydrolysed chemically, sooner or later to release the parent drugs (**45** and **49**), to show their normal anti-inflammatory activity without affecting the GIT and other body tissues.

It would not be out of place to mention here that the radiolabeling and biodistribution studies for these and other compounds need to be performed in more detail, may be at a later date.